CALIFORNIA INSTITUTE OF TECHNOLOGY
EARTHQUAKE ENGINEERING RESEARCH LABORATORY

LABORATORY EVALUATIONS AND INSTRUMENT CORRECTIONS OF STRONG-MOTION ACCELEROGRAPHS

by

M. D. Trifunac and D. E. Hudson

Report No. EERL 70-04
A Report on Research Conducted Under a
Grant from the National Science Foundation

Pasadena, California

August, 1970

TABLE OF CONTENTS

INTRODUCTION

Since the first strong-motion accelerographs for the measurement of the ground motion associated with destructive earthquakes appeared in the early 1930's there has been a continual development of instruments and data handling techniques. These developments have resulted in improved field reliability, increased frequency response range, better resolution and accuracy, and reduced costs. As new instrument types appear it is necessary to carry out comprehensive programs of laboratory and field evaluation to ensure adequate performance capabilities.

The advent of high speed digital computer systems has completely altered data processing procedures associated with strong-motion instrumentation. Modern digitization and digital filtering techniques, for example, have made it possible to use new approaches to transducer design, and to the optimal retrieval of information from instrument records.

The Earthquake Engineering Research Laboratory of the California Institute of Technology considers the continued reliable operation, expansion, and data processing functions of a network of strong-motion accelerographs to be one of the key requirements of earthquake engineering research. To this end, this laboratory has for many years conducted numerous studies and research programs aimed at improvements in all aspects of this subject. In cooperation with the Seismological Field Survey of the U. S. Coast and Geodetic Survey, the

Caltech group has been engaged in accelerograph design, testing, network design and installation, accelerogram digitizing and corrections, and the use of accelerograms for structural response determinations.

The present report brings together a number of special studies related to accelerograph evaluations and data processing, which may be of interest to others engaged in instrument development or in the use of accelerograph records. It is our feeling that the best use can be made of the basic data only by those persons thoroughly familiar with the details of instrument design, and the special problems that may be associated with both the basic measurements themselves and with the handling and interpretation of the data. Some repetition of test method descriptions has been retained to ensure a reasonable independence of the various sections.

A. LABORATORY DYNAMIC TESTS OF STRONG-MOTION ACCELEROGRAPHS

The characteristics of seismic-type transducers can be defined by specifying a relatively small number of system parameters such as natural frequency, damping, sensitivity and resolution. In particular, however, there may be questions as to the extent to which simple idealizations of transducer behavior are justified. For example, does the transducer act effectively as a single-degree-of-freedom system for the whole frequency range of interest? Are the effects of cross-axis sensitivity reducing the effective accuracy of the device? Do variations in paper speed or position introduce practical difficulties in data analysis? It is thus important that some overall tests be conducted on the instrument,which will impose conditions on the device reasonably similar to those it will encounter in the field during the recording of actual earthquakes.

The method adopted for such evaluation is illustrated in Figure A. 1. The strong-motion accelerograph (in this case the Japanese SMAC-B) is mounted on a table which is constrained to move horizontally in one direction. The table is driven by a Ling 1500 lb electromagnetic vibration generator with a test signal derived from a General Radio random noise generator. The test signal from the noise generator first goes to the Ling Clipper Mixer and then to the Krohn-Hite filter, Ling Booster Amplifier and the master gain control, before it is used to produce motions of the vibration generator. No attempt is

Figure A.1

made to apply an exactly prescribed motion to the table. The actual table acceleration is measured with a laboratory accelerometer having a wide frequency range. The accelerometer standard is a Statham strain gage accelerometer having a natural frequency of about 100 cps, whose overall accuracy and stability have been ascertained by several years of calibration and experience in the laboratory.

The filtered random input signal to the vibration generator is selected to have approximately the same amplitude and frequency spectral properties as typical strong-motion earthquakes. In this way the transducer test is carried out under transient conditions similar to its intended use in the field.

No attempt is made to confine this table motion accurately to a uni-directional configuration. Because of lack of precision in the supporting structure, and low relative rigidity of the whole assembly. the table has significant vertical and lateral components of acceleration. Those do not, of course, disturb the measurements because the laboratory accelerometer has a low cross-axis sensitivity and accurately measures the component of acceleration in the desired direction. The three-dimensional character of motion is believed to be an advantage, in that it more closely simulates the field conditions to which the accelerograph will be exposed in practice.

In conducting the test, the laboratory accelerometer can be rigidly attached to the frame of the accelerograph being tested at a point near the transducer element. Alternatively it can be ascertained by monitoring measurements that over the frequency range of interest

all parts in the system have the same motion in the desired direction.

The output of the laboratory accelerometer is amplified by a carrier amplifier system and recorded on a Brush Mark 280 pen-writing oscillograph. Laboratory checks of the speed of the oscillograph against standard time transmissions have established the accuracy of the paper drive.

Since the major application for the recorded strong earthquake ground motions is as inputs for structural response calculations, it seems appropriate to base accelerograph evaluations on the accuracy of such response calculations. To this end the Fourier Spectrum has been adopted as a quantity which is closely related to structural response calculations (Hudson, 1962) which would clearly reveal instrument differences of a type that would be of primary concern to the earthquake engineer. By superimposing accelerograms and calculated Fourier amplitude spectra from the laboratory accelerometer and the accelerograph under test, one can evaluate in a very direct way the overall effectiveness of the whole instrumentation system.

The methods used to digitize the analog records obtained from the laboratory accelerometer and the test accelerograph have been described and discussed in detail by Hudson, Nigam and Trifunac (1969). Figure A. 2 shows a general view of the digitizer equipment which is currently being used at the Earthquake Engineering Research Laboratory of the California Institute of Technology, for accelerograph evaluation as well as for the routine processing of strong-motion accelerograms obtained in the field. Techniques of operator training have been

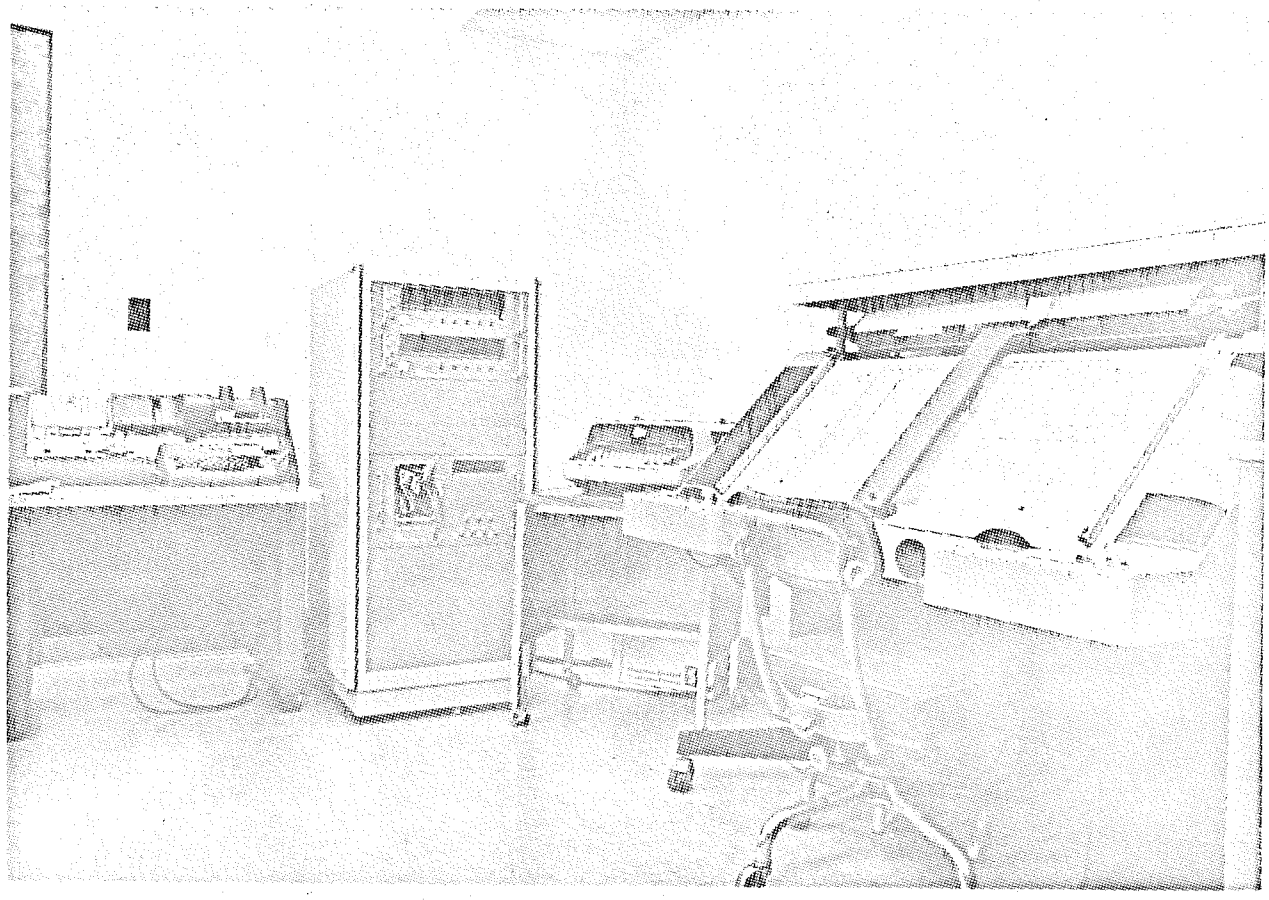

Figure A.2

developed to make the digitizing process compatible in accuracy with the basic accelerograph data itself.

As will be noted in the following sections of the present report, many additional tests enter into a complete evaluation of an accelerograph system. The above described shaking table is, however, considered to be the single most important process in the overall evaluation process.

For additional studies of special tests on a magnetic tape type strong-motion accelerograph refer to the report by Peters (1968).

B. LABORATORY EVALUATION OF SEVERAL MODERN MECHANICAL-OPTICAL TYPE ACCELEROGRAPHS

Random shaker tests of strong-motion accelerographs are performed in order to evaluate their overall accuracy in the field during actual strong earthquake ground motion. In these tests the instruments are subject to motions which are generated in the laboratory by an electro-magnetic shaker. The character of the motion is nearly random and corresponds to the band of frequencies typical of destructive earthquake ground motion.

The frequency content of such motion, characterized by the Fourier amplitude spectra or the maximum relative velocity spectra, varies considerably from one earthquake to another. It depends, among other parameters, on the earthquake mechanism, the type of the medium along the path of wave propagation, and on ground attenuation factors and distance. By observing many Fourier amplitude spectra of ground acceleration records one can approximately conclude that the predominant frequency band usually extends to 10 to 15 cps.

For a random vibration test an accelerograph is bolted to a table 20 inches wide and 38 inches long. The table is supported on two rows of well lubricated steel balls which ensures predominately longitudinal displacements of several inches. At one end the table is connected to an electro-magnetic shaker which generates the motion. During the test, table acceleration is monitored by a Statham $\pm 2g$ accelerometer whose natural frequency is above 100 cps. The signal from the accelerometer is amplified by a carrier amplifier system and

then reproduced on a Brush recorder. This record serves as the reference to which the other accelerograph records are compared.

Two types of comparison are usually made. In one, digitized records from the reference accelerometer and from the test accelerograph are superimposed on the same plot. This permits a visual estimate of the degree to which the two records agree. In the other comparison, Fourier amplitude spectra are calculated for both the reference and accelerograph records and plotted on the same graph. This second method indicates the degree of agreement in frequency space and represents a more informative and more complete comparison than the first one. This is mainly because the two records may visually appear similar and yet may differ significantly at high frequencies.

Fourier amplitude spectra for four different strong-motion accelerographs, tested as described above, are given in Figures B.1 to B.4. The frequency bands of the random noise excitation varied from 0 cps to 6 cps up to 0 cps to 20 cps and are indicated in each figure.

As may be seen, the agreement between the spectral curves in all figures is good. The spectral differences in Figures B.1, B.2 and B.4 are not much larger than the fluctuations introduced by the repeated digitization of the same accelerograph record (Hudson, et al, 1969). In Figure B.3 one can see a deviation of the spectra for frequencies greater than about 11 cps. This increase of the AR-240 spectral amplitude is attributed to the fact that this particular

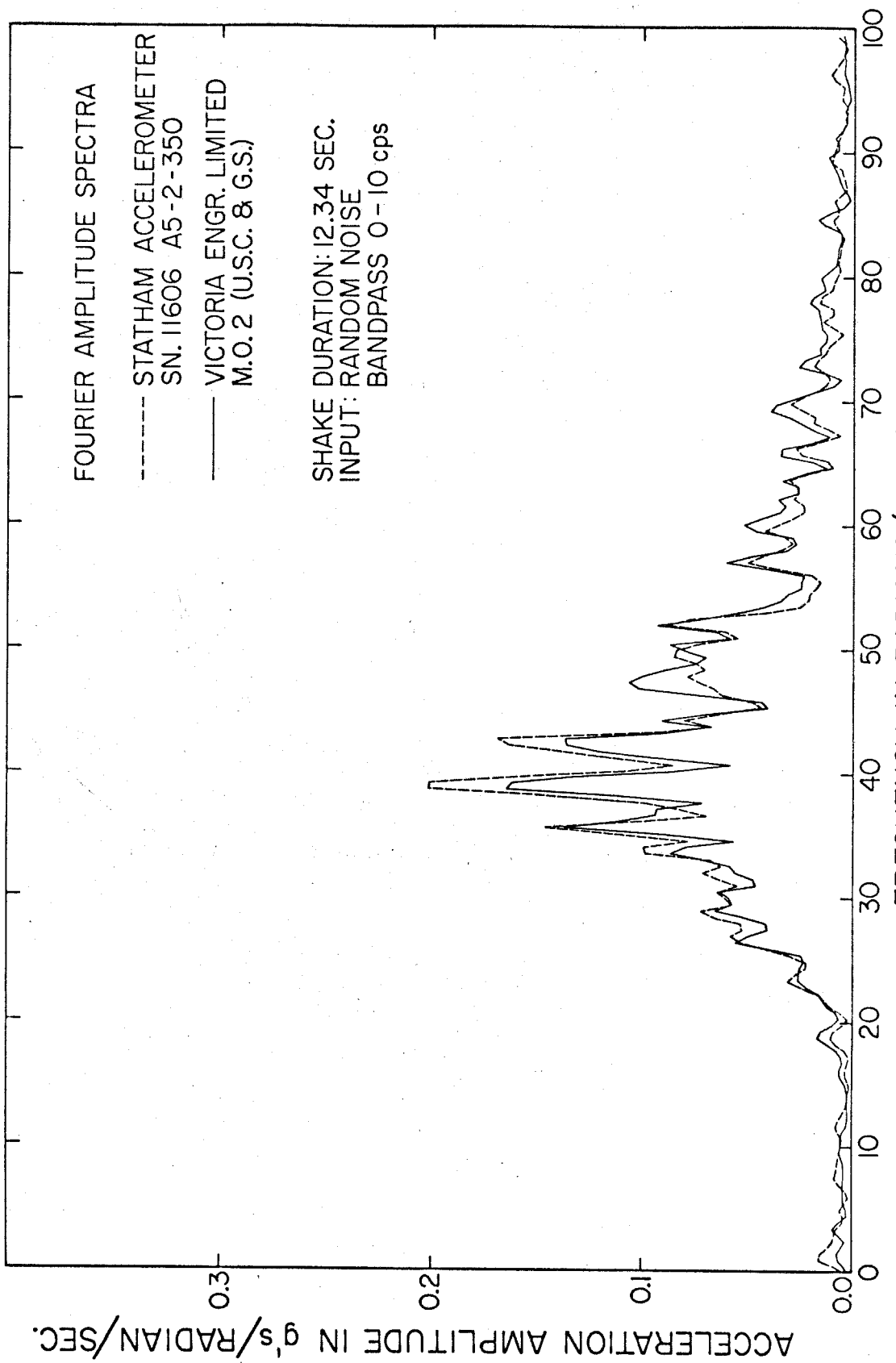

Figure B1. A comparison of the Fourier amplitude spectra for the M_L 0.2 and the reference Statham accelerograms recorded simultaneously during the random table motion.

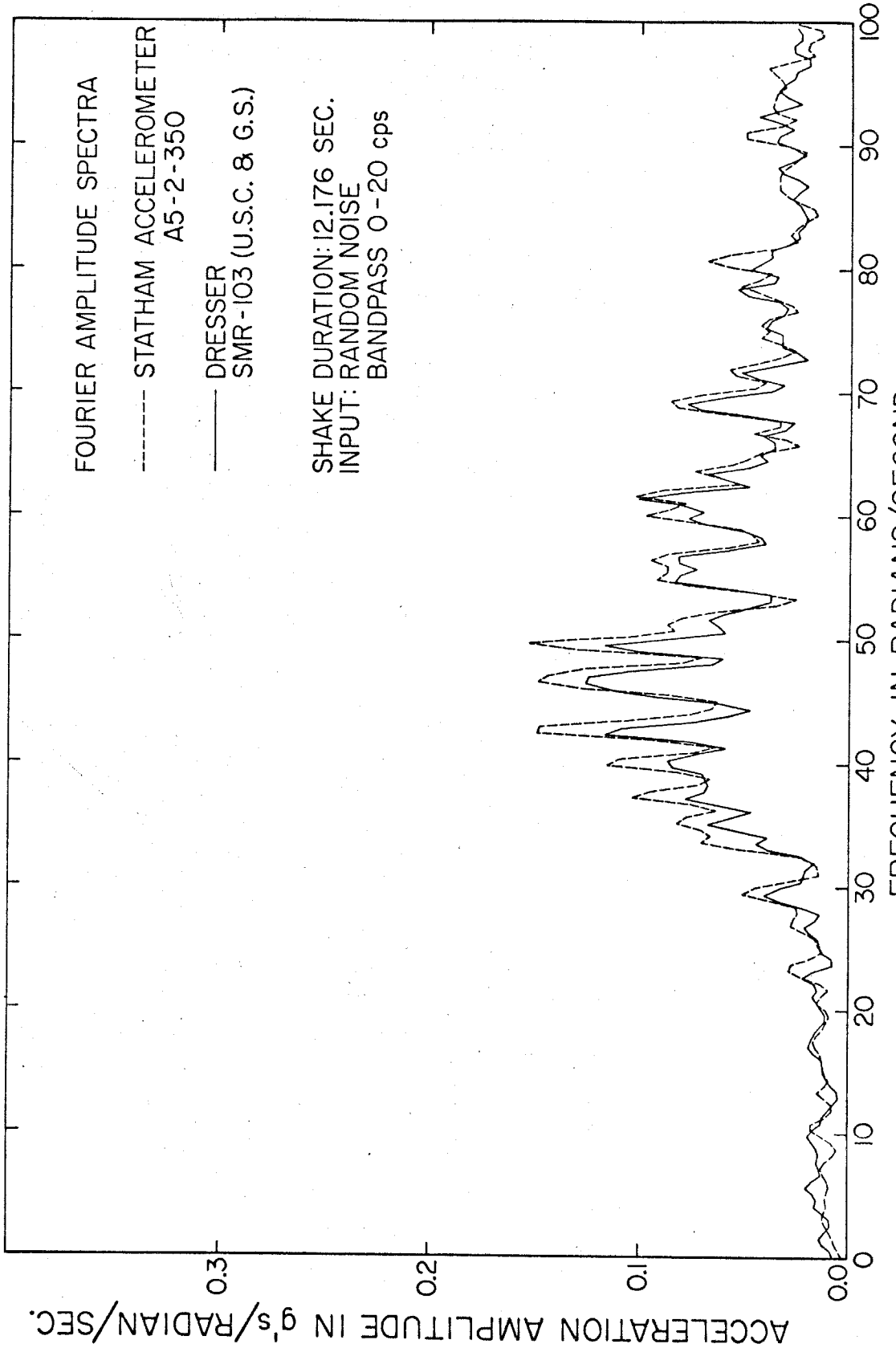

Figure B 2. A comparison of the Fourier amplitude spectra for the DRESSER and the reference Statham accelerograms recorded simultaneously during the random table motion.

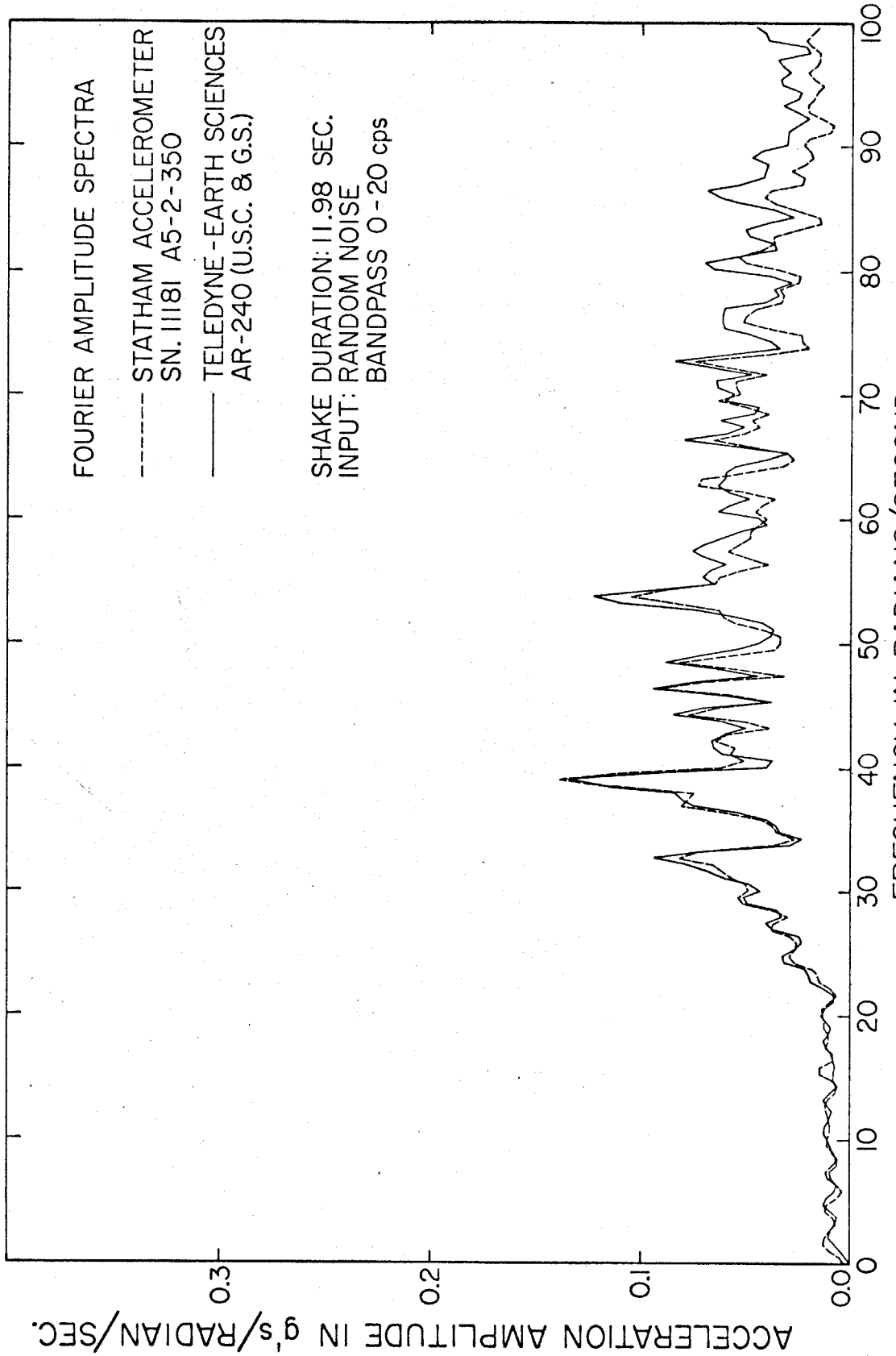

Figure B 3. A comparison of the Fourier amplitude spectra for the AR-240 and the reference Statham accelerograms recorded simultaneously during the random table motion.

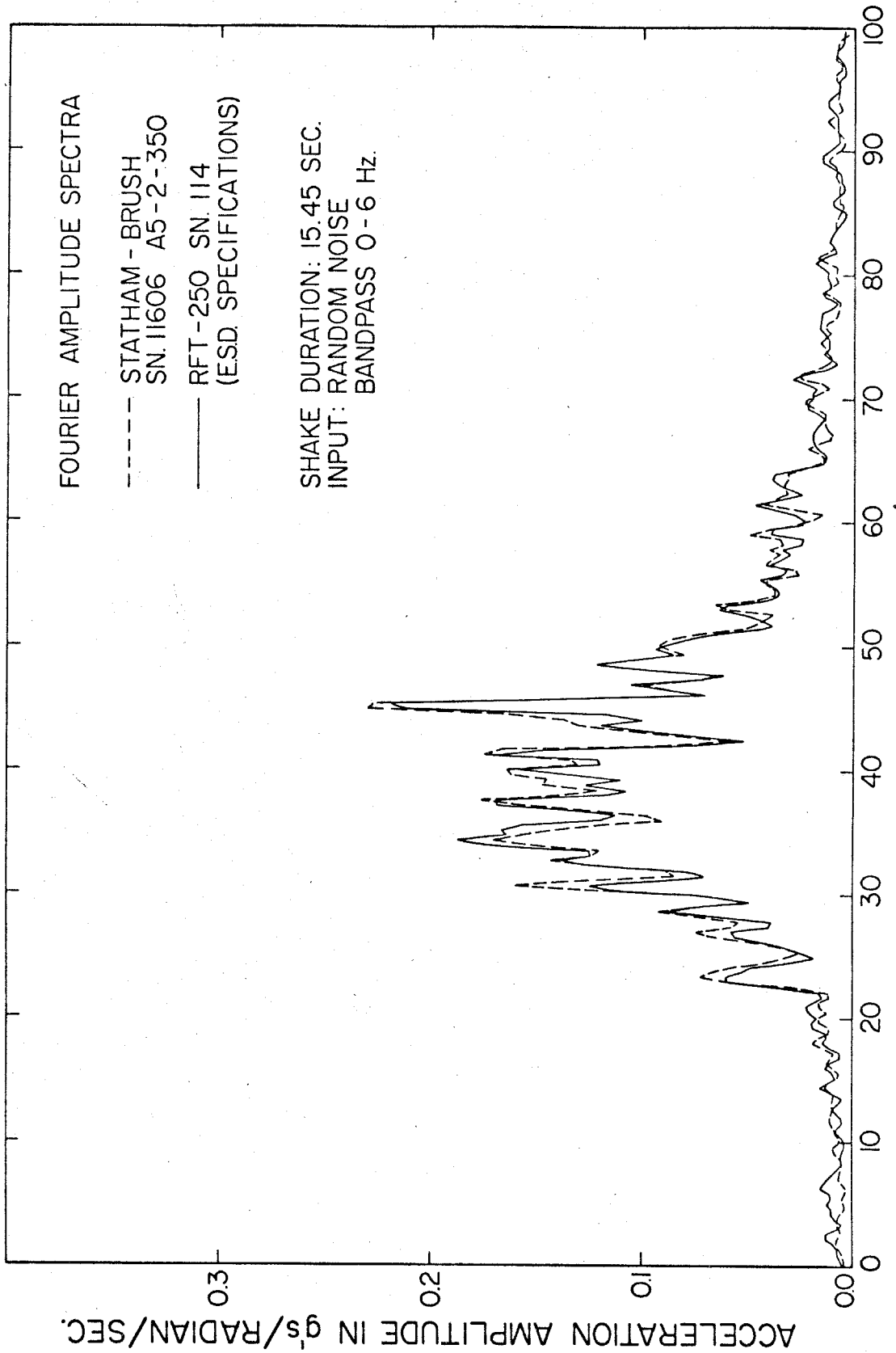

Figure B 4. A comparison of the Fourier amplitude spectra for the RFT-250 and the reference Statham accelerograms recorded simultaneously during the random table motion.

instrument had a significantly smaller damping than the specified 70%. The natural frequency of the AR-240 is about 18 cps, and the deviation in the spectrum curves becomes significant only at frequencies above 10 cps.

C. LABORATORY TESTS OF THE SMAC-B STRONG-MOTION ACCELEROGRAPH

Abstract

Laboratory tests of the performance of the SMAC-B, 10 cps critically damped, strong-motion accelerograph indicate that it can yield satisfactory records of strong earthquake ground motion for a wide range of conditions. However, the fact that critical damping is used requires that instrumental corrections be made before the records may be considered as ground accelerations for frequencies up to about 10 cps. Smoothing techniques allow accurate numerical differentiation and sufficiently accurate instrumental corrections can be performed directly from the differential equation. The SMAC-B mechanical system of connecting springs, pivots, and levers for amplification and recording has extraneous frequencies which range from about 10 cps to about 25 cps. The presence of such frequencies could interfere with accurate recording of high frequency ground acceleration, although this would be in a frequency range normally considered to be outside the range of applicability of the instrument.

Introduction

Research and trial production of the strong-motion seismograph SMAC were initiated in 1951 and in 1957 an improved version SMAC-B was developed. Presently, there are about 450 strong-motion accelerographs of the SMAC-B type in Japan (Strong-Motion Earthquake Observation Council, Tokyo, 1968) and many small and intermediate earthquakes have been recorded since 1957.

A visual comparison of Japanese SMAC records and accelerograms obtained in the western United States gives the impression that the Japanese records appear to have a rather smaller content of high frequency oscillations than is present in most of the American records. Part of this apparent difference might of course be attributed to basic differences in earthquake ground motion or in conditions of mounting and installation in structures. Part of the difference could perhaps also be accounted for by basic differences in accelerograph design, and it is this aspect of the problem that is here investigated. Through a recent exchange program of the USCGS and the Strong-Motion Earthquake Observation Committee of Japan, a SMAC-B strong-motion accelerograph has been available for laboratory investigation. Among other findings, the results of these tests now confirm and explain some of the previous observations regarding frequency content of many accelerograms recorded in Japan.

Destructive earthquakes do not occur very often and consequently there are not many strong earthquake ground motion records available

for earthquake engineering studies. For this reason the records which are available must be used with the maximum efficiency. Therefore, it is hoped that a brief study of the dynamic properties of the SMAC-B strong-motion instrument may help in the interpretations of the SMAC accelerograms recorded in Japan and in other parts of the world.

A Brief Description of the SMAC-B Strong-Motion Instrument.

The SMAC-B strong-motion instrument belongs to a general group of mechanical seismic type accelerographs. It has three pendulums, recording vertical, and two mutually perpendicular horizontal motions. The natural period of each seismic mass is 0.1 second. Damping is introduced by air damper having the form of a rectangular dashpot. The sensitivity is 25 gal/mm on the record, involving a mechanical lever magnification of the pendulum motion of 16 times. Recording paper 288 mm wide moves with a nominal speed of 10 mm/sec, while a record is written by a sapphire stylus on an arm 15 cm long. Laboratory experiment indicated actual paper speed to be on the average 10.15 mm/sec, for the instrument tested. If necessary the speed may be increased four times. The paper is driven by a hand wound spring motor and the recording time is about 3 minutes for each single operation, with five automatic consecutive operations possible. The instrument is equipped with electrical and mechanical starters. The electrical starter has a natural period of 0.3 seconds and the sensitivity of 10 gals, while the mechanical starter has the sensitivity of 100 gals. Time marking is by a clock controlling an electric relay

contact and stylus assembly which makes marks at an interval of one second. For the instrument tested the error in the time marking was found to be less than 0.2%. Electric power is supplied by four dry cells.

The relative motion of the seismic mass is magnified mechanically by means of a spring-loaded single lever for two horizontal pendulums and by two spring-loaded levers for the vertical pendulum. The behavior of these mechanical connections was studied with a stroboscope during a steady-state sinusoidal vibration test. When tuned to the frequency of oscillation, the stroboscope light allows critical observation of particular configurations of a mechanical system. For one horizontal pendulum it was found that steady-state vibrations close to and greater than 13 cps can cause an extension of the connecting spring in the lever system so that the connecting rod and recording pen could loose contact for a short period of time. This one-sided effect is clearly undesirable because it may cause incorrectly recorded amplitudes.

The vertical pendulum recording system was not similarly investigated, but it would be expected that similar problems would exist. A similar phenomenon was observed for the time marking stylus which is of the electromagnetic type. At about 12.5 cps vibration in the direction of the stylus motion, the stylus begins to vibrate leaving very light pulses on the time trace. At a frequency of about 13.5 cps these pulses become quite clear. Such behavior of the recording pen may lead to incorrect time marks if an earthquake has a few high frequency

pulses. These pen vibrations could perhaps be eliminated partially or completely by the choice of an appropriate higher pressure between the stylus and the paper.

In addition to the above steady-state vibrations, a simple test was made in which the recording stylus was displaced by hand for an angle of about 30 to 40 degrees and then released to vibrate freely. During this test the seismic mass was free to move. As a result, a typical record obtained from the horizontal pendulum indicated fast decaying vibrations with frequencies of the order of 25 cps over the first 0.2 seconds followed by a decaying 10 cps vibration for another 0.4 to 0.5 seconds. The 10 cps vibration lasted longer than would be expected in a critically damped single-degree of freedom system, and must somehow be a consequence of an interaction between the mechanical lever system and the main seismic mass. The recording system of the vertical pendulum indicated a different behavior. A typical free vibration started with about one cycle of 9 to 10 cps frequency and rapidly decayed with increasing frequency reaching about 25 cps. Complete decay took less than 0.6 seconds.

Linearization of the SMAC-B Record.

As previously mentioned, the SMAC-B recording stylus is supported by the arm 15 cm long, which introduces a circular curvature into the record. In addition, the recording arm may not be parallel to the direction of the paper motion so that all vibrations may be recorded with respect to some angle α. The first step in correcting

the SMAC-B record consists of determining the angle α and then transforming digitized data to account for this offset rotation. The second step consists in transforming a cylindrical coordinate system into a rectangular system.

These corrections must be applied before the SMAC-B record can be used for further computations. Although the procedure can easily be programmed and performed automatically on the digitized SMAC-B record, it represents an additional process not required by many other strong-motion accelerographs.

Natural Frequency and Damping.

In order to determine the natural frequency of the SMAC-B pendulum system, the damping cylinder had to be removed. In that case small damping effects are caused by friction in the material of pendulum H-spring, the mechanism of connecting springs and pivots, stylus friction, and air resistance. This test was performed by displacing the pendulum mass by hand and then releasing it to perform free oscillations. For typical initial displacements the record consisted of 10 to 40 cycles before the motion stopped. The result was 10 cps for the natural frequency based on the actual paper speed. This is in agreement with the instrument specifications within the accuracy of the measurements.

During the free vibration test various stylus pressures were used to see the effect of this pressure on free vibration decay. The instrument instruction book suggests 4 to 6 grams to leave a clear

recording trace on the paper. It was estimated that a pressure of about 2 grams is near a minimum required to produce a visible record. The maximum pressure applied was about 9 grams.

Two free vibration decay curves were studied to determine the character of the damping, for 2 and for 9 grams pressure between the stylus and the paper. First, the fraction of equivalent viscous damping ζ was estimated by measuring the ratio of the successive amplitudes. These results are plotted in Figure C.1 versus the amplitude measured in mm on the SMAC-B recording paper. If the damping is of the coulomb type (dry friction), one obtains the following relation for the equivalent viscous damping:

$$\zeta = \frac{2F}{\pi k A}$$

where

ζ = fraction of the critical viscous damping

F = friction force between the pen and the recording paper

A = the amplitude of pen motion

k = spring constant of the pendulum

It is seen that this relation represents a hyperbola. A least squares criterion was used to fit the curves through the data points in Figure C.1. This gave $\frac{2F}{\pi k} = 0.365$ for the pressure of 9 grams and $\frac{2F}{\pi k} = 0.135$ for the pressure of 2 grams. For the lower curve, least squares fit was performed only on amplitudes greater than 5 mm.

From the above results, it may be concluded that the damping introduced by friction between the stylus and the recording paper is

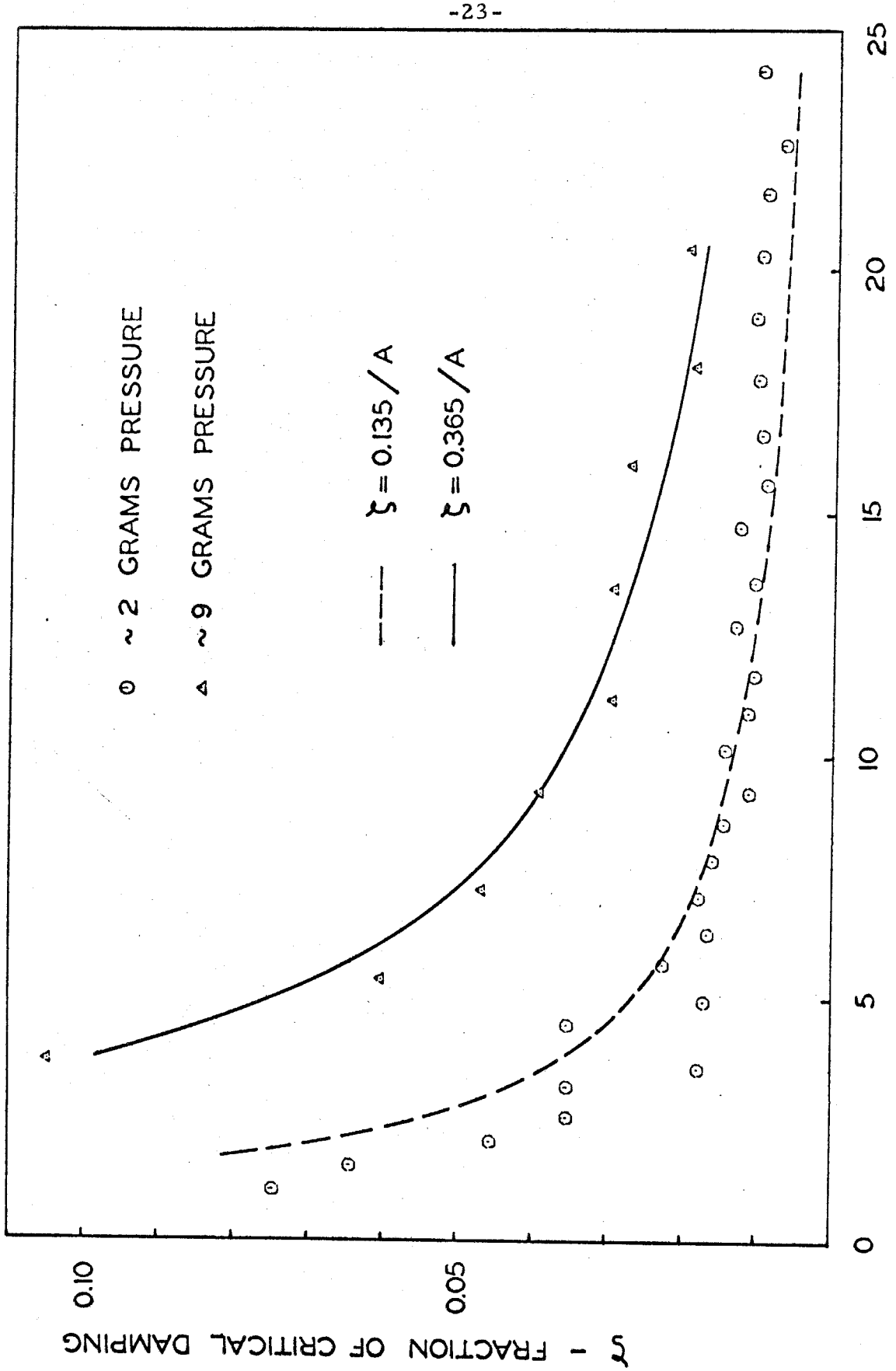

Figure C1. Experimental determination of the ζ a fraction of equivalent viscous damping for various stylus to paper pressures plotted versus the record amplitude in mm for SMAC-B accelerograph. Least square fitted hyperbolas for two cases considered are also shown in the figure.

essentially of the coulomb type, while the other dissipative forces in the system are very small. The equivalent viscous damping is less than about 5% for stylus amplitudes greater than a few millimeters, i.e., for ground accelerations greater than about 0.05 g.

The Tilt Test.

The sensitivity of accelerometers is usually determined by a tilt test in the earth's gravitational field. During this test, the instrument is tilted with respect to the vertical through an angle α, and as a result the seismic mass is deflected by a constant fraction of gravity equal to $g \sin\alpha$. By deflections of the recording stylus corresponding to various α's, it is easy to determine the sensitivity — normally given in units of g per mm on the recording paper. The tilt test was performed for six angles α ranging from about 6 degrees to about 22 degrees. The resulting average sensitivity was 0.0251 g/mm. This determination is in excellent agreement with the 0.0250 g/mm specified by the SMAC-B instruction manual.

SMAC-B Response Curve Determined by the Steady-State Vibration Test.

For a steady-state vibration test, the SMAC-B and an electric motor driven sinusoidal shaker were bolted to a table 24 inches wide and 36 inches long. The table was supported on two rows of steel balls which allow one-dimensional longitudinal motion. By changing motor speed and transmission ratio between the motor and the shaker, the table can be excited in sinusoidal steady-state motion with frequencies from about 1 to 15 cps.

The table motion was monitored by a Statham ±2g accelerometer with a natural frequency of about 100 cps. Before it was recorded on the Mark 280 Brush recorder the signal from the accelerometer was amplified by a carrier amplifier system and low-pass filtered by a Krohn-Hite variable filter. This filter has a 20 db per octave fall off above the cut off frequency which was set at 20 cps. The signal from the accelerometer was low-pass filtered in order to eliminate some of the high frequency noise which was partly caused by the table motion.

A response curve gives the ratio of the sinusoidal acceleration amplitude recorded by SMAC-B and the acceleration of table motion recorded by Statham, at a given frequency. The data from 67 response curve tests are given in Figure C. 2, and correspond to various frequencies of table motion ranging from 1 to about 11 cps. For low frequencies the SMAC-B record becomes small and hence the experimental errors in measuring the amplitudes increase. This is the reason for somewhat greater scatter of experimental points in Figure C. 2 in the region of lower frequencies. On the same Figure C.2 a set of response curves is plotted for a single degree of freedom viscous damped oscillator, with a natural frequency of 10 cps and damping ratios ranging from 0. 95 to 1. 20 of critical. It is assumed here that an air damper of the dashpot type can be well represented by viscous damping. Experimental data in Figure C. 2 indicate the best equivalent viscous damping to be about 1. 05 of critical, in good agreement with the instrument specifications of 100% critical damping.

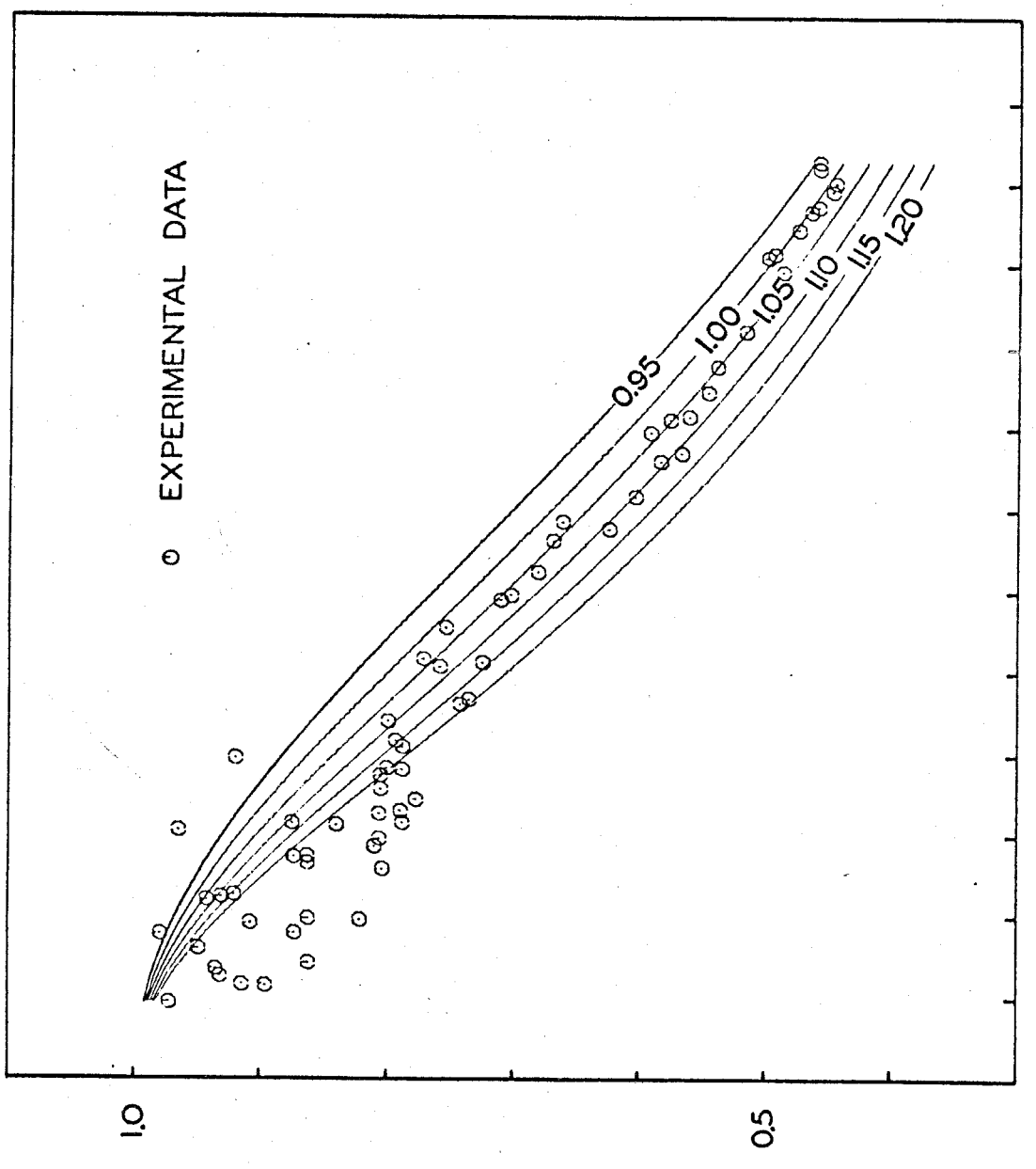

Figure C 2. The data from experimental determination of the SMAC-B amplitude response curve. Superimposed in same figure are the amplitude response curves for the single degree of freedom systems, with various fractions (0.95, 1.00, 1.05, 1.10, 1.15, and 1.20) of critical viscous damping, and natural frequency of 10 cps.

Random Shaker Test.

This test is designed to evaluate the overall behavior during motions similar to the strong earthquake ground motions. During this test the SMAC-B was bolted to a table similar in construction to a table used for the steady-state response curve, and vibrations were produced by a random motion generator. The frequencies of table motion were predominately from 2 to 10 cps. As in the previous test, table motion was monitored by the Statham ±2g accelerometer. Figure C.3 compares the Statham and the SMAC-B linearized records. As may be seen, there is considerable variation in speed of the SMAC-B paper. The difference of time coordinates between the corresponding SMAC-B and Statham amplitudes is indicated at the top of the figure. Although fairly nonuniform, this difference shows a clear long period trend of about 6 seconds and an average peak amplitude of about 0.04 seconds.

Figure C.4 shows the Fourier amplitude spectra calculated for both Statham and SMAC-B records. This comparison for the uncorrected records shows that the agreement is relatively poor. First, above about 7 cps frequency, the locations of the two sets of peaks do not agree. Second, the average of the SMAC-B spectral amplitudes is considerably lower than for the Statham record. The overall average amplitude ratio of the two spectra is about 2 at 10 cps and becomes greater at bigger frequencies, in agreement with the experimentally determined SMAC-B response curve of Figure C.2.

An accurate representation of ground acceleration is frequently required for frequencies up to about 10 cps and sometimes higher. The

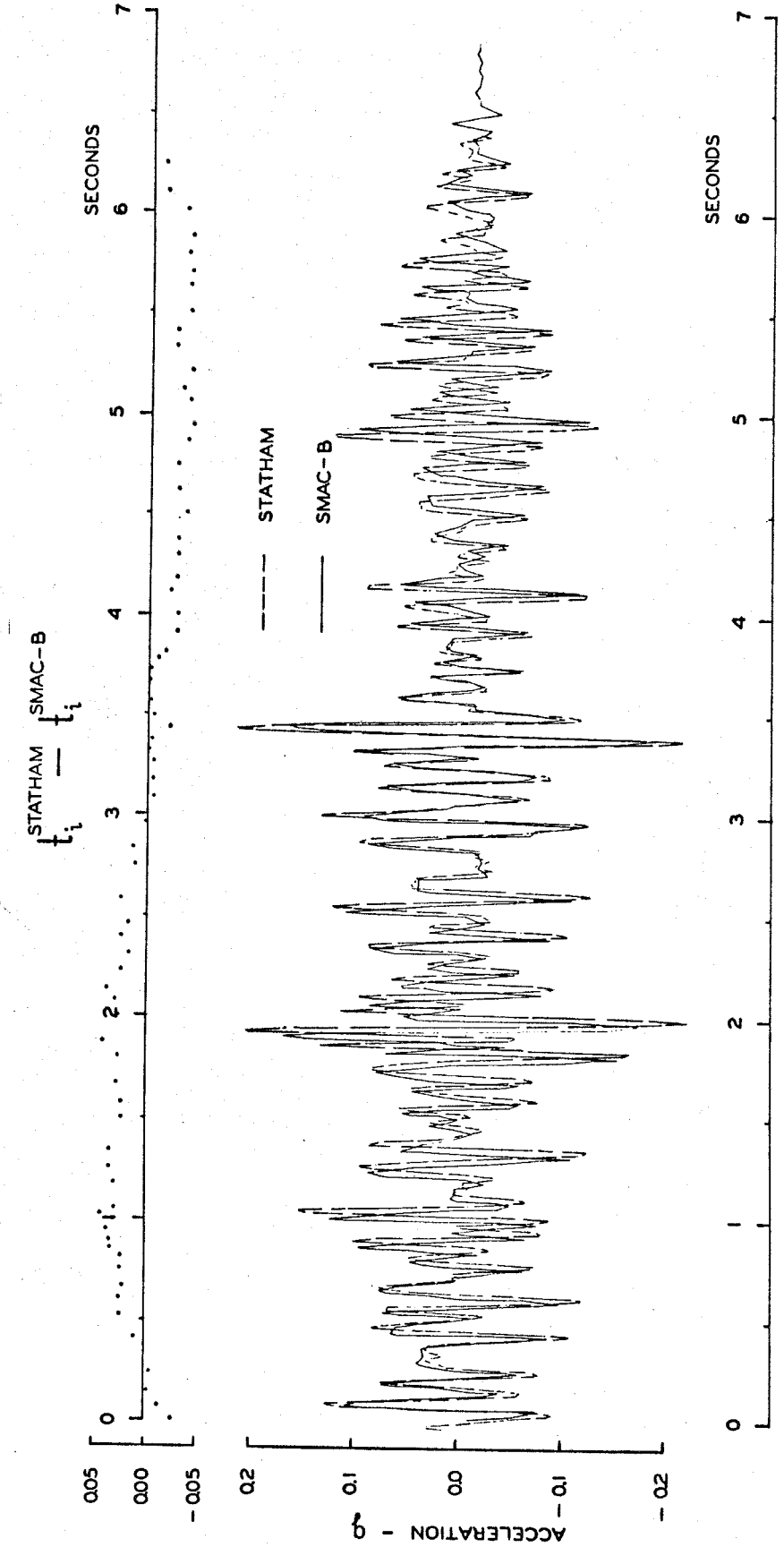

Figure C 3. A comparison of linearized SMAC-B and Statham acceleration records for a random table motion. The difference of time coordinates between the corresponding SMAC-B and Statham amplitudes is indicated at the top of the figure.

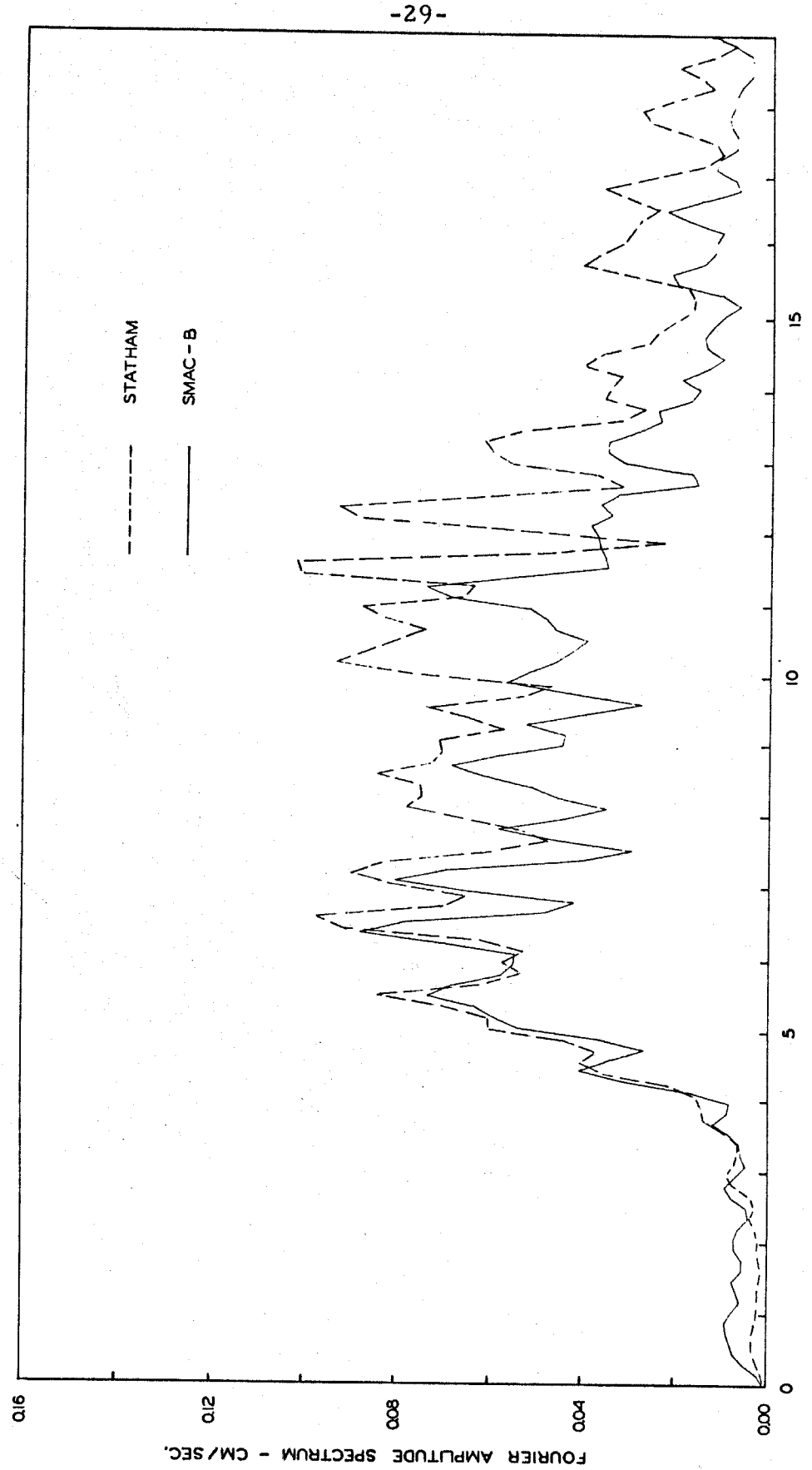

Figure C 4. Fourier amplitude spectra for SMAC-B and Statham records given in Figure 3.

SMAC-B spectrum shown in Figure C. 4 thus requires an instrument correction of the original accelerogram.

Accelerogram Correction.

In order to improve the accuracy of the SMAC-B record two different corrections were made. First, the SMAC-B time coordinates were changed by correcting for the nearly sinusoidal long period trend of 6 seconds and 0. 04 seconds amplitude. After this approximate correction, agreement (Figure C. 5) between the Statham and SMAC-B records is considerably better. It appears, however, that all high frequency peaks of SMAC-B record are smaller than those of the Statham. This is caused by the partial filtering of high frequencies in accordance with the SMAC-B response curve (Figure C. 2).

The Fourier amplitude spectrum of the Statham record is now compared with the time corrected SMAC-B record in Figure C. 6. By comparing this spectrum and the one for the original SMAC-B record in Figure C. 4, we observe that the agreement of the peak positions is considerably improved. The position and shape of nearly all spectral peaks for the SMAC-B record now agrees well with the spectra of the Statham record. The amplitudes are, however, still in error.

The second correction performed on the SMAC-B record was the so-called instrumental correction. The governing differential equation of the pendulum in a seismic type transducer is

$$\frac{\ddot{x}}{\omega_n^2} + \frac{2\zeta}{\omega_n}\dot{x} + x = -\frac{V_s}{\omega_n^2}\ddot{z} \qquad (1)$$

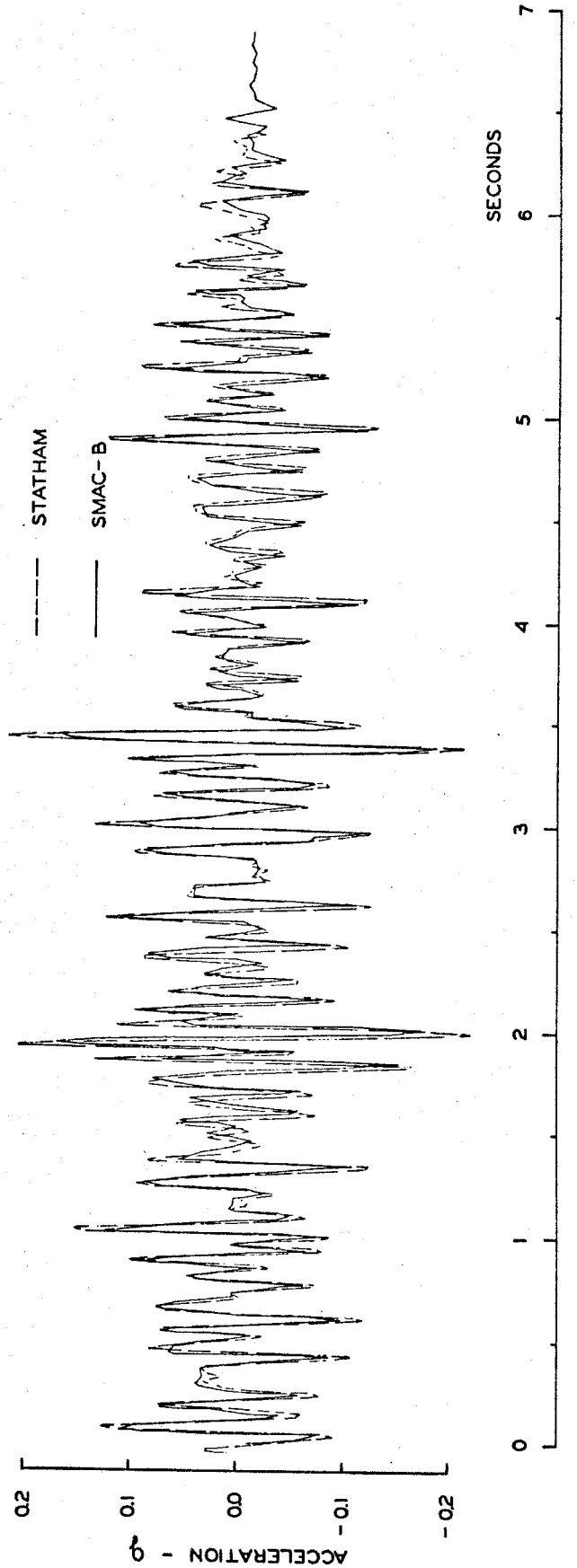

Figure C 5. A comparison of linearized and corrected SMAC-B and Statham acceleration records.

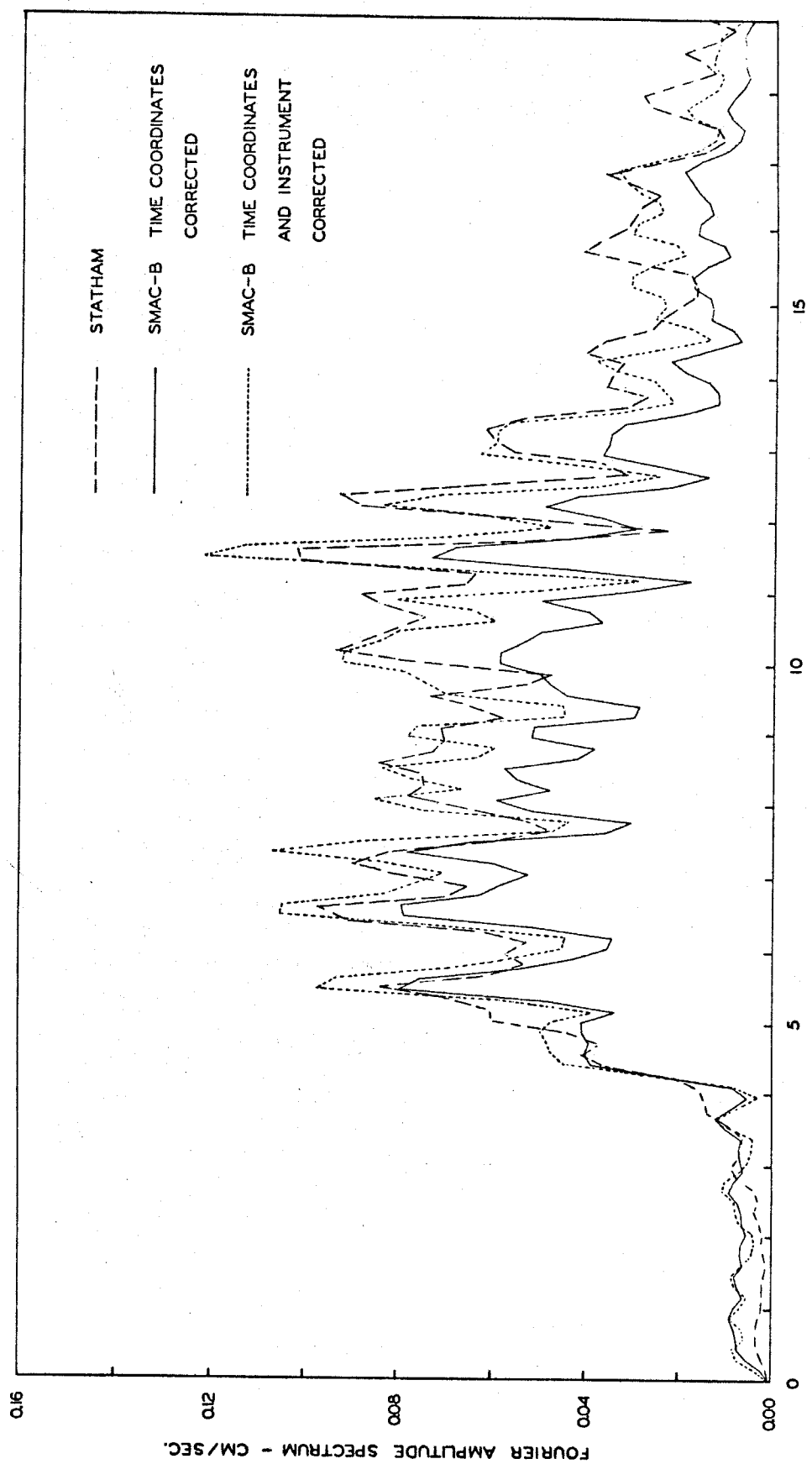

Figure C 6. Fourier amplitude spectra of the Statham acceleration record together with the spectra of linearized and time corrected SMAC-B accelerogram. Fourier amplitude spectrum for linearized time and instrument corrected SMAC-B accelerogram is also indicated.

where

x = relative motion of SMAC-B pendulum

$\ddot{z}$ = ground acceleration

ω_n = natural frequency of SMAC-B pendulum

ζ = fraction of the critical damping

V_s = static magnification

As is well known, the first approximation to $\ddot{z}$ is to assume that ω_n is a large number, in our case, 62.8 radians per second, and to neglect the first two terms in the differential equation so that

$$x \approx -\frac{V_s}{\omega_n^2}\ddot{z}$$

where $-V_s/\omega_n^2$ is a constant. The errors of this approximation cause the large spectral differences evident in Figure C.6. Knowing the response curve amplitudes (Figure C.2) we could merely divide the SMAC-B Fourier amplitude spectrum by the corresponding amplitudes on the response curve. This simple process would correct the SMAC-B Fourier spectra in Figure C.6, but the SMAC-B accelerogram would remain uncorrected. Our objective here is to correct the SMAC-B record itself since it represents the basic data about the ground motion, which is necessary for example for structural response calculations.

In order to correct for instrument properties by using the differential equation (1) it is necessary to differentiate the original SMAC-B record twice. A smoothing method may be used to eliminate high frequency fluctuations and digitization noises which are amplified

by the differentiation process (Trifunac and Hudson, 1970). Successive filtering by equally weighted running means over time intervals $T_1 = 0.030$ sec, $T_2 = 0.018$ sec, and $T_3 = 0.010$ sec were used. This smoothing was applied to interpolated equally spaced data with $\Delta t = 0.002$ seconds which were generated from the original SMAC-B record. After filtering, every fifth point of the smoothed record was kept for further analysis thus giving equally spaced data with $\Delta t = 0.01$ seconds. The differentiation was then performed by using a central difference scheme. The SMAC-B record corrected in this way agreed well with the Statham record and it would in fact be indistinguishable at the scale of Figure C. 5. The Fourier amplitude spectrum of the time and instrument corrected SMAC-B record appears in Figure C. 6. As it may be seen, the agreement with the Statham spectrum is very good. Some of SMAC-B spectral peaks are higher than those of Statham spectrum. This might be caused by an imperfect time correction of the SMAC-B record. The general level of the two spectra however agrees very well. The above spectral differences are not much larger than the fluctuations caused by repeated digitization of the same accelerograph record (Hudson, et al, 1969) by the same person. Remembering the many steps required in the correction procedure it may be concluded that the agreement between Statham and SMAC-B spectra in Figure C. 6 is remarkable.

Significant differences between the corrected SMAC-B spectrum and Statham spectrum at low frequencies (Figure C. 6), from about 0 cps to about 3 cps, are most probably caused by the lateral fluctuations in

the position of the SMAC-B recording paper. This fluctuation can be as much as 4 mm.

Conclusions.

Laboratory tests of the SMAC-B strong-motion accelerograph lead to the following conclusions:

1. The natural frequency of 10 cps, the sensitivity of 25 gal/mm, and the damping of 100% critical determined by the laboratory tests are in excellent agreement with the instrument specifications.

2. The shape of the SMAC-B response curve, obtained by steady-state vibration tests, indicates that the air damper closely approximates viscous damping.

3. It is not clear why the SMAC-B is adjusted to a damping of 100% critical in ordinary use rather than about 70%, which would significantly improve high frequency components in the Fourier spectrum of the recorded acceleration.

4. Damping produced by friction between the stylus and recording paper is of the coulomb type. For recorded amplitudes greater than about five millimeters it does not exceed 5% of the equivalent viscous damping.

5. The SMAC-B stylus supported by a 15 cm lever gives an acceleration record in a cylindrical rather than in a rectangular coordinate system. Although it is simple to linearize the record, this feature requires additional data processing.

6. Steady-state vibration tests indicate that various parts of the mechanical amplification and recording system and the time marker

have their own natural frequencies. At about 13 cps and greater, the time marking stylus starts to vibrate and leaves undesired marks on the time trace. At about 13 cps a spring, which is a part of the mechanical lever amplification system, may be extended by inertial forces so that the stylus arm does not precisely follow the seismic mass. The amplification and stylus recording mechanism of the vertical pendulum indicated amplitude dependent frequencies from about 10 to 25 cps. Such behavior of the recording system may leave some doubt about the validity of high frequencies if they happen to be observed on the accelerogram.

7. The paper speed of 10 mm/sec is rather nonuniform and erratic on the unit tested. Besides long period variations in the paper speed, many short (less than about 0.2 seconds) pulse-like changes in the paper motion were observed. This may have been caused by mechanical imperfections, or dirt in the paper driving mechanism. This behavior may be a consequence of the lack of adjustment or maintenance of this particular unit.

8. A comparison of the records and the Fourier amplitude spectra obtained from the linearized SMAC-B record and Statham ±2g accelerometer from the recording of random table motion, shows that the linearized and uncorrected SMAC-B accelerogram does not give an accurate table acceleration versus time at the high frequencies, greater than about 7 cps.

9. It was demonstrated that an adequate time correction of the SMAC-B record combined with an instrument correction based on a smoothing technique can significantly improve the accuracy of the recorded acceleration.

10. The tolerances in the SMAC-B paper drive system can allow the recording paper to drift laterally about 4 mm. This may introduce large errors in the long period spectral components of the ground motion record. In order to permit corrections for these long period drifts, it is recommended that two fixed baselines be recorded.

D. LABORATORY EVALUATION OF THE RFT-250 PIVOT SUSPENSION STRONG-MOTION ACCELEROGRAPH

A Brief Description of the RFT-250 Accelerograph

The RFT-250 accelerograph is a strong-motion recorder with three seismometers of the torsional type with a natural frequency of 17 to 20 cps. The model tested differs from the other RFT-250 instruments in that a cross spring pivot suspension is used in place of the simple torsion wire supported torsional pendulum. Other features of the instrument are essentially the same as standard RFT-250 models which do not use pivot suspension. Three seismometers record support acceleration for two mutually perpendicular horizontal and one vertical direction. The damping is provided by a coil-magnet system. The damping, adjustable by means of various shunt resistors, is normally set at 60 percent of critical. The seismometer motions are recorded on 70 mm photographic film by means of light beams. The sensitivity is about 1.9 cm per 1 g on the recording film. The film speed is 10 mm/sec. There is one timing trace, programmed for two marks per second with nominal accuracy of ±2 percent. This accuracy was confirmed by measurement on the instrument tested.

Starting is provided either by an inverted horizontal pendulum sensitive to tilt, or remotely by an electric signal. The 12 volt power supply consists of two 6 volt rechargeable batteries connected in series.

Natural Frequency and Damping

The internal pendulum damping and the natural frequency for the instrument tested were determined from free vibration decay curves. The damping computed from the decay curves did not appear to be dependent on the amplitude of motion. For the transverse pendulum, the damping ζ for the "undamped" pendulum was $0.0410 < \zeta < 0.0515$ and for the vertical pendulum $0.0493 < \zeta < 0.0662$.

The periods of the free vibration of the pendulums did not appear to be dependent on the amplitude of motion. The expermentally determined periods were $T_T = 0.0583$ sec. for transverse, $T_V = 0.0584$ sec. for the vertical, and $T_L = 0.0587$ sec. for the longitudinal pendulums. These periods are nearly the same and correspond to a frequency of about 17 cps.

Static Tilt and the Alignment Tests

During the static tilt test the RFT-250 was rotated by the same amount about all four edges of a square tilt table. The following sensitivities were determined in this way: 18.85 mm/g for transverse, 19.60 mm/g for vertical and 18.55 mm/g for the longitudinal pendulums. As may be seen, these values agree favorably with the nominal sensitivity of 19 mm/g. The relative errors are less than about 3%.

During the same tilt table test the degree of misalignment of the pendulums was measured. Ideally the sensitivity vectors of the three accelerograph pendulums should be mutually perpendicular. Also the sensitivity vector of the longitudinal pendulum should be parallel to the longitudinal axis of the instrument base, etc. We shall call here any deviation from this ideal orientation "misalignment."

To determine the misalignment of any of the horizontal pendulums in the horizontal plane an instrument can be rotated about the longitudinal and transverse axis of the base. This is illustrated in Figure D.1. The angles of the horizontal misalignment are obtained from the relative deflection of the traces A and B for rotations about the longitudinal and transverse axes. These angles are

$$\alpha_L = \tan^{-1} \frac{h_2}{h_1} \quad ; \quad \alpha_T = \tan^{-1} \frac{h_4}{h_3}$$

where α_L = angle of misalignment w.r.t. the longitudinal instrument axis in the horizontal plane.

α_T = angle of misalignment w.r.t. the transverse instrument axis in the horizontal plane.

h_1 = deflection of the longitudinal trace A away from the unperturbed static state for the rotation about the transverse axis.

h_2 = deflection of the longitudinal trace A away from the unperturbed static state for the rotation about the longitudinal axis.

h_3 = deflection of the transverse trace B away from the unperturbed static state for the rotation about the longitudinal axis.

h_4 = deflection of the transverse trace B away from the unperturbed static state for the rotation about the transverse axis.

For the instrument tested, the misalignment of the longitudinal pendulum relative to the longitudinal axis in the horizontal plane was found to be $\alpha_L = 6.75^\circ$ and the misalignment for the transverse pendulum relative to the transverse axis, also in the horizontal plane, $\alpha_T = 6.76^\circ$. The equality of these two angles α_L and α_T indicates that the two horizontal

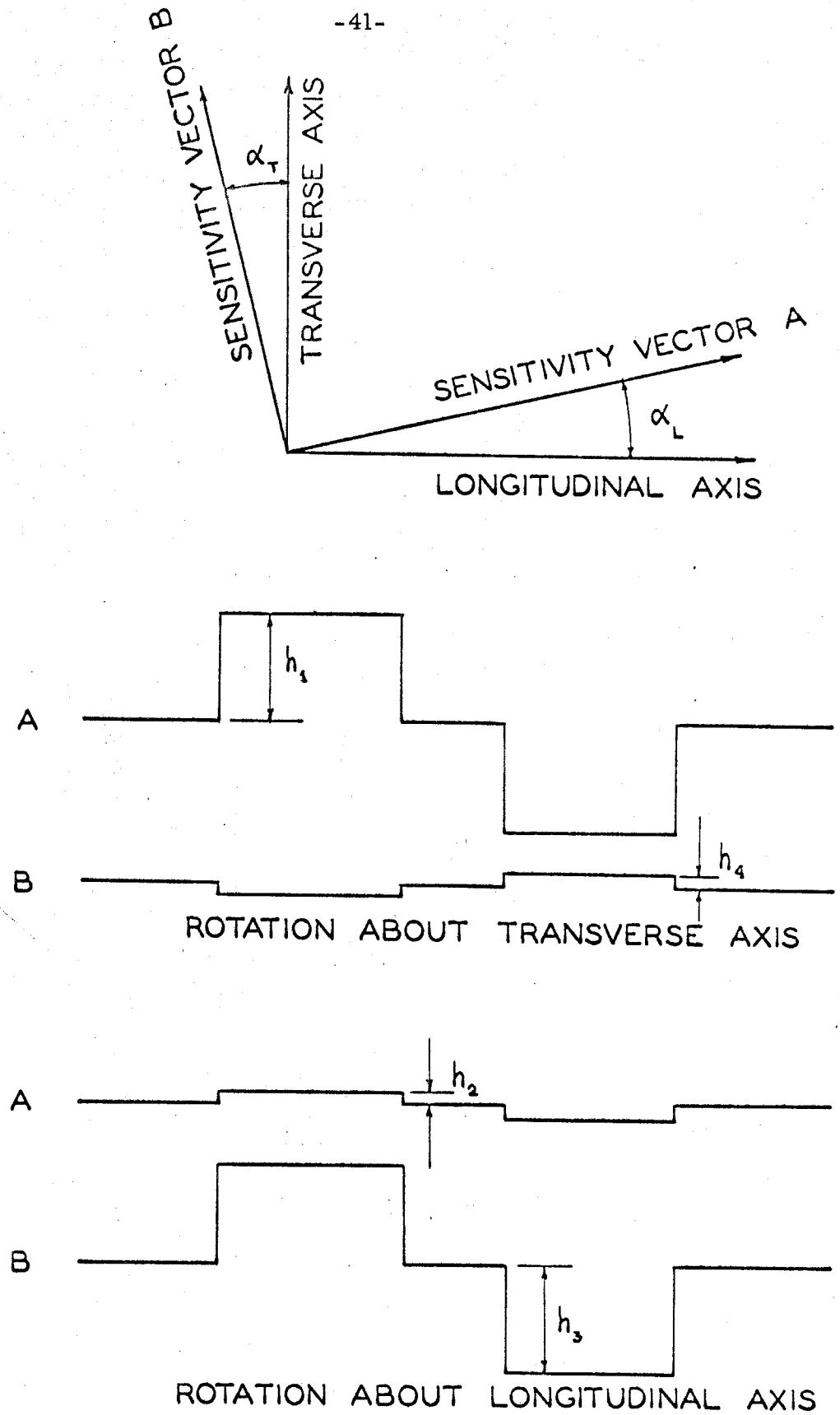

Figure D 1. The misalignments of the horizontal pendulums α_L and α_T in the horizontal plane determined by the tilt tests.

pendulums are mutually perpendicular in the horizontal plane. No deviations of horizontal pendulums from the horizontal plane could be detected.

The measurement of the deviation of the horizontal pendulum from the horizontal plane is illustrated in Figure D.2 and is equal to

$$\alpha_H = \tan^{-1}\left[\frac{(R-1)\sin\theta}{(R+1)(1+\cos\theta) - 2}\right]$$

where α_H = angle of misalignment of the horizontal sensitivity vectors w.r.t. the horizontal plane.

R = trace deflection for tilt up/trace deflection for tilt down.

θ = angle of tilt.

The scheme for the measurement of the misalignment of the vertical pendulum in either transverse or longitudinal direction when the deviation in the other perpendicular direction is small, is illustrated in Figure D.3. The angle of misalignment in this case becomes

$$\alpha_{V_P} = \tan^{-1}\left[\frac{(R-1)(1-\cos\theta)}{(R+1)\sin\theta}\right]$$

where

α_{V_P} = angle of misalignment of the vertical sensitivity vector w.r.t. the true vertical for the rotation about the P axis.

R = trace deflection for tilt to the right/trace deflection for the tilt to the left.

θ = angle of tilt.

The misalignment of the vertical pendulum for the rotation about the transverse axis was found to be $\alpha_{V_T} = 0.13^\circ$ and for the rotation about the longitudinal axis $\alpha_{V_L} = 5.1^\circ$.

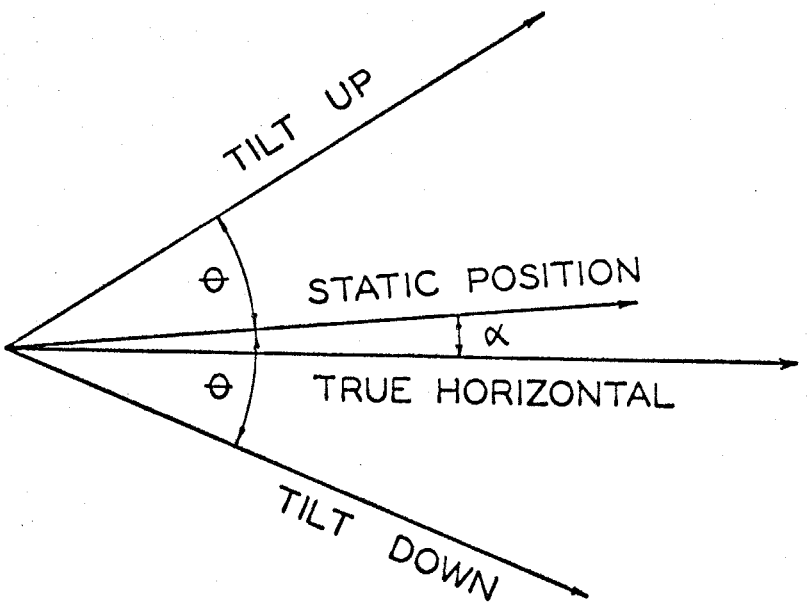

Figure D 2. The deviation α of the horizontal pendulum from the horizontal plane.

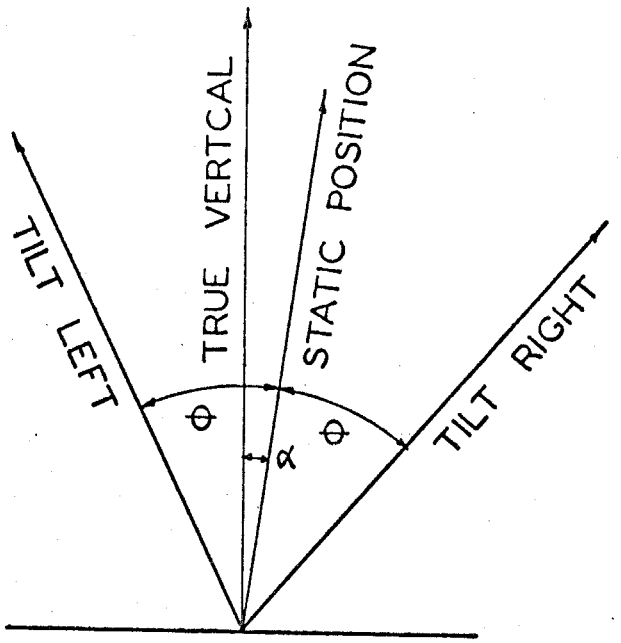

Figure D 3. The misalignment α of the vertical sensitivity vector from the true vertical.

The question of the alignment of the transducers may be an important matter since any misalignment may lead to considerable cross axis sensitivity.

Dynamic Test of the RFT-250 Pivot Suspension Instrument

During this test the RFT-250 was mounted on a horizontal shake table driven by a random signal filtered through a band pass filter 0.02 cps to 40 cps. A Statham ±2g accelerometer, with a Brush carrier amplifier and recorder, having a frequency response nearly flat to approximately 60 cps, also measured table accelerations. The longitudinal axis of the RFT-250 coincided with the axis of the Statham accelerometer, but the pendulums in the RFT-250 were several inches above the Statham, so that table rocking about the transverse axis would produce different motions of the two transducers. This effect is expected to be insignificant.

A comparison of the records produced by the Brush-Statham system and the RFT-250 is shown in Figure D.4 for the first four seconds of the recording, and appears to be very good. The Fourier spectrum analysis of about 8 seconds of the recording is given in Figure D.5. Again, this comparison shows that the agreement between the RFT-250 pivot suspension accelerograph and the Statham-Brush system is very good for all frequencies greater than about 3 cps. For frequencies smaller than about 3 cps the two spectra show considerable deviations, which among other factors, could be caused by the small transverse play of the recording film, which seems to be a common difficulty for many accelerographs. This could be corrected for by

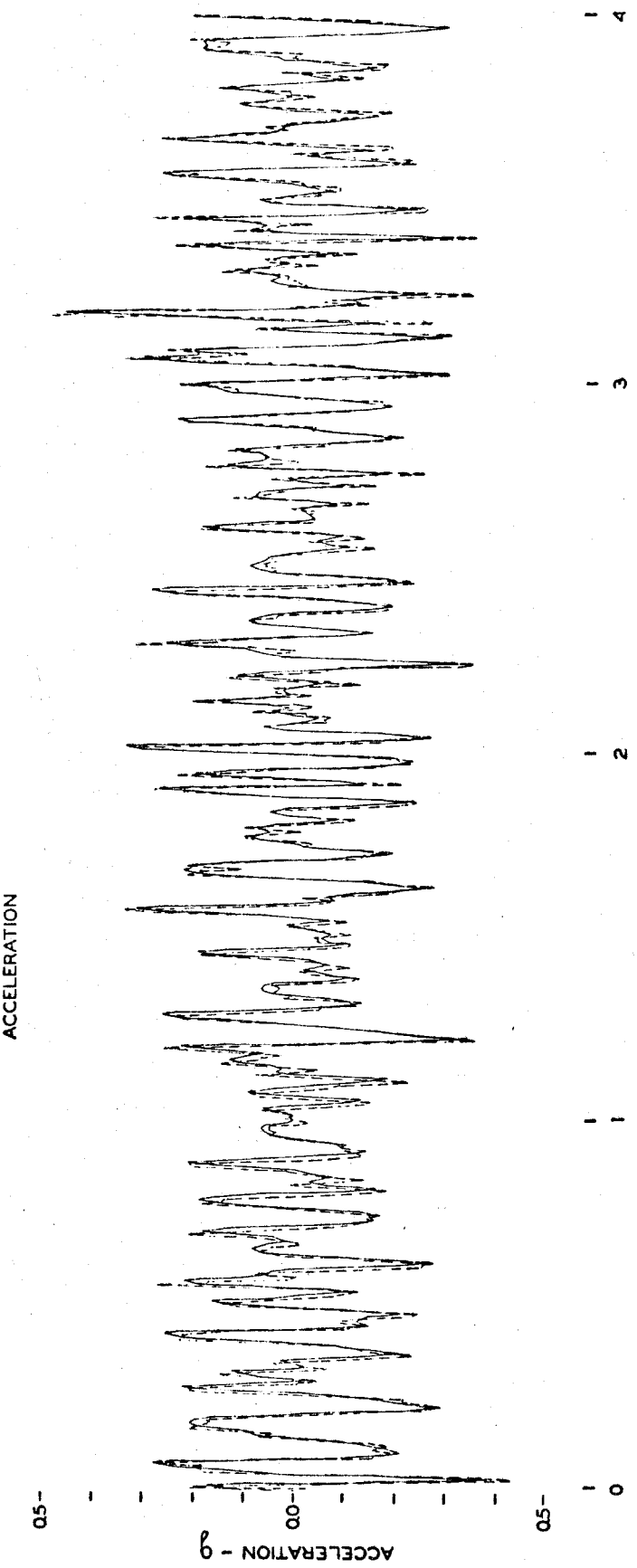

Figure D 4. A comparison of the records produced by the brush-Statham system and the RFT-250 pivot suspension accelerograph.

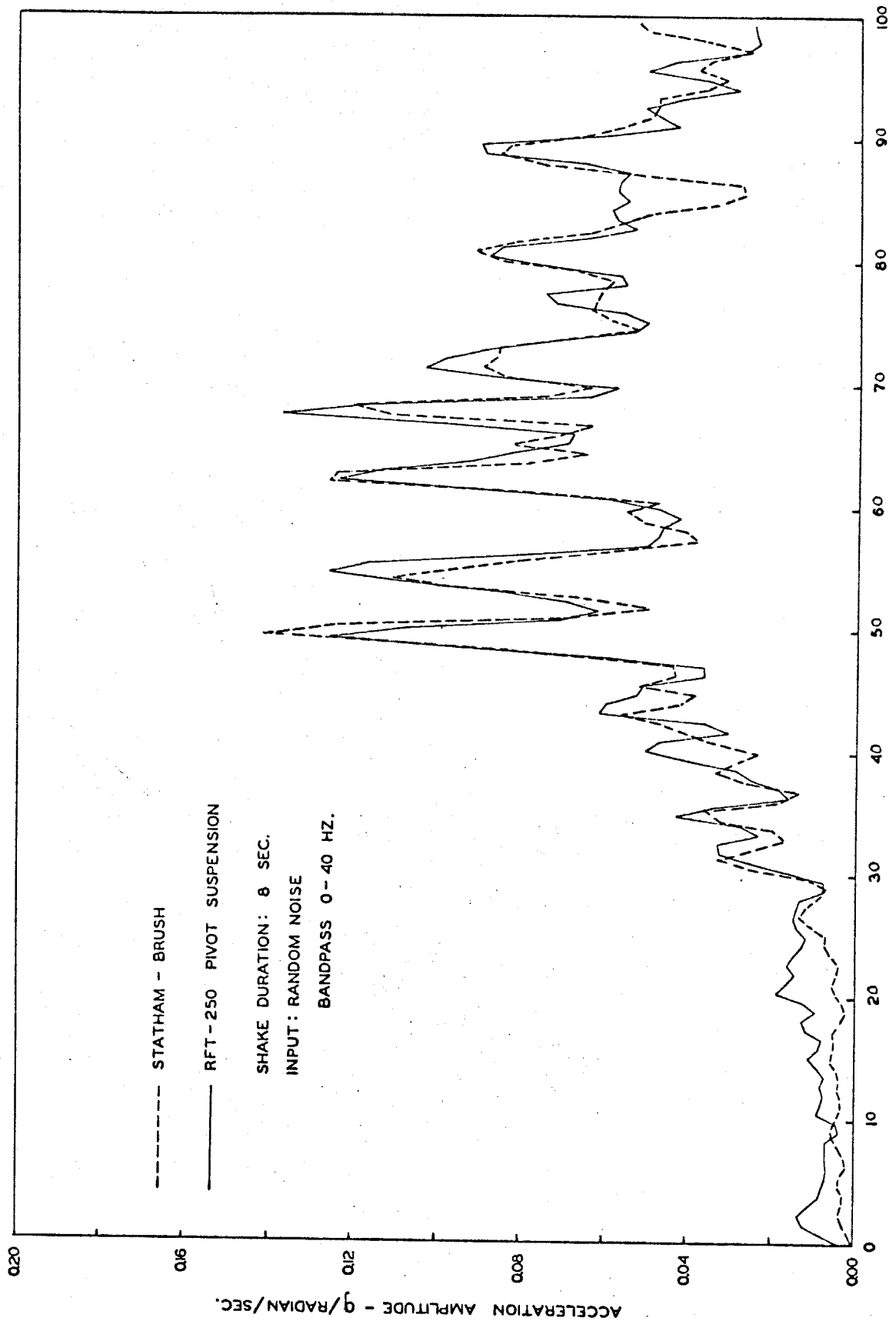

Figure D 5. A comparison of the Fourier amplitude spectra for the RFT-250 pivot suspension and the reference Statham accelerograms recorded simultaneously during the random table motion.

digitizing the fixed instrument trace, which was not considered necessary for this particular study.

Conclusions

Laboratory tests of the RFT-250 strong-motion accelerograph with the pivot suspension system did not detect any adverse effects relative to the other accelerographs in operation.

The tests for misalignment of the sensitivity vectors of the transverse, longitudinal and vertical transducers show that for the instrument tested two horizontal pendulum sensitivity vectors are mutually perpendicular. The vertical sensitivity vector had an inclination with respect to the true vertical of about 5^{o} in the transverse direction. It is important that the three sensitivity vectors be mutually perpendicular in order to avoid cross axis sensitivity.

E. LABORATORY EVALUATION OF THE SMA-1 STRONG-MOTION ACCELEROGRAPH

Description of the SMA-1 Accelerograph

The SMA-1 is a new general purpose accelerograph for measuring strong earthquake ground motion and structural response. (Figure E.1) The transducer mass consists of a plastic plate supporting a coil cantilivered on two flexible flat cantilever springs. The coil moves in a magnetic field providing equivalent viscous damping. Nominal damping of 0.6 to 0.7 of critical is attained with a shunt resistance of approximately 100 ohms. The typical coil resistance is 26 Ω. The nominal natural frequency of the transducer is about 25 cps. The accelerometer optics consists of a double mirror system similar to that used on the Wood-Anderson seismometer. The distance of the folded optical path from the light source to the accelerometer is approximately 39 cm.

Recording is on a 70 mm perforated photographic film whose speed is 10 mm/sec. There is one timing trace giving two marks per second. The nominal accuracy of the timer is ±1%. On the instrument tested, timer accuracy was within 0.57 percent. In the stand-by condition, the instrument draws 0.15 MA current, required for the vertical starter. The standard 12 volt power supply consists of eight "D" size, 1.5 volt disposable or rechargeable batteries. Other types of batteries or battery-charger combinations can also be accomodated. When actuated, the whole unit draws about 1 amp. current during recording.

The instrument is triggered by a built-in VS-1 vertical electromagnetic starter (described in Section F). It is believed that this starter

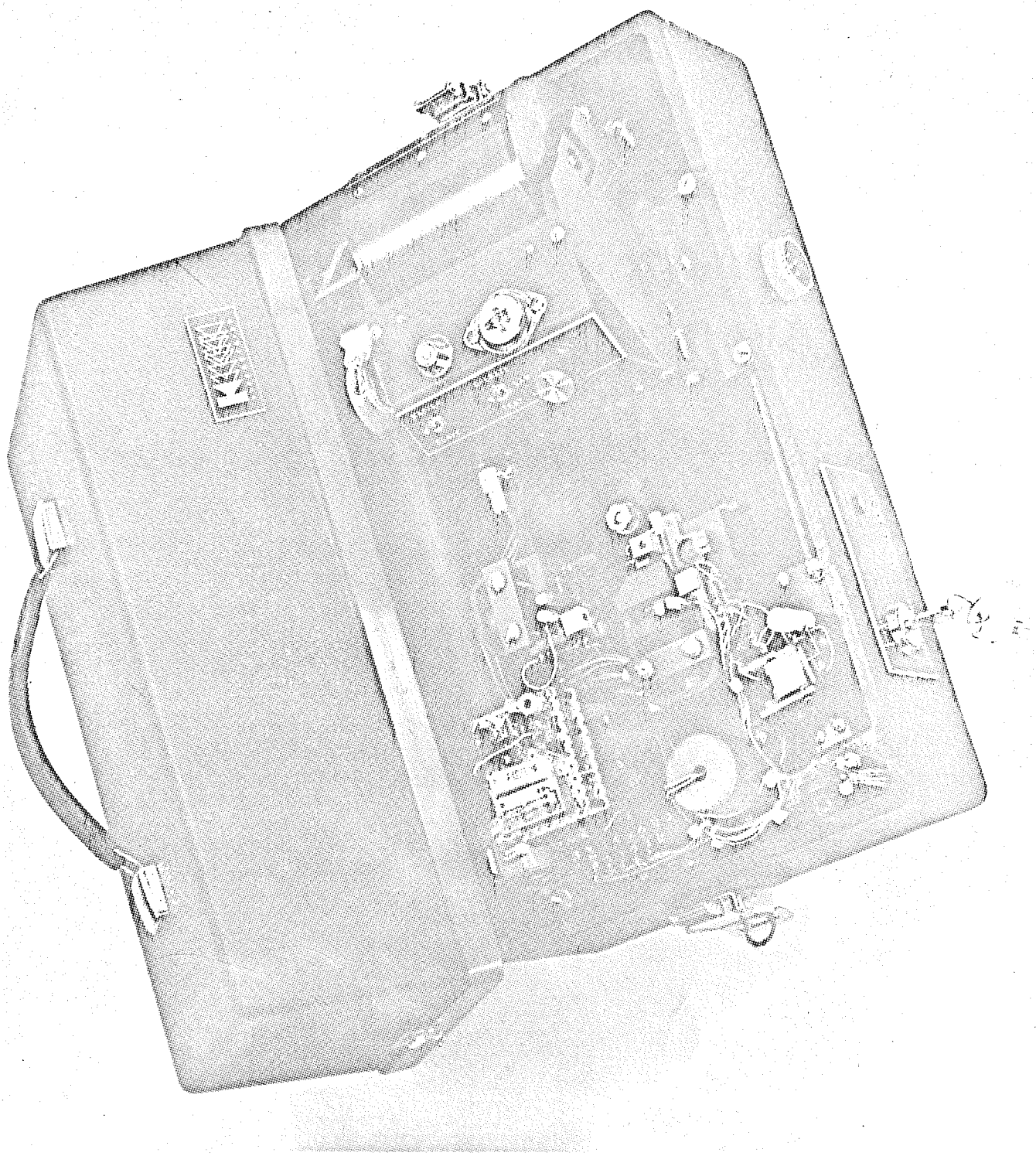

Figure E.1 The SMA-1 accelerograph.

will trigger the instrument for most earthquakes somewhat earlier than would a horizontal starter, since it is sensitive to the vertical P wave motions which normally propagate with the biggest velocities. Once the VS-1 is triggered it is designed to actuate the SMA-1 to full operation within 0.1 second. Starter damping is approximately 1.5 times critical, with nearly flat response to acceleration from 1 to about 10 cps. The actuating level of the vertical starter is adjustable from about 0.005 g to about 0.05 g.

Natural Fequency and Internal Damping

The natural frequency of the transducer and the internal damping are determined by removing the shunt resistor, pulsing the seismometer mass and recording vibration decay. The internal damping computed from the decay curves varied from 2 to 5 percent for the three components.

Experimental values of natural frequency were found to be $f_n^T = 26.3$ cps for the transverse, $f_n^V = 25.4$ cps for the vertical and $f_n^L = 26.6$ cps for the longitudinal transducers of the instrument tested. These frequencies correspond to the first mode of vibration of the spring-mass cantilever system. The spring-mass system possesses additional vibration modes and frequencies. The evaluation experiments also revealed a characteristic frequency of about 30 cps which was superimposed on the 25 cps motion during the free vibration decay test and produced small but observable beats. The analysis of the typical records obtained from the instrument also indicated the presence of the same 30 cps "noise" superimposed on the main signal. This

frequency, perhaps representing torsional vibrations of the transducer mass, could be eliminated in future designs. This small amplitude 30 cps motion does not adversely affect the accuracy of the recorded signal or its Fourier transform, but it may affect the convenience of the manual digitization process in that the operator may have to digitize more data points.

Static Tilt and Alignment Tests

As described in the previous section (Section D), during static tilt and alignment tests the instrument is rotated about all four edges of a square tilt table. For the SMA-1 tested, the following sensitivities were found: 18.50 mm/g for transverse, 19.45 mm/g for vertical and 18.35 mm/g for the longitudinal transducers.

Ideally the sensitivity vectors of the three transducers should be mutually perpendicular and at the same time parallel to the longitudinal and transverse axis of the instrument base. As described in Section D, the angles indicating the amount of deviation from the ideal configuration can be determined from the simple static tilt tests. For the instrument tested the misalignment* of the longitudinal transducer sensitivity vector relative to the longitudinal axis in the horizontal plane was found to be $\alpha_L = 1.32^o$, and the misalignment of the transverse transducer sensitivity vector relative to the transverse axis, also in the horizontal plane $\alpha_T = 5.22^o$. These two angles indicate that the two horizontal

---

* For the meaning and the notation used for the different angles of misalignment see Section D.

transducer sensitivity vectors are not mutually perpendicular in the horizontal plane projection. The deviation of the horizontal pendulums from the horizontal plane was found to be: $\alpha_H = 0.32^o$ for longitudinal axis and $\alpha_H = -0.42^o$ for the transverse axis. Here, α_H positive indicates that the sensitivity vector lies above the horizontal plane.

The misalignment of the vertical transducer sensitivity vector for the rotation about the transverse axis was found to be $\alpha_{V_T} = 0.22^o$ and for the rotation about the longitudinal axis $\alpha_{V_L} = 1.23^o$.

Dynamic Test of the SMA-1 Accelerograph

During this test the SMA-1 mounted on a horizontal vibration table was driven by a random noise filtered through a band pass filter 2 cps to 20 cps. The table acceleration was measured with a Statham ±2g accelerometer and recorded on a Brush recorder. The frequency response of the Statham accelerometer is nearly flat to about 60 cps.

A comparison of the Fourier spectra for the SMA-1 acceleration record with the Statham-Brush system for records about 9 seconds long is shown in Figure E.2. This comparison indicates good agreement of the two spectra from about 25 radians/second to about 150 radians/second. As noted for many other similar comparisons of the Statham-Brush system and accelerograph records, deviations in the Fourier spectra for low frequencies up to about 3 cps is probably caused by small transverse play of the recording film in the accelerograph and the paper in the Brush recorder.

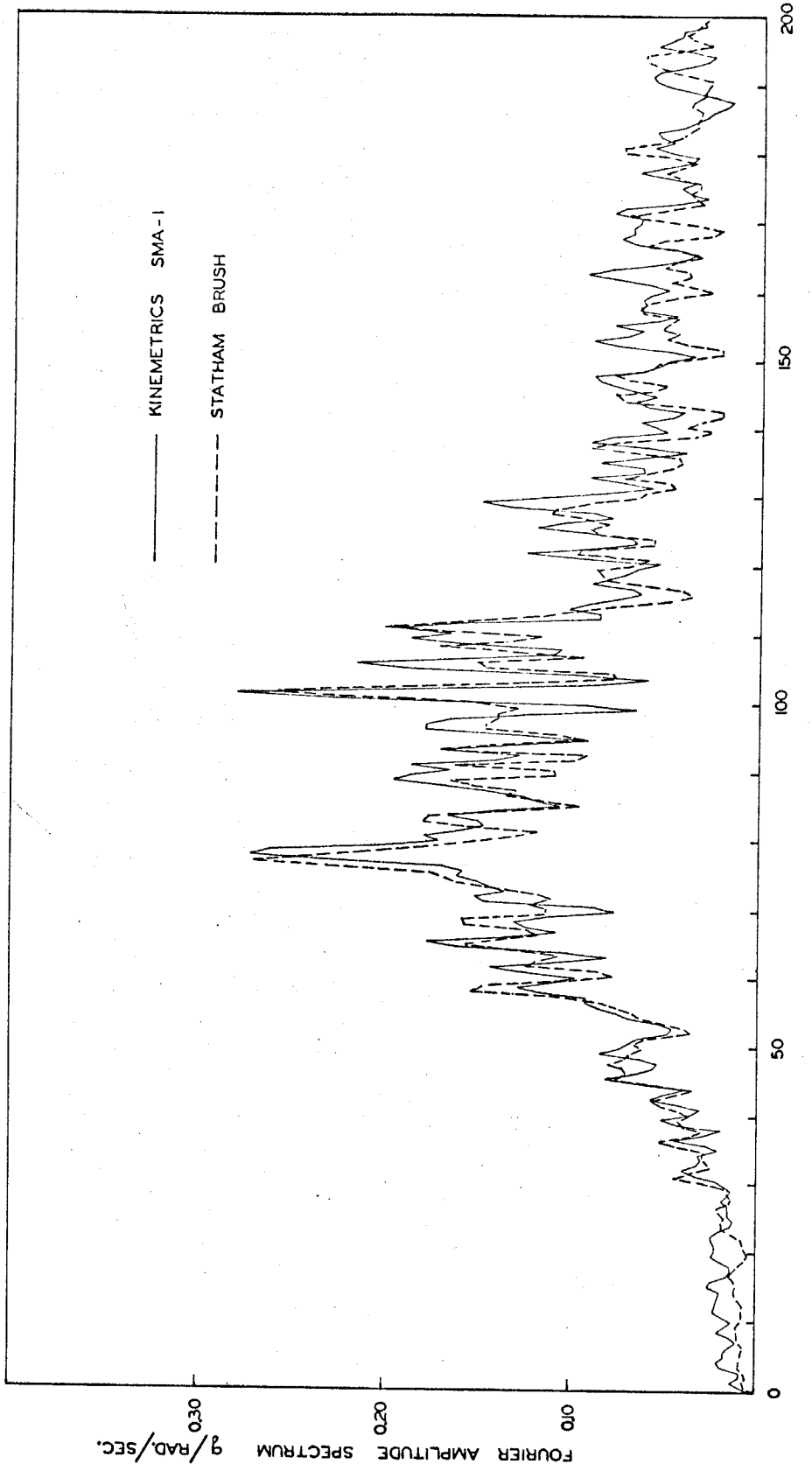

Figure E 2. A comparison of the Fourier amplitude spectra for the SMA-1 and the reference Statham accelerograms recorded simultaneously during the random table motion.

Test of the Battery Power Supply

The film storage magazines in the SMA-1 have a capacity of 50 feet of 70 mm film. With the regular speed of 1 cm/sec continuous running time is about 25 minutes. Thus under the worst and most unlikely field conditions the instrument power supply should be able to maintain normal operation for more than 25 minutes.

The unloaded voltage level of eight new 1.5 volt, size D, batteries connected in series was 13.6 volts. After the SMA-1 was actuated the battery voltage dropped to 12.0 volts and after 18 minutes of continuous running it was down to 11 volts. The experiment was then interrupted for a short time to see the degree of the battery recovery while in a stand-by condition. After one hour the unloaded voltage was 12.7 and after the SMA-1 has been actuated it was down to 11.5 volts. The motor for the film advance mechanism stopped 25 minutes later. At that time the power supply voltage was 10.5 volts.

The above simple test indicates that the power supply in the SMA-1 is adequate. It shows that the initial voltage, immediately after the SMA-1 has been actuated, should be above 11.5 volts in order to provide for at least 25 minutes of continuous normal operation. In the recording mode of operation the actuated SMA-1 draws approximately 1 amp. current.

Conclusions

Evaluation tests of the SMA-1 strong-motion accelerograph indicated that the design specifications were satisfactorily met. The new type vertical starter VS-1, if it proves reliable in the field

operation, should provide earlier triggering time and better defined triggering level than the old horizontal starter.

Analysis of the records obtained from the SMA-1, indicate the presence of 30 cps "noise" superimposed on the main signal. This extraneous motion is probably associated with a torsional or higher transverse mode of vibration of the transducer element and could be eliminated in a future design. The small amplitudes of this noise do not seriously affect the quality of the recorded acceleration.

The tests for the misalignment of the sensitivity vectors of the transducers indicated that the deviations from mutually perpendicular axes are less than about 1^{o} in all but one case for which it was about 5^{o}. This is considered to be satisfactory for the normal use of the instrument.

The evaluation of the battery power supply indicates that while the instrument is running, at least 11.5 volts is required to ensure continuous normal operation of the SMA-1 for the following 25 minutes.

F. THE VS-1 VERTICAL ELECTROMAGNETIC STARTER FOR STRONG-MOTION ACCELEROGRAPHS

PART I. THEORY AND OPERATION

Introduction.

An examination of strong-motion earthquake accelerograms from past earthquakes shows that in practically all cases the vertical ground acceleration has attained relatively large values at the time the horizontally actuated starter triggers the instrument. It would of course be expected for vertically arriving waves that vertical motions corresponding to the higher velocity P waves would arrive ahead of the horizontal motions associated with the slower S wave. It thus seems likely that for most earthquakes a vertical starter would ensure an earlier triggering of the accelerograph, and would thus permit the recording of the very beginning of the strong horizontal motion.

Early experiments by the U.S. Coast and Geodetic Survey with a displacement type vertical starter were eventually abandoned because of long-term instabilities and difficulties of adjustment. Such a vertical starter has been successfully incorporated into the Japanese SMAC accelerograph, although here again the adjustment of the device has given rise to some operational difficulties.

The New Zealand MO-2 Accelerograph employs a vertical electromagnetic velocity type starter, which by eliminating the D.C. zero frequency response and the necessity for closely-spaced switch contacts, avoids long-term drift problems, the difficulties of adjustment, and the possibility of malfunctions caused by foundation tilt, etc. In its commercial form, the starter in the MO-2 was not provided with

a sensitivity adjustment nor with a convenient means for setting, checking or calibrating the device. Since such electromagnetic systems inevitably involve rather more complicated associated circuitry than a simple displacement switch type, some means for testing and checking is a virtual necessity to ensure field reliability.

The starter described herein is that built into the SMA-1 Strong-Motion Accelerograph developed and marketed by Kinemetrics, Inc. The same device is also available as the VS-1 Vertical Starter in the form of an externally mounted unit which can be used for other accelerographs or equipment, as a replacement for or addition to other starting devices.

Principles of Operation.

Since the calibration and testing of the electromagnetic type starter requires an understanding of the basic relationships involved, the theory of such devices will be outlined. Figure F.1 (a, b) shows the configuration of the device, and defines the following quantities:

$y(t)$ = absolute displacement of base = ground motion

$\ddot{y}(t)$ = ground acceleration which triggers starter

$x(t)$ = absolute displacement of starter coil, measured from position of static equilibrium

$z(t) = (x-y)$ = relative displacement between starter coil and base (magnet system)

$\dot{z}(t)$ = relative velocity between coil and magnet

m = mass of starter coil (M = mass in kg.)

k = spring constant of coil suspension system

c = viscous damping coefficient of coil suspension system

E_c = voltage generated in starter coil

i_c = current in starter coil

R_c = resistance of starter coil

R_d = parallel damping resistance

R_p = total resistance of sensitivity adjust potentiometer

E_p = voltage across sensitivity adjust potentiometer

i_p = current in sensitivity adjust potentiometer

G = "generator constant" for the coil-magnet system, where $E_c = G\dot{z}$

F = electromagnetic force on starter coil, where $F = -Gi_c$

The equation of motion for the starter coil spring-mass system is:

$$m\ddot{x} = -c(\dot{x}-\dot{y}) - k(x-y) - Gi_c$$

or

$$m\ddot{z} + c\dot{z} + kz = -m\ddot{y} - Gi_c$$

putting $\frac{k}{m} = \omega_n^2$, and $\frac{c}{m} = 2\omega_n\zeta$ where ζ is the fraction of critical damping due to viscous damping only, this becomes:

$$\ddot{z} + 2\omega_n\zeta\dot{z} + \omega_n^2 z = -\ddot{y} - \frac{G}{m}i_c$$

Writing the voltage drop equations around the loops in Figure F.1(b):

$$E_c - R_c i_c - R_d(i_c - i_p) = 0$$

$$R_p i_p + R_d(i_p - i_c) = 0$$

from which

$$i_p = \frac{R_d}{R_p + R_d} i_c$$

and

$$E_c = \frac{R_c R_p + R_c R_d + R_d R_p}{R_p + R_d} i_c = (R_c + R_x)\, i_c$$

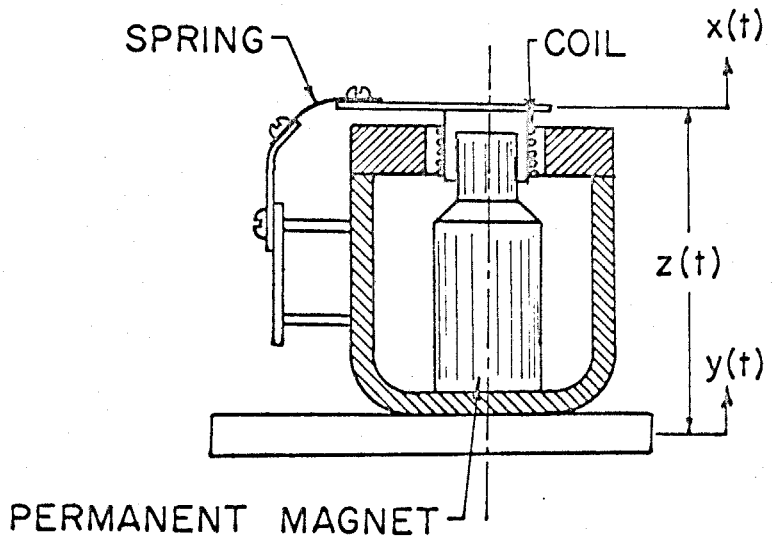

Figure F.1(a)

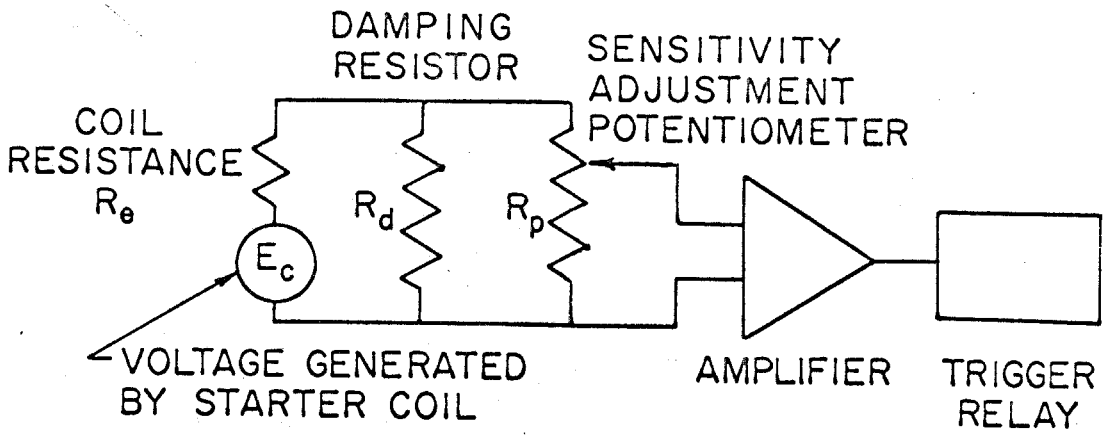

Figure F.1(b)

where $$\frac{1}{R_x} = \frac{1}{R_d} + \frac{1}{R_p}$$

thus $$i_c = \frac{E_c}{R_c + R_x} = \frac{G\dot{z}}{R_c + R_x}$$

and the system equation becomes:

$$\ddot{z} + \left[2\omega_n \zeta + \frac{G^2}{m(R_c + R_x)} \right] \dot{z} + \omega_n^2 z = -\ddot{y}$$

if h = fraction of critical damping for the whole system, then

$$2\omega_n h = \left[2\omega_n \zeta + \frac{G^2}{m(R_c + R_x)} \right]$$

The total h is to be at least 1.0, whereas the viscous damping ζ is only a few percent, so that the first term in the square bracket can be neglected, and:

$$2\omega_n h \approx \frac{G^2}{m(R_c + R_x)}$$

This relationship affords one way of determining the generator constant G. If m, R_c, R_x and ω_n are known and ζ is sufficiently small then a measurement of h will permit the calculation of G. If ζ is not small, G can be determined in the following way. First one can set $R_x = \infty$ which gives

$$2\omega_n h_\infty = 2\omega_n \zeta$$

Since ζ is now determined to be h_∞ and m, R_c, R_x and ω_n are known, the generator constant is given by

$$G = \left(2\omega_n \, m \, (h - h_\infty) \, (R_c + R_x) \right)^{1/2}$$

where h is the measured quality.

The system equation of motion thus becomes:

$$\ddot{z} + 2\omega_n h\dot{z} + \omega_n^2 z = -\ddot{y} \quad .$$

If a sinusoidal acceleration input

$$\ddot{y}(t) = \ddot{y}_o \sin \omega t$$

is introduced, z_s the steady-state solution of the equation is: (note that since damping is very large, $h > 1$, transient terms are unimportant)

$$z_s = \frac{\ddot{y}_o / \omega_n^2}{\sqrt{\left[1 - \left(\frac{\omega}{\omega_n}\right)^2\right]^2 + \left[2\left(\frac{\omega}{\omega_n}\right) h\right]^2}} \sin(\omega t - \phi)$$

Differentiating to find $\dot{z}$, then from $E_c = G\dot{z}$ and assuming ζ is small we have:

$$E_c = \frac{m\ddot{y}_o (R_c + R_x)}{G\sqrt{1 + \left[\frac{1 - \left(\frac{\omega}{\omega_n}\right)^2}{2h\left(\frac{\omega}{\omega_n}\right)}\right]^2}}$$

We want the voltage across the sensitivity adjust potentiometer E_p rather than E_c, so

$$E_p = R_p i_p = \frac{R_p R_d}{R_p + R_d} \cdot i_c = \frac{R_x}{(R_c + R_x)} E_c$$

and finally

$$E_p = \frac{mR_x \ddot{y}_o}{G\sqrt{1 + \left[\frac{1 - \left(\frac{\omega}{\omega_n}\right)^2}{2\left(\frac{\omega}{\omega_n}\right) h}\right]^2}}$$

This is the response curve for the electromagnetic starter. This is

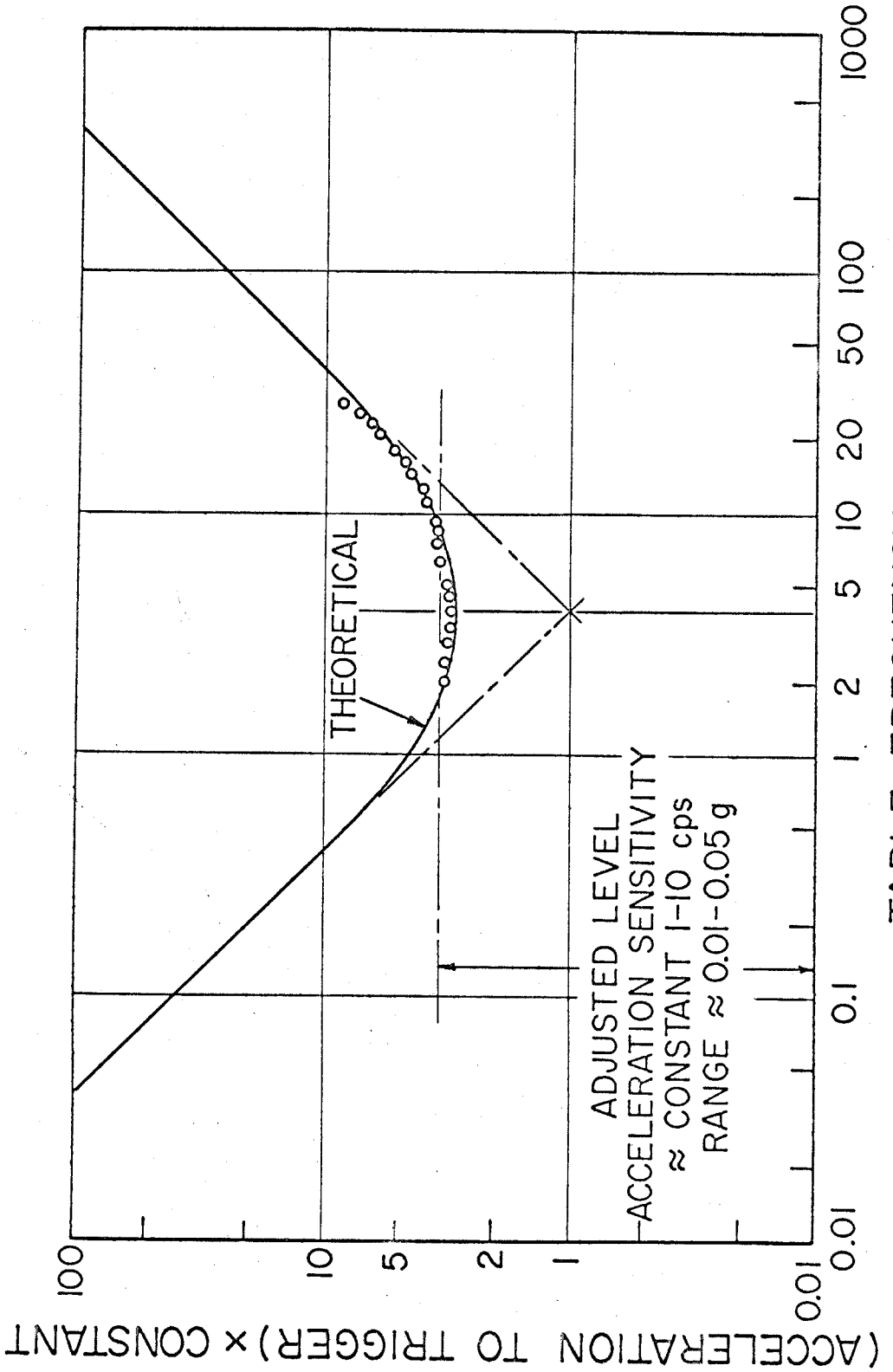

Figure F 2.

Vertical starter response curves

plotted in Figure F.2 for a particular starter having the following constants:

$h = 1.35$

$m = 3.85$ grams (weight)

$\omega_n = 3.9$ cps

$R_x = 83.3$ ohms

The starter has been designed to have an acceleration response which is approximately flat over the frequency range 1 to 10 cps. The triggering level is adjusted to the desired value in the range 0.01 to 0.05 g by the sensitivity adjustment potentiometer of Figure F. 1(b).

Sensitivity Adjustment

It is desirable that there be a simple means of adjusting and checking the starter in the field. For this purpose the "field calibrator" shown in Figure F.3 has been developed.

To use this device, the output terminals are connected by means of alligator clips across the damping resistor on the vertical terminal board of the VS-1 starter. No changes in the starter wiring are required, and no wires need to be disconnected. Referring to the diagrams of Figures F.1(b) and F.3, it will be seen that this connects the resistance R_e across the output of the field calibrator, where:

$$\frac{1}{R_e} = \frac{1}{R_c} + \frac{1}{R_d} + \frac{1}{R_p} \quad .$$

The voltage E_p produced by the field calibrator across this R_e resistance can now be calculated. This voltage corresponds to that generated by the starter coil.

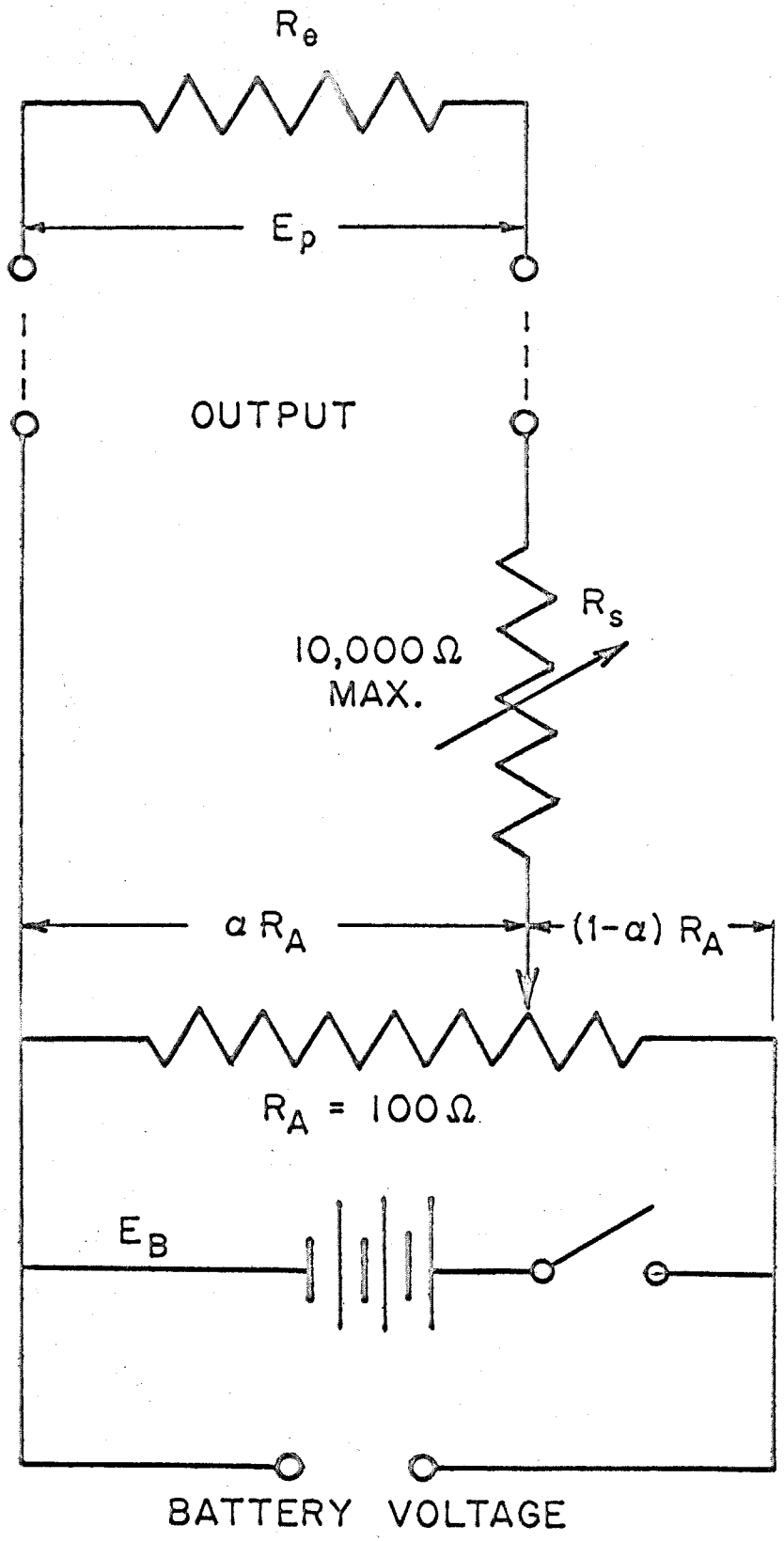

Figure F 3.

Field Calibrator

Writing the expressions for voltage drop around the two loops of the circuit of Figure F.3, the following expression for E_p is found:

$$E_p = \frac{\alpha R_e E_B}{R_s + R_e + \alpha(1 - \alpha) R_A}$$

The variable resistance R_s has a maximum resistance of 10,000 ohms, and is usually set in range of 2000-3000 ohms. The value of R_e is about 20 ohms, and R_A is 100 ohms. It is evident that to a good approximation only the first term in the denominator of the preceding expression for E_p need be retained, so:

$$E_p \approx \frac{\alpha R_e E_B}{R_s}$$

Returning now to the general expression for the response of the starter, we have for the flat portion of the curve: (putting $\frac{\omega}{\omega_n} = 1$)

$$E_p \approx \frac{m R_x \ddot{y}_o}{G}$$

equating the two expressions for E_p gives:

$$\ddot{y}_o = \alpha \left(\frac{R_e E_B G}{m R_s R_x} \right)$$

the term in the parentheses can be made equal to unity by putting

$$R_s = \frac{R_e E_B G}{m R_x}$$

in which case we obtain:

$$\ddot{y}_o = \alpha$$

In other words, for this particular value of R_s, the setting of the R_A potentiometer is just equal to the flat acceleration sensitivity of the starter.

The above relationships thus permit a simple procedure for measuring and setting the starter sensitivity, as follows:

(1) Measure the battery voltage E_B. (Use a calibrated voltmeter for accurate work.)

(2) Measure R_e across the damping resistor, or calculate from known values of R_c, R_d, and R_p. Calculate R_x from known values of R_d and R_p.

(3) The setting of the "sensor" potentiometer R_s can then be calculated from the following relationship

$$R_s = \frac{R_e E_B G}{m R_x (.981)}$$

where G is the known generator constant in volts per m/sec; the factor (.981) comes from 981 cm/sec^2 per g, the desired final units of acceleration, and the fact that the R_s potentiometer is a 10,000 ohm potentiometer with 1000 divisions on the dial scale.

(4) With the R_A potentiometer set at 0 ($\alpha = 0$), connect the output of the field calibrator across the starter damping resistor using alligator clips.

(5) Slowly increase the α setting on R_A until the starter actuates, as indicated by an audible click from the starter relay, or by a start of the SMA-1 accelerograph. The α dial reading will then

be the starter acceleration sensitivity in units of 0.0001 g. Note that to avoid transients from a moving starter coil, the potentiometer setting should be slowly changed; otherwise it will be necessary to mechanically block the starter coil from motion to get repeatable readings.

(6) To set the starter sensitivity to a particular value, set the R_A potentiometer to the desired α setting, and adjust the starter sensitivity potentiometer (screw-driver adjustable pot on vertical terminal board, CCW-insensitive) until the starter just actuates.

(7) To check the balance of the differential amplifier in the starter assembly, repeat the above checks with reversed polarity. The starter should operate at approximately the same setting for both polarities.

Note that the relationship between the setting of the starter sensitivity potentiometer and the acceleration is nonlinear because of the reciprocal relationship involved. At high values of acceleration level ($> 0.04 - 0.05$ g), the adjustment will become very critical.

Measurement of Generator Constant

Most of the parameters in the above relationships for setting and calibrating the starter involve components having stable properties little influenced by time or the usual environmental conditions. Such parameters as the mass of the moving coil and the values of the resistors should remain constant and should not vary significantly from unit to unit. The parameter most likely to vary for different units is the generator constant G, which

depends upon the magnetic field strength of the permanent magnet system. It is therefore desirable to have a relatively simple means of measuring this generator constant.

The generator constant could of course be directly derived from a vibration table test of the unit. Suitable vertical vibration tables having a good wave form at low frequencies are not readily available and in any event are laboratory instruments not easily adaptible to field use. Although such vibration table tests have been used for laboratory evaluation of the starter, it is useful to have alternative methods which can be used in the field.

Two tests of this kind immediately suggest themselves: (a) from the measured damping, the generator constant can be calculated from the theoretical relationships given above; (b) by measuring the coil current required to lift a known weight, the generator constant can be calculated from the relationship $F = -Gi$.

The basic difficulty in the damping test arises from the high value of damping ($h > 1$), which means that no oscillations occur and it is difficult to get an accurate measure of the system response. In practice, two methods will give an acceptable accuracy. (1) By disconnecting the damping resistor, thus leaving the sensitivity adjust potentiometer as the sole damping resistor, the damping is decreased to the point where several cycles of oscillation occur, so that the decrease in amplitude per cycle can be directly measured. (2) Alternatively, with the damping resistor disconnected, a parallel variable resistor can be adjusted to give critical damping as observed on a recorder or storage

oscilloscope. Knowing the value of the resistor to give critical damping will then permit a calculation of the actual damping with the prescribed damping resistor. These methods have two disadvantages. First, they require breaking of a soldered joint in the starter assembly, and second, they require some kind of a recorder which is inconvenient for field applications. For these reasons, the damping method of measuring the generator constant is not considered to be generally useful for field use.

Force-Current Test

The same field calibrator described above for checking and setting the starter acceleration sensitivity can be used to measure the generator constant. By connecting the output of the field calibrator across the damping resistor, without breaking any connections, a known current can be introduced into the transducer coil. From the circuit diagrams of Figures F.1(b) and F.3, the value of this current can be written as:

$$i_c = \frac{\alpha R_e E_B}{R_c \left[R_s + R_e + \alpha(1-\alpha)R_A\right]}$$

To measure the force associated with this current, place a small piece of plastic material weighing about 1 gram on the coil in a central position and note the vertical deflection in the earth's gravitational field. Increase the current in the coil by increasing α for the R_A potentiometer in the field calibrator until the coil is just lifted to its initial position. The force is then just equal to the weight of the test mass, which can be accurately measured on a balance. From the calculated value of the current i_c, the generator constant can then be calculated from $F=mg= -Gi_c$.

This test has as advantages the fact that no connections need be broken in the starter, and no recorder or indicating instruments are needed. The disadvantage is the necessity for an accurate measurement of the vertical positioning of the coil. A fine scribed line on the coil stop assembly will assist in this measurement, which can be carried out with a satisfactory accuracy provided that considerable care is taken. In this test the value of R_s should be of the order of 500 ohms in order to produce suitable currents from the field calibrator unit. To calculate the numerical value of the generator constant G from the definition $G = \frac{F}{i}$, note that if F is the force in Newtons, and i is the current in amperes, G will have the units volts per meter per second. The force in Newtons will be given by the mass of the test strip in kilograms multiplied by 9.81 meters per second.

PART II

Evaluation Tests

To determine the overall performance characteristics of the starter, and to ascertain the extent to which the preceding simple theory describes its behavior, a series of tests were made on a vertical vibration table. For this purpose a small vibration table was constructed consisting of a square aluminum plate 11" x 12" x 3/8" supported by bars which are mounted on flexure hinges so that the table can move on a radius of 20 inches with an approximately vertical motion. The table is driven by a Goodman's Model V5 electromagnetic vibration generator driven by Hewlett-Packard Harrison Model 6823A Power Amplifier. The basic test signal was supplied by either a Hewlett-Packard Model 3310A Function Generator for sinusoidal motions, or by a Hewlett-Packard Model 3722A Noise Generator for more complex wave shapes. The table motion was measured by a Statham AS-2-350 strain gage type accelerometer having a natural frequency of approximately 100 cps. The accelerometer signal was amplified by a Brush Carrier System Amplifier and recorded on a Brush Pen Recorder. The accelerometer-amplifier-recorder system was statically calibrated by rotating the accelerometer transducer in the earth's gravitational field.

With the above vertical shaking table, it was possible to generate good sinusoidal wave forms at the triggering level of acceleration down to a frequency of about 2-3 cps, which sufficed to cover the response range of major interest.

Natural Frequency

The natural frequency of the VS-1 vertical starter transducer element can be determined by recording the voltage proportional to the velocity of the transducer mass during a vibration decay test. During this test the damping resistor (100Ω) must be removed to eliminate most of the electromagnetic damping. For this purpose the transducer coil was connected to the high impedance input amplifier of the Brush Mark 280 Recorder and the vibration decay was recorded for some 30 seconds. This gave $f_n = 3.97$ cps as the natural frequency for the unit tested which is in agreement with the nominal frequency of $f_n = 4.00$ cps specified for VS-1 starters.

Generator Constant

The G constant for the VS-1 vertical starter was measured by two methods. The first method was the Force-Current Test described in Part I. For the starter tested the measured quantities were: $R_e = 21.5\Omega$ and $R_c = 29\Omega$. The voltage of the field calibrator battery supply, with the switch on, just before the test was $E_B = 6.05$ Volts, and R_s was set to 450 ohms. A small piece of plastic material weighing 1.034 gms was centered on the transducer coil. The coil was lifted to its original position prior to the loading with the mass, by a current corresponding to a measured $\alpha = 0.207$. The test mass was $M = 1.034$ gms, and current in the coil then is calculated as:

$$i_c = \frac{\alpha R_e E_B}{R_c\left[R_s + R_e + \alpha(1-\alpha)R_A\right]} = \frac{(0.207)(21.5)(6.05)}{29\left[450 + 21.5 + 0.207(1-0.207)100\right]}$$

$$= 0.00190 \text{ AMP}.$$

and the G constant is:

$$G = \frac{F}{i} = \frac{(0.001034)(9.81)}{0.00190} = 5.33 \text{ V/m/sec.}$$

The second method used to measure G is based on the steady state excitation of the system on a vertical shaking table. First, the 100Ω damping resistor is replaced by a bigger resistance to decrease the equivalent viscous damping. With the 100Ω damping resistor the starter is normally overdamped so that the fraction of critical damping cannot be determined by a vibration decay test from the ratio of successive peak amplitudes. Using an arbitrarily chosen resistor of measured value 1441Ω resulted in a fraction of critical damping $\zeta = 0.126$. For this value the steady sinusoidal table velocity is amplified $\frac{1}{2\zeta} = 3.97$ times by the transducer unit when excited at its natural frequency $f_n = 3.97$ cps. By definition, G is the voltage generated in the open circuit by the coil moving in the magnetic field with velocity equal to 1 m/sec. Thus if one monitors the output of the transducer coil during the steady state excitation simultaneously with the amplitude of the steady sinusoidal table velocity, G_L is given by

$$G_L = \left(\frac{\text{Amplitude of sinusoidal transducer voltage output}}{\text{Velocity amplitude of the sinusoidal table motion}}\right) \cdot (2\zeta)$$

The subscript L indicates that the output of the seismometer is attenuated because of the presence of the damping resistance (1441Ω) in the circuit. The open circuit generator constant G then becomes

$$G = \frac{R_x + R_c}{R_x} G_L$$

where

R_x = external damping resistance, ohms

R_c = coil resistance, ohms

With $R_x = 1441\Omega$ and $R_c = 29\Omega$ we compute G=5.36 V/m/sec. This value agrees very well with the determination of G using the Force-Current Test. This second method is of course not well adapted to field use because of the requirement of a vertical vibration generator.

Sensitivity

Once the generator constant is determined one can proceed to measure the sensitivity adjustment level of the VS-1 vertical starter as described in Part I. With $E_B = 6.15$ volts, $R_e = 21.5\Omega$, $R_d = 100\Omega$, $R_p = 500\Omega$, m=3.85 gm, for the starter tested, one can compute R_x from

$$\frac{1}{R_x} = \frac{1}{R_d} + \frac{1}{R_p} \quad \text{to be} \quad R_x = 83.3\Omega$$

and R_s then becomes

$$R_s = \frac{R_e E_B G}{m R_x (0.981)} = 2240\,\Omega$$

With the R_s potentiometer set at 2240Ω, the α setting on the R_A potentiometer, when starter is just actuated gives the sensitivity setting in units of $g \times 10^{-4}$.

To check the accuracy of such a sensitivity level determination, the starter can be mounted on the vertical table, and excited with a steady sinusoidal acceleration with slowly increasing amplitude. At triggering, the acceleration level should agree with that obtained from the test with the field calibrator. By changing the setting on the

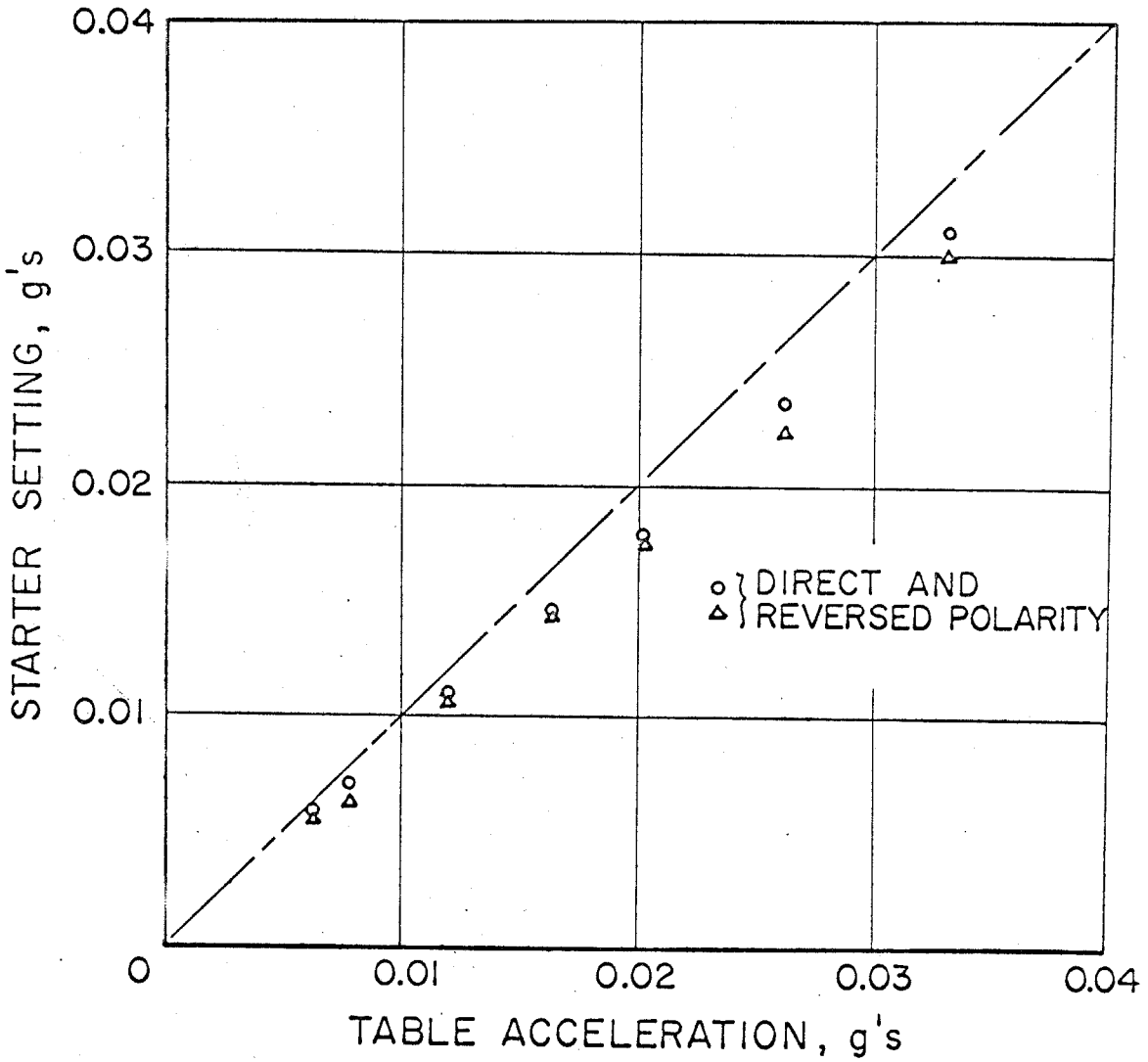

Figure F 4.

Starter sensitivity calibration

sensitivity potentiometer the two sensitivity determination methods were compared for seven different sensitivity levels. The results of this test are given in Figure F.4.

As seen in Figure F.1(b), the recorded signal from the velocity transducer goes from the sensitivity adjustment potentiometer to the amplifier and then to the trigger relay. One way to check whether the amplifier in the VS-1 is properly balanced is to change the polarity of the alligator clips in the field calibration and to repeat the sensitivity level determination test. This was done for all seven tests and the results are indicated in Figure F.4 by two sets of points, one set belonging to the positive and the other to the negative polarity. Ideally one would expect the experimental points to fall on a 45 degree straight line, if the agreement between the steady state vibration table test and the field calibrator test is perfect. In the present case the points do fall on a straight line but slightly off the ideal 45 degree slope, indicating that there is a systematic error of about 10 percent. This error can be caused by errors in determining m, G, R_x, R_e and E_B which together yield the value of R_s, and by errors in measuring the actual acceleration levels recorded by the Statham-Brush system. These discrepancies indicate the errors that may be expected in field work when the field calibrator only is used, without measurements of the other parameters. The difference between the two sets of points for the two polarities (Figure F.4) does indicate a slight asymmetry in system response but is considered to be within tolerance limits for satisfactory starter operation.

Triggering Response to Sinusoidal Motions

This test consisted of steady state sinusoidal excitation of the VS-1 vertical starter mounted on the vertical shaking table. For each frequency the amplitude of the table motion was gradually increased until the starter triggered. When actuated, the starter gives a 12 V D.C. output which may be recorded on the Brush pen recorder or indicated on a meter. This output was monitored on the Brush pen recorder simultaneously with the output from the Statham accelerometer which was calibrated to give table acceleration in g's.

The purpose of this test was to check the validity of the theoretical starter response curve. The points experimentally determined in this way were superimposed on the theoretical curve of Figure F.2 with an arbitrary vertical scale. This comparison indicates an excellent agreement.

During this experiment the sensitivity level was constant and set to an arbitrary value of 0.0129 g at the natural frequency f_n=3.97 cps for the starter tested. This level was determined with the field calibrator test described above.

Change of the Sensitivity Response Curve

The VS-1 vertical starter response curve is nearly constant from about 1 cps to 10 cps. Outside of this region the sensitivity monotonically decreases as shown in Figure F.2. It has been observed that although the sensitivity decreases with increasing frequencies above 20 cps, inadvertant high frequency pulses may actuate the VS-1 starter. This may be an important consideration, since many instruments are located in buildings where elevator noise, people moving about and accidentally falling small objects may trigger the instrument. Such

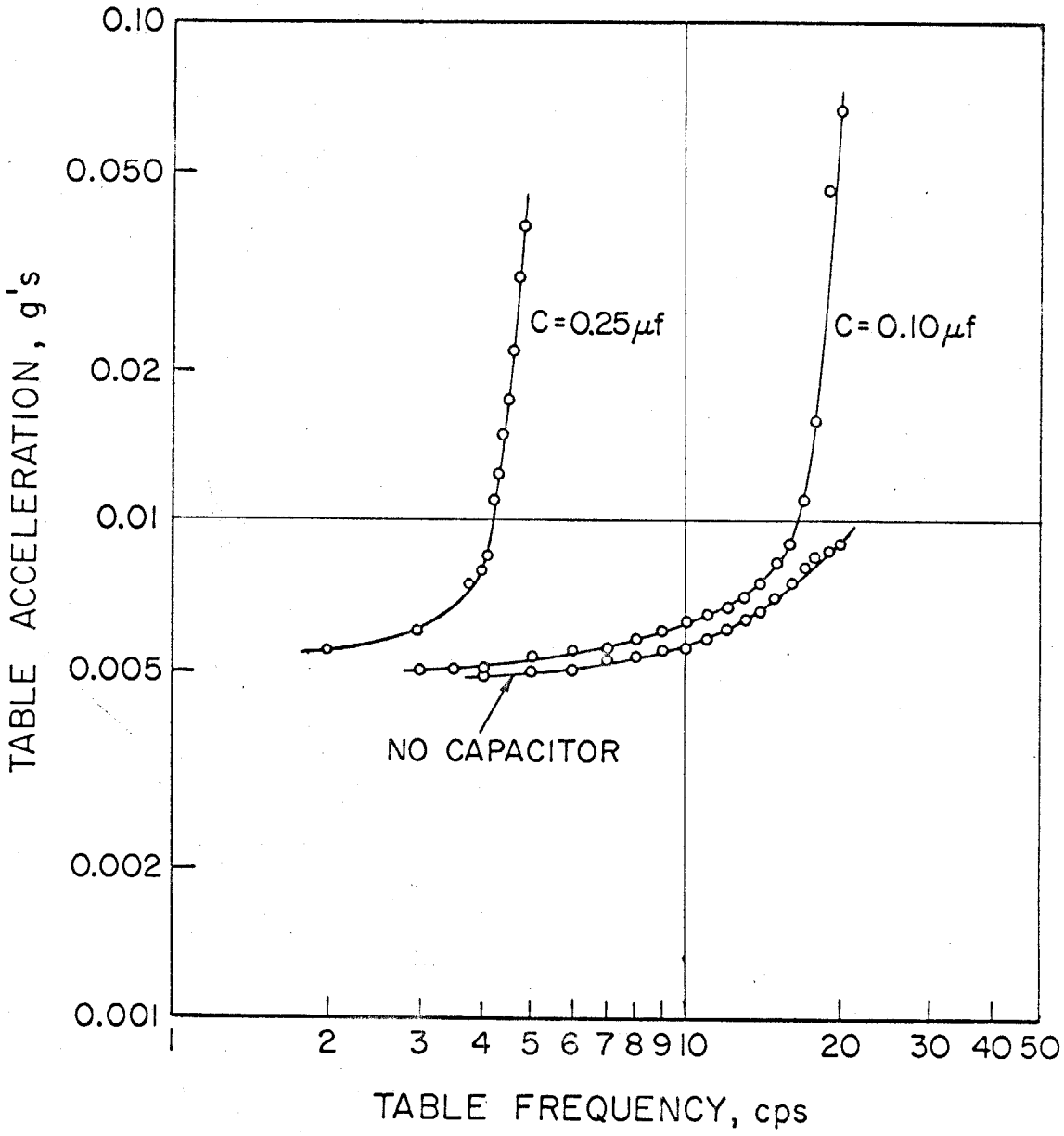

Figure F 5.

Frequency response of vertical starter plus output capacitor.

excitations are usually characterized by high frequency components sometimes of rather high magnitude.

This situation can be improved by attenuating the high frequency sensitivity by adding a capacitor across the amplifier output. The shape of the new response curve is shown in Figure F.5. As may be seen, the addition of a 0.10 μf capacitor sharply attenuates the sensitivity level above 15 cps, while a capacitor of 0.25 μf attenuates the sensitivity above about 4 cps.

As is well known, the P waves recorded on the accelerograms for several past earthquakes show a somewhat higher frequency content than the horizontal wave components. Since these frequencies may well extend to about 10 cps it seems that the additional capacitor should be at most about 0.10 μf.

Conclusions

The vertical starter VS-1 is a significant step forward in the design of an accelerograph starter to trigger as early as possible. Since P wave arrivals with predominantly vertical motions are expected to be the first motions in most earthquakes or explosion generated ground motions, vertical starters should ensure an earlier triggering and so permit the recording of the initial horizontal motions. This electromagnetic starter with a velocity transducer eliminates D.C. zero frequency response and in this way avoids problems associated with long-term drift and tilt.

Laboratory evaluation tests of the transducer element based on steady state vertical excitation and on the field calibrator, indicate that the starter functions in a satisfactory manner. The determination of the

generator constant G and the sensitivity level adjustment can both be made with a simple field calibrator and a standard Volt-ohmmeter.

The vertical starter VS-1 is more complicated than the old horizontal starter in that it incorporates additional relays and electronic components whose long-term performance and reliability in field use have still to be evaluated over a period of years. The new vertical starter can be added to accelerographs already in operation, and used to replace or supplement existing horizontal starters.

G. CALCULATION OF TRUE GROUND MOTION FROM SEISMIC INSTRUMENT RECORDS — TRANSDUCER CHARACTERISTIC CORRECTIONS

Abstract

The correction of seismic type transducer outputs to determine true ground motion is a well known process that involves in one way or another a differentiation of transient signals. The numerical computation of such derivatives is a process which normally leads to large errors. It is shown in this paper that a simple smoothing technique can be used to reduce such errors and to yield accurate first and second order derivatives. This method opens new possibilities in seismic instrument design and enables one to perform simple and accurate instrument corrections for the instruments which are already in use.

Introduction

Ground acceleration versus time is often used to describe the character of strong earthquake ground motion. The direct measurement of ground acceleration has some advantages compared to the measurement of ground velocity or ground displacement. The most important advantage is that it gives directly the time variation of ground acceleration which is used to determine structural response. Also, if necessary, the acceleration can be integrated to obtain ground velocity or displacement.

Most of the currently used strong-motion accelerographs

have natural frequencies of 15-25 cycles per second and about 60% - 70% of critical damping. It may be seen that the measured ground accelerations in the frequency range of 0 to about 10 cycles per second will have relatively small amplitude or phase distortions. However, if the signal to be measured contains higher frequencies or if the motion is measured with an instrument which has longer natural period, it may be necessary to apply certain corrections to the measured quantities.

The objective of this paper is to outline a simple method for such instrumental corrections. Although the method presented here is not new in principle, it is felt that it may be useful to outline the procedure in a form suitable for typical strong-motion accelerograph applications. Since strong earthquake ground acceleration is the most important information for studies of structural response, it would be advantageous to have an accurate scheme which would generate ground acceleration from any recording of strong-motion instruments. In addition, if it is possible to perform instrument corrections accurately, the measurement of the acceleration will not necessarily require that direct recording accelerographs be used for that purpose. This is another important aspect of this problem because it releases many constraints imposed on the instrument design.

Transducer Equation

The general transducer equation can be written in vector

form as:

$$\underset{\sim}{f}(\underset{\sim}{x}, \dot{\underset{\sim}{x}}, \ddot{\underset{\sim}{x}}, \ldots, \alpha_1, \alpha_2, \ldots) = \underset{\sim}{\alpha}(z, \dot{z}, \ddot{z}, \ldots) \tag{1}$$

where $\underset{\sim}{f}(\cdot)$ and $\underset{\sim}{\alpha}(\cdot)$ are functions which depend on the particular instrument in question, $\underset{\sim}{x}$ is a measure of relative instrument response, $\alpha_1, \alpha_2, \ldots$ are instrument constants and z is the absolute ground motion. Depending on the construction, the directly recorded instrument output could be either $\dot{\underset{\sim}{x}}, \underset{\sim}{x}$, or some combination of $\dot{\underset{\sim}{x}}$ and $\ddot{\underset{\sim}{x}}$. In particular, most strong-motion and some other seismic instruments can be described by the following special form of differential equation (1) which represents a single degree of freedom viscous damped oscillator:

$$\ddot{x} + 2\omega_n \zeta \dot{x} + \omega_n^2 x = - V_s \ddot{z}(t) \tag{2}$$

Here ω_n is the natural frequency of the mass-spring system, ζ is the fraction of critical damping, and V_s is a scaling constant. In the case of accelerographs with displacement transducers, the recorded quantity is x. However for some other instruments with the velocity transducers $\dot{x}$ is recorded.

It may be seen that if one can differentiate the function x twice to get $\dot{x}$ and $\ddot{x}$ the absolute ground acceleration can be obtained from (2) immediately. It is this differentiation process that may introduce some difficulties and thus has to be considered in some detail.

Errors of Digitization

Most strong-motion instruments which are presently in the operation employ photographic recording on paper or film. These records are normally hand digitized on a device which consists of a cross-hair system coupled to a digital output device. Successive x-y coordinates are thus converted to digital signals and may be read out to a card punch or a typewriter.

The accuracy of such digitization will depend on the operator, the system used and the quality of the recorded trace. A description of typical digitizing procedures and errors involved may be found in the paper by Hudson et al.(1969). For the present work it will be assumed that the quality of the record is good and that the digitizing machine is sufficiently accurate so that the only errors are those introduced by the operator. Fig. G.1 shows an enlarged portion of a typical recorded trace. While digitizing, the operator attempts to align the cross-hair on the center of the recorded trace which is indicated by the dashed line in Fig. G.1. If it is assumed that the operator is careful, is not biased in choosing the points, and that the error of every digitization is independent of the previous one, the chosen points will be in some sense randomly distributed about the center of the recorded trace. These digitizing errors are the predominant reason why one cannot simply take digitized x(t) data as in Fig. G.1 and carry out repeated differentiations in a conventional way with a satisfactory accuracy. As Jenschke and Penzien (1964) have pointed out "any numerical method of

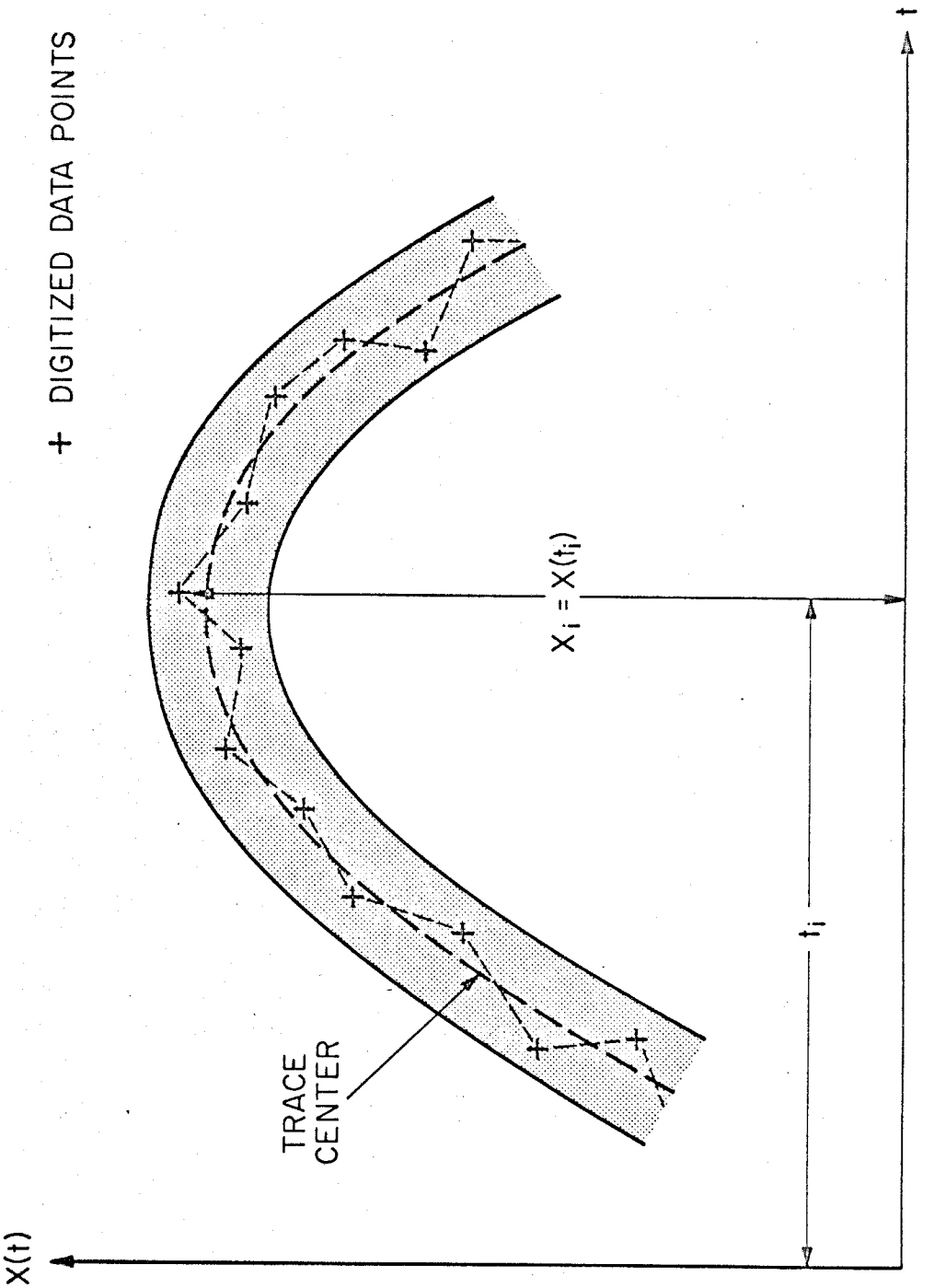

Figure G 1. Enlarged portion of a typical optically recorded instrument output x(t). Digitized points x_i (t_i) are indicated by small crosses.

calculating the second derivative of x(t) by means of finite differences leads to such large errors that this method is impractical".

To compute the derivatives of a x(t) function given in tabulated form two methods can be considered. One method would consist of smoothing the digitized x(t) function so that digitizing errors are filtered out. The other method would consist of interpolating, in the least square sense, a function defined by an analytically differentiable series to the function x(t) given in the tabulated form. In both cases low-pass filtered or interpolated functions would be used to estimate the derivative of the digitized x(t) function.

Smoothing

Numerical smoothing and filtering of time series are frequently used procedures in many fields of data processing. For a general review on the subject the reader could consult various books and papers (e.g. Holloway, 1958). In this section we shall outline only some basic principles of smoothing techniques in order to present some of the essential background.

The reason for performing a smoothing operation on a time series is to attenuate high-frequency Fourier components that are present in the data. The main justification for doing this is based on the assumption that the high-frequency components result from some randomly introduced errors during recording or processing of the data. For example in the case of the records from strong earthquake ground motion these errors may be introduced during hand

digitization as explained above (Fig. G.1). Another important assumption is that the high-frequency components which may be present in the record, but are smoothed out together with the frequencies resulting from randomly introduced errors, are of no importance for further data processing. In the case of the records of strong earthquake ground motion it would then be important that the high-frequency error components introduced by digitization be in the frequency band well above those frequencies belonging to the real ground motion. Since it is intuitively clear that frequencies introduced by digitization are closely related to the average time interval between the successive digitized data points, it follows that one should aim at digitizing as many closely spaced points as is feasible.

Numerically smoothed values x_i^* corresponding to discrete observations x_i are normally computed from:

$$x_i^* = \sum_{k=-n}^{m} w_k x_{i+k} \tag{3}$$

where w_k are weights of the smoothing function, and m and n depend on the particular kind of filter used. It is normally desired to have the mean of the time series x_i unchanged. To meet this requirement the sum of the weights w_k has to be one, i.e.

$$\sum_{k=-n}^{m} w_k = 1 \tag{4}$$

The frequency response of a continuous filter w(t) which would approximate the above discrete filter is characterized by the complex

quantity

$$R(f) = \int_{-\infty}^{\infty} w(t)\, e^{2\pi i f t} dt \tag{5}$$

The absolute value of R(f) represents the ratio of the Fourier amplitude after and before the smoothing. Phase distortion φ between a Fourier component of the original and the filtered function is given by

$$\varphi(f) = \tan^{-1}\left[\frac{\mathrm{Im}\{R(f)\}}{\mathrm{Re}\{R(f)\}}\right] \tag{6}$$

It is often required that the smoothing function w(t) does not shift phases. This will be true if $\mathrm{Im}\{R(f)\} = 0$ and from equation (5) it then follows that w(t) must be even function w.r.t. the origin t = 0.

The frequency response of an equally-weighted running mean over the time interval T can be well approximated by using the continuous envelope w(t) of the discrete weights w_i as

$$w(t) = \begin{cases} 1/T \text{ for } |t| \le T/2 \\ 0 \quad \text{otherwise} \end{cases} \tag{7}$$

and is found to be

$$R(f) = \frac{\sin(\pi f T)}{\pi f T} \tag{8}$$

If it is necessary to use certain prescribed forms of R(f), the weighting function w(t) can be computed from

$$w(t) = \int_{-\infty}^{\infty} R(f)\, e^{-2\pi i f t} df \tag{9}$$

On the other hand it may be advantageous to arrive at the desired form of R(f) by successive filtering. If successive filtering

is performed with n different filtering functions w_m, m=1, 2,..., M(k) having frequency response functions $R_k(f)$, k=1, 2...n, then the resulting frequency response function R(f) is given by

$$R(f) = \prod_{k=1}^{n} R_k(f) \tag{10}$$

In the present work this simple method of successive filtering to smooth out high-frequency errors introduced by digitization is used.

This short outline of the smoothing method has been based mostly on the paper by J.L. Holloway (1958), which treats many other aspects of smoothing and filtering in greater detail.

Differentiation

In order to qualitatively examine the possibilities of the above method of filtering out high-frequency components in the digitized record a simple mathematical experiment was performed. A random function generator was used to produce an acceleration curve which is given in Fig.G.2. This acceleration curve was digitized on a Benson Lehner data reducer and was baseline corrected by fitting a parabola to the acceleration curve. The corrected acceleration was then integrated two times to give velocity (Fig. G. 3) and displacement (Fig. G. 4) functions. The displacement function from Figure G. 4 was then digitized so that there were about 200 points per second. Smoothing is easier to perform on equally spaced data points; therefore, the usual assumption was made that the digitized function

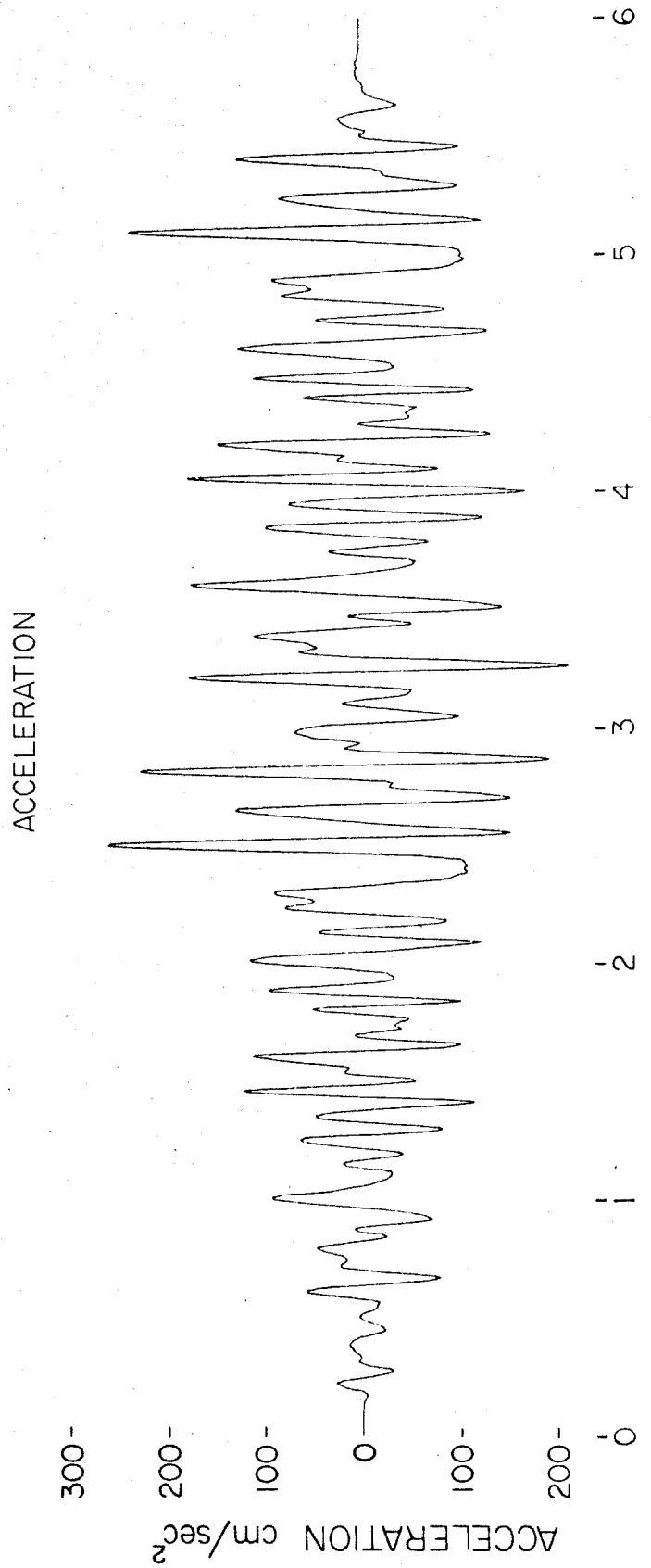

Figure G 2. Acceleration generated on a random function generator.

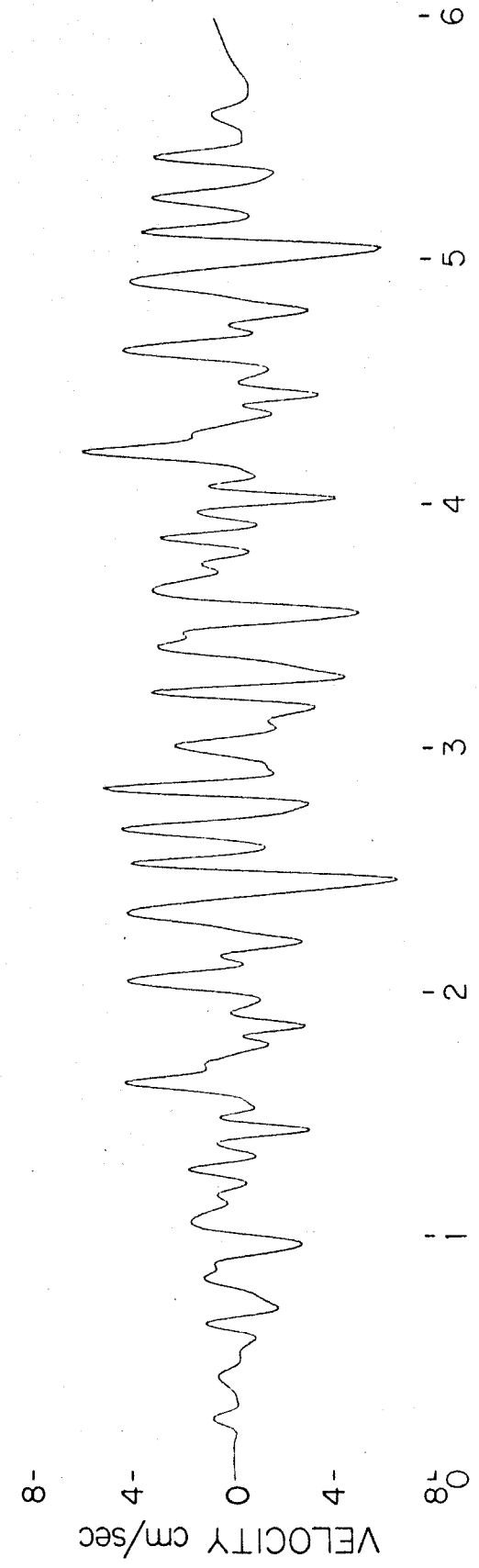

Figure G 3. Computed velocity.

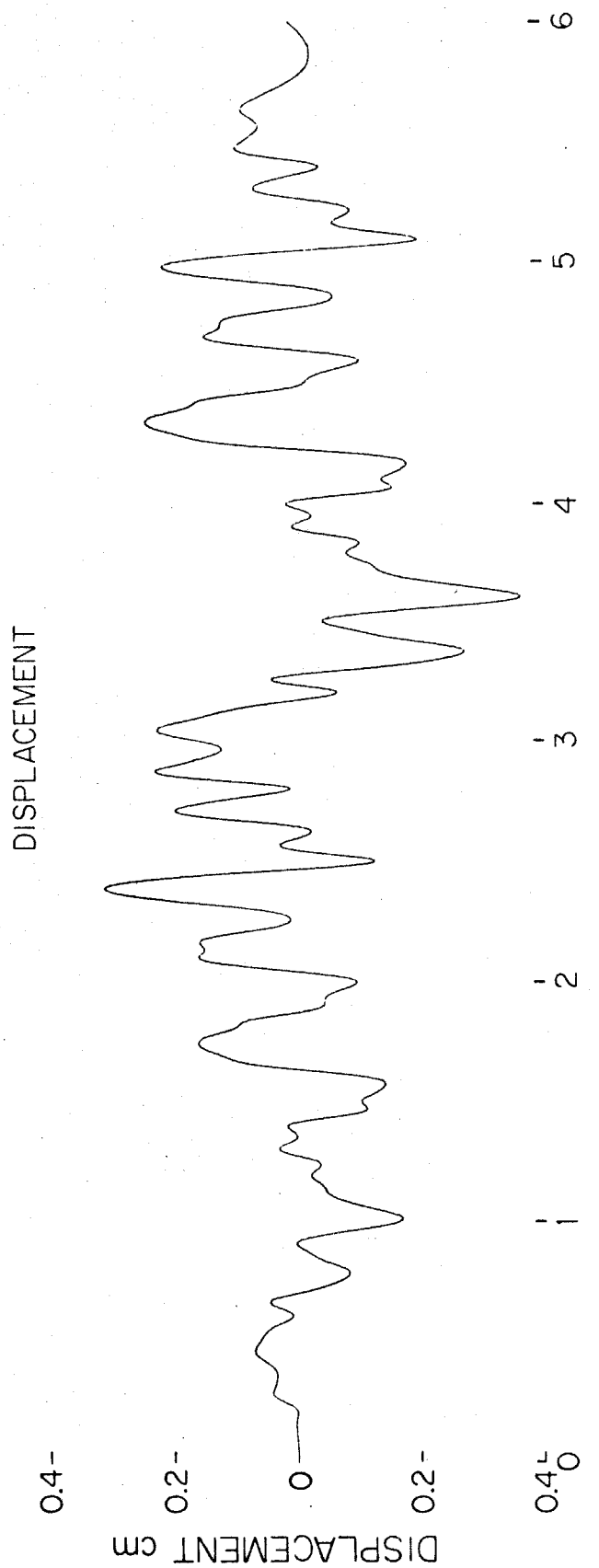

Figure G 4. Computed displacement.

is straight between successively chosen points and equally spaced data with $\Delta t = .002$ sec. (or 500 points/second) were interpolated. Successive smoothing using equally weighted running means was performed on this data. Three windows were employed in succession having the averaging interval T equal to 0.020, 0.012 and 0.008 seconds respectively. With reference to equation (8) it is seen that for $fT \gtrsim 1$, R(f) is essentially zero. Therefore all frequencies greater than and approximately equal to $f = \frac{1}{0.02} = 50$ cps were essentially filtered out.

The reason for using three smoothing intervals in succession is that the frequency response of equally weighted mean filter over T=0.020 seconds introduces negative response for frequencies that satisfy $1 < fT < 2$, $3 < fT < 4$, etc. One of the simplest ways to filter out the negative response is to employ equation (10) and to filter again the smoothed data but now in such a way that the zero of the next filter is conveniently located between the first and second zeroes of the frequency response of the first filtering function.

Numerical differentiation of the smoothed displacement x(t) was performed by using a centered difference scheme:

$$\frac{dx(t)}{dt} = \frac{x(t+\Delta t) - x(t-\Delta t)}{2\Delta t} + O(\Delta t^2) \qquad (11)$$

$$\frac{d^2x(t)}{dt^2} = \frac{x(t+\Delta t) - 2x(t) + x(t-\Delta t)}{\Delta t^2} + O(\Delta t^2) \qquad (12)$$

Velocity and acceleration curves obtained in this way are given in Figures G.5 and G.6. After a detailed comparison with

Figures G.2 and G.3 it may be concluded that the agreement is very good. The derived acceleration curve has some higher frequency irregularities and some of the sharper peaks have smaller amplitudes, because of the partially smoothed intermediately high frequencies.

It should be mentioned here that some of the minor imperfections observed in comparing Figures G.2 and G.6 could be eliminated by using a sharp cut-off filter with

$$R(f) = \begin{cases} 1 & 0 \le f \le f_c \\ 0 & f > f_c \end{cases} \tag{13}$$

where f_c is the cut-off frequency. The filtering function with zero phase shifts belonging to this filter becomes

$$w(t) = \frac{\sin(2\pi f_c t)}{\pi t} \tag{14}$$

There are however certain practical disadvantages in using this filtering function because it requires much longer intervals of smoothing for every filtered point. On the other hand, as will be seen in the following section, simple succesive filtering by equally weighted running means can give quite good results in many instances.

The Computation of Ground Acceleration

In this section we will employ the smoothing technique, briefly described above, to perform instrument corrections and to compute ground acceleration. Our attention will be restricted to the

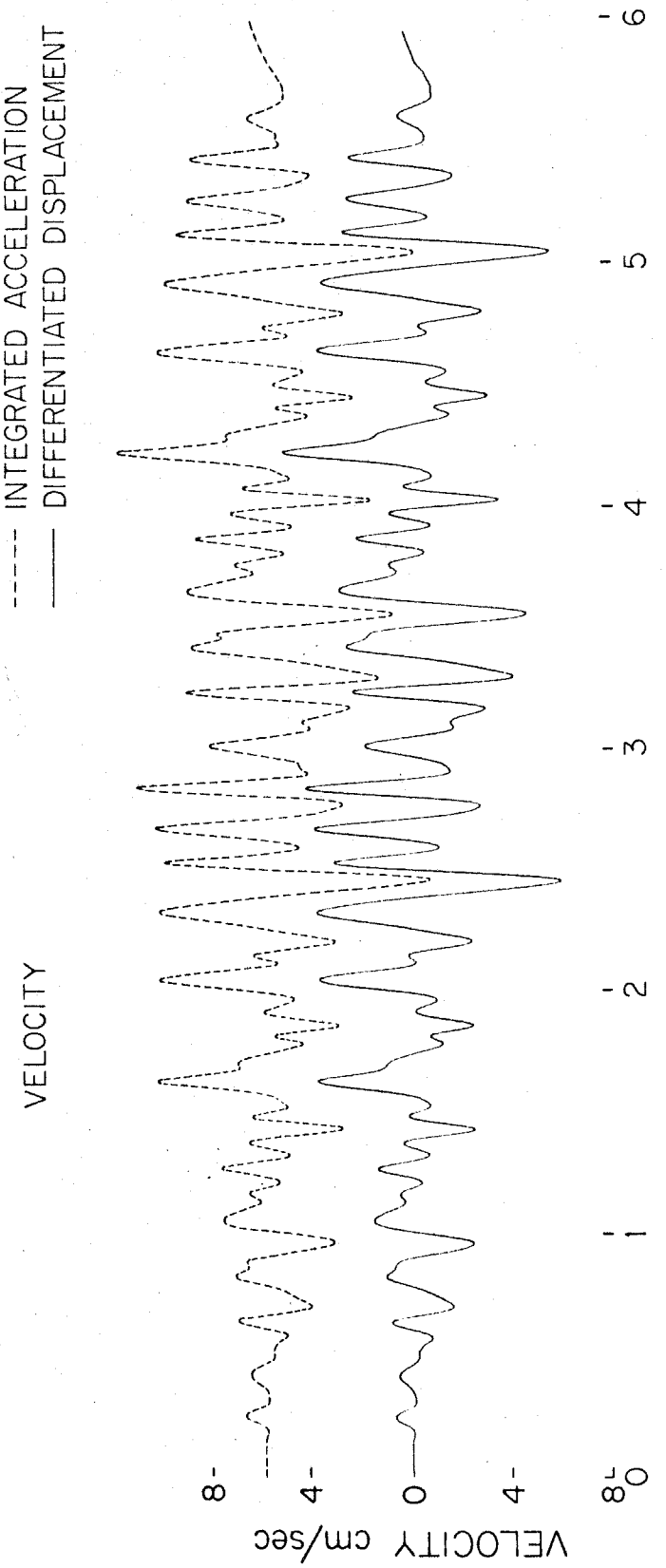

Figure G 5. Velocity derived from the displacement in Figure G 4. Digitized data were smoothed by successive equally weighted running means over intervals T = 0.020, 0.012 and 0.008 seconds. Dashed scale displaced for visibility.

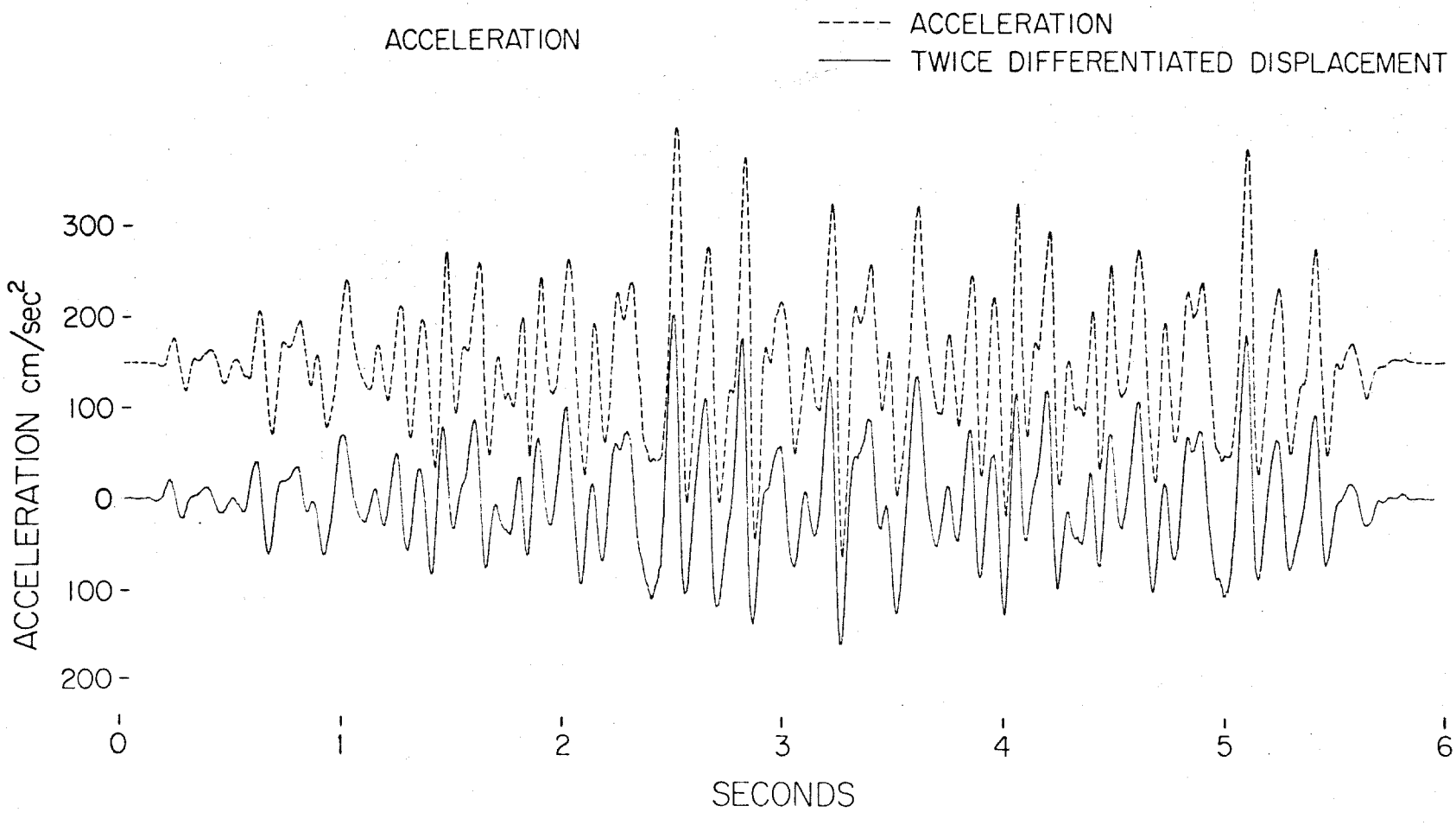

Figure G 6. Acceleration derived from the displacement in Figure G 4. Digitized data were smoothed by successive equally weighted running means over intervals T = 0.020, 0.012 and 0.008 seconds. Dashed scale displaced for visibility.

equation of a single degree of freedom system with viscous damping,

$$\ddot{x} + 2\omega_n \zeta \dot{x} + \omega_n^2 x = -\ddot{z} \tag{15}$$

As before ω_n is the natural frequency of the pendulum, ζ is the fraction of the critical damping and we assume here that $V_s = 1$. We note that in using equation (15) as an example no loss in generality is involved because once we are able to differentiate a function of the instrument response with sufficient accuracy we can use almost any physical system defined by the differential equation to compute the variation of the forcing function in time.

Fifteen seconds of typical recorded strong earthquake ground acceleration was adopted by definition as the exact acceleration $\ddot{z}(t)$ and is given in Figure G.7. This acceleration was then used as the forcing function in differential equation (15) which was integrated using the third order Runge-Kutta method. The natural frequency of the instrument ω_n was taken as 6.28 rad./second and the fraction of critical damping ζ as 0.60. Computed velocity and displacement of this mathematical instrument are given in Figures G.8 and G.9. Two experiments were then performed.

First it was assumed that the instrument in question is a velocity pick-up, i.e. that the instrument output is proportional to $\dot{x}(t)$ (Figure G.8). The computed instrument velocity was digitized and used to reconstruct $\ddot{z}(t)$. This was done in the following way. To obtain $x(t)$, $\dot{x}(t)$ was baseline corrected by a parabolic baseline and integrated once. Also, $\dot{x}(t)$ was smoothed with two successive equally

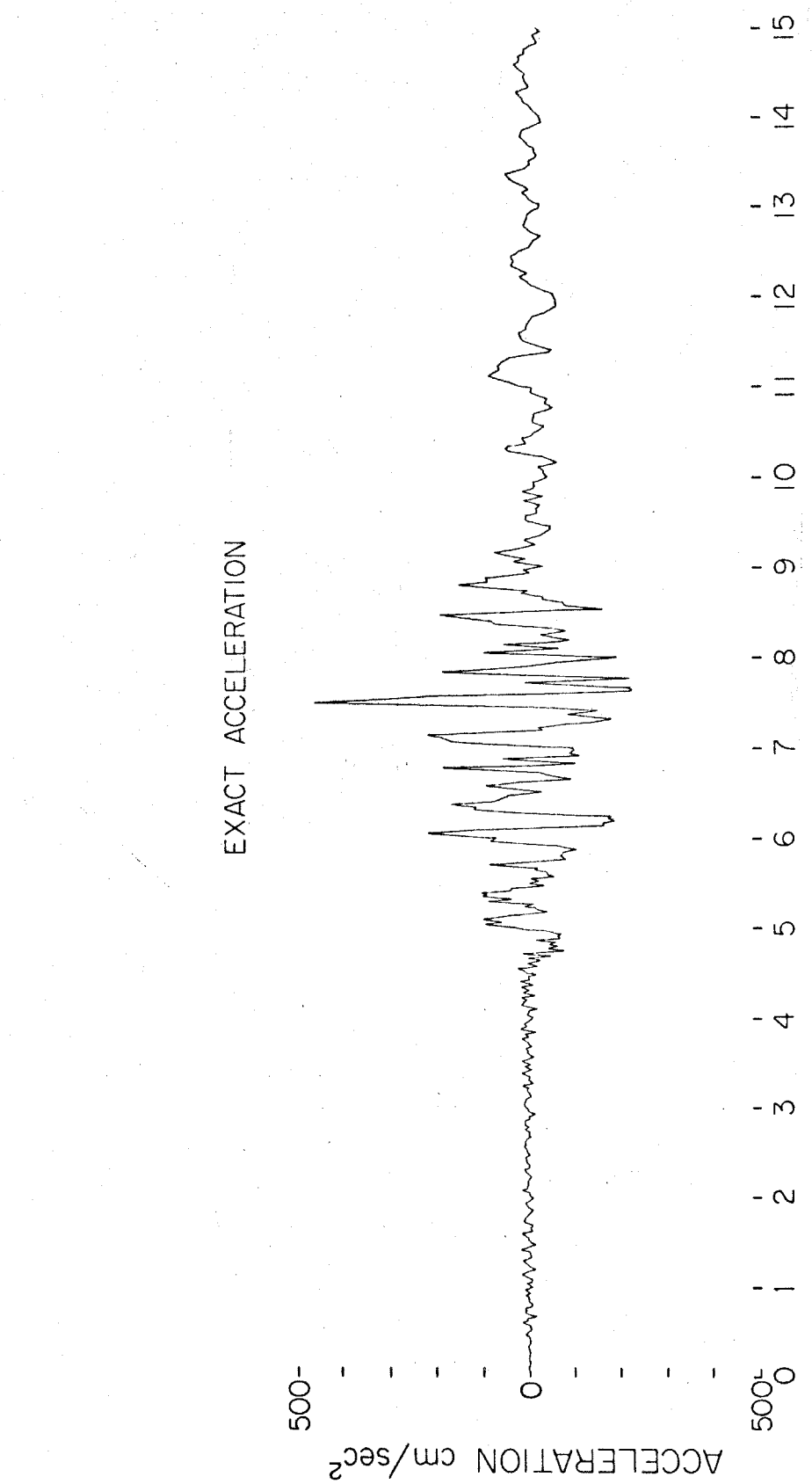

Figure G 7. Strong earthquake ground motion accelerogram adopted as the exact acceleration $\ddot{z}(t)$.

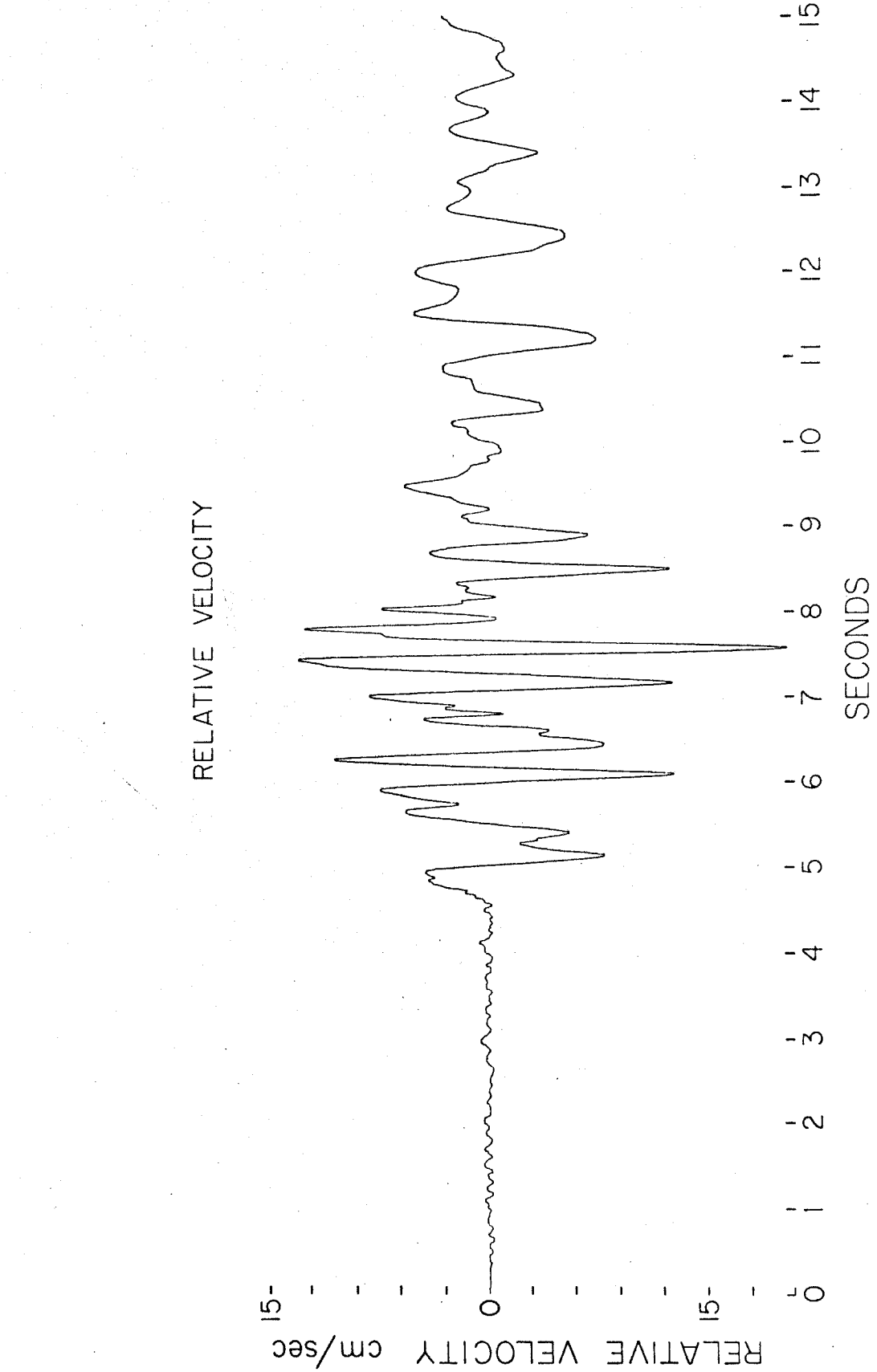

Figure G 8. Relative velocity response of a single degree of freedom system with natural period T_n = 1 second and 60% of critical viscous damping, excited by the acceleration $\ddot{z}(t)$ given in Figure G 7.

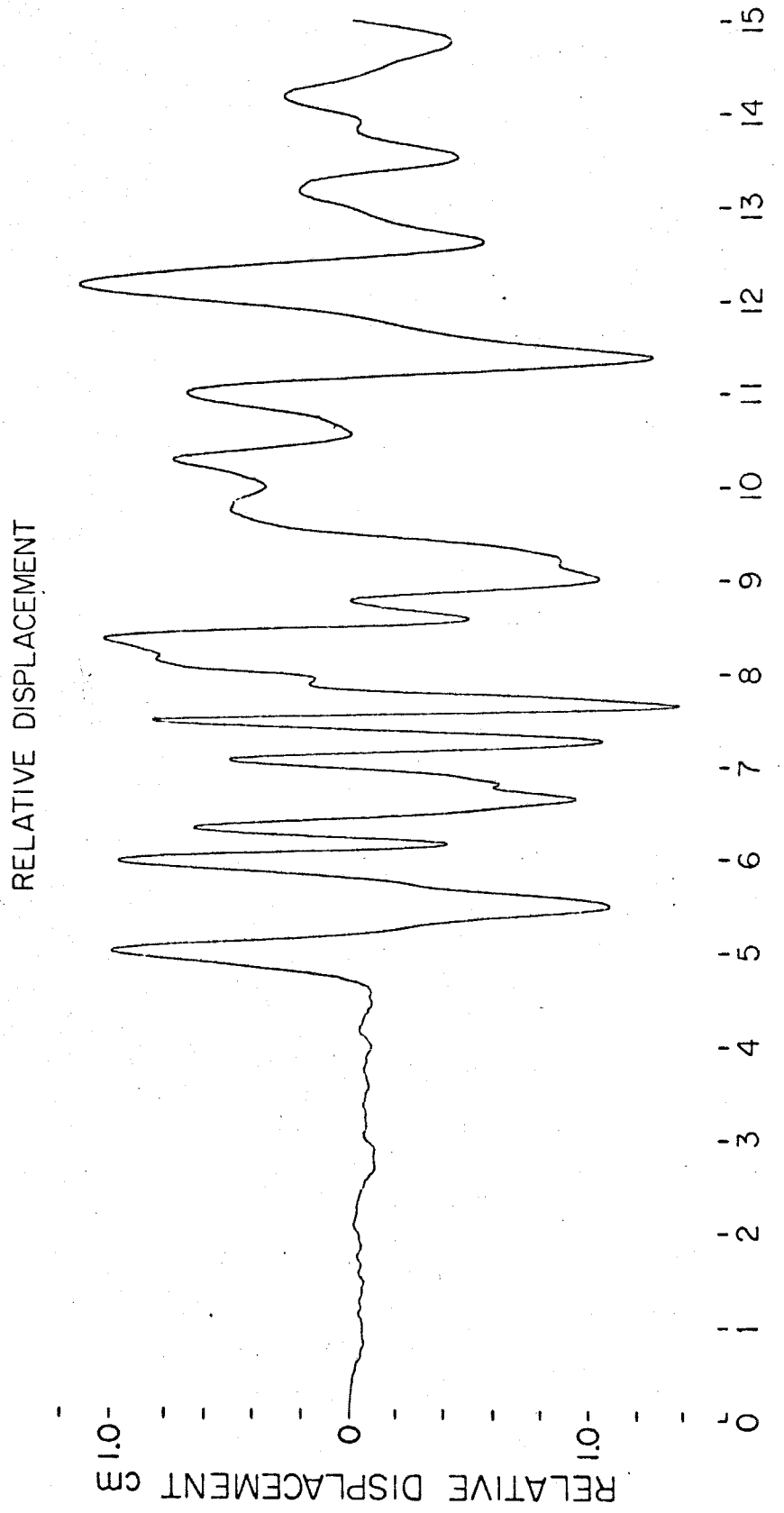

Figure G 9. Relative displacement response of a single degree of freedom system with natural period T_n= 1 second and 60% of critical viscous damping, excited by the acceleration $\ddot{z}(t)$ given in Figure G 7.

weighted running means first over the interval T=0.016 and then over T=0.008 seconds, and differentiated to get $\ddot{x}(t)$. The resulting $\ddot{z}(t)$ constructed by using $\ddot{x}(t)$, $\dot{x}(t)$ and $x(t)$ in equation (15) is given in Figure G.10. The agreement with the original acceleration $\ddot{z}(t)$ in Figure G.7 is very good. It may be noted here that since only one differentiation of the digitized $\dot{x}(t)$ data is necessary to obtain $\ddot{x}(t)$, the filtering does not have to be so severe as in the following case.

In the second experiment it was assumed that the instrument output is proportional to x(t) (Figure G.9). The digitized x(t) function was smoothed by successive filters with filtering intervals 0.048, 0.032 and 0.016 seconds. The smoothed x(t) was differentiated and $\dot{x}(t)$ and $\ddot{x}(t)$ were used again in equation (15) to compute $\ddot{z}(t)$ which is given in Figure G.11. As it may be seen from Figure G.11, the reconstructed $\ddot{z}(t)$ is in good agreement with the original $\ddot{z}(t)$ but of somewhat reduced quality when compared with $\ddot{z}(t)$ in Figure G.10 obtained from $\dot{x}(t)$. The reason for this is that when starting from x(t) much stronger filtering of high-frequency components is necessary in order to eliminate digitizing errors which are increasingly emphasized by every additional differentiation. The frequency dependence of the R(f) resulting from successive application of running mean filters with T=0.048, 0.032 and 0.016 sec. on the equally spaced data for x(t) with $\Delta t = 0.004$ sec. is given in Figure G.12.

It may be concluded then that by careful hand digitization and a simple smoothing technique, one can correct for the instrument response and reconstruct ground acceleration with a high degree of

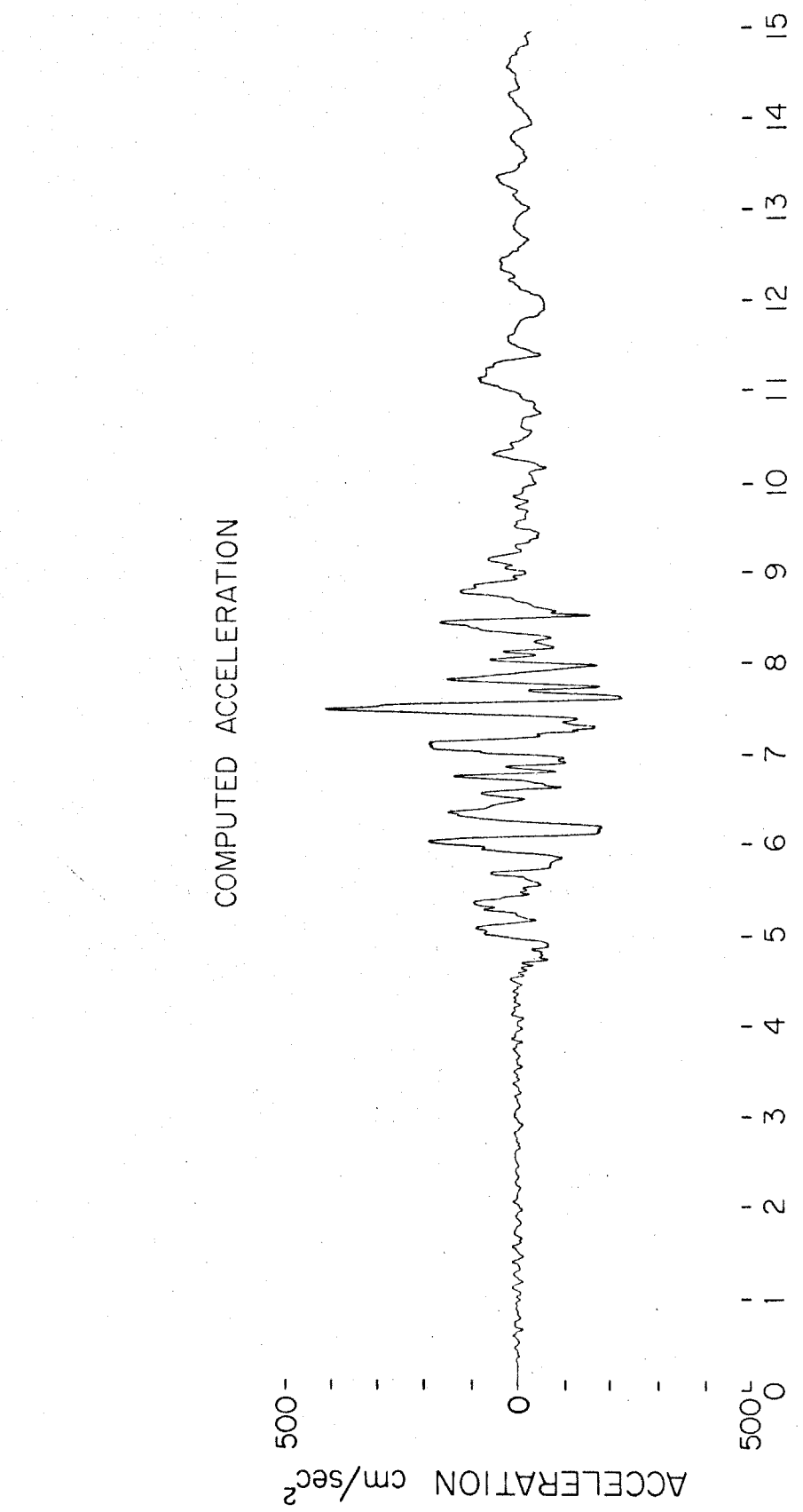

Figure G 10. Ground acceleration $\ddot{z}(t)$ reconstructed by using velocity response of a single degree of freedom oscillator given in Figure G 8.

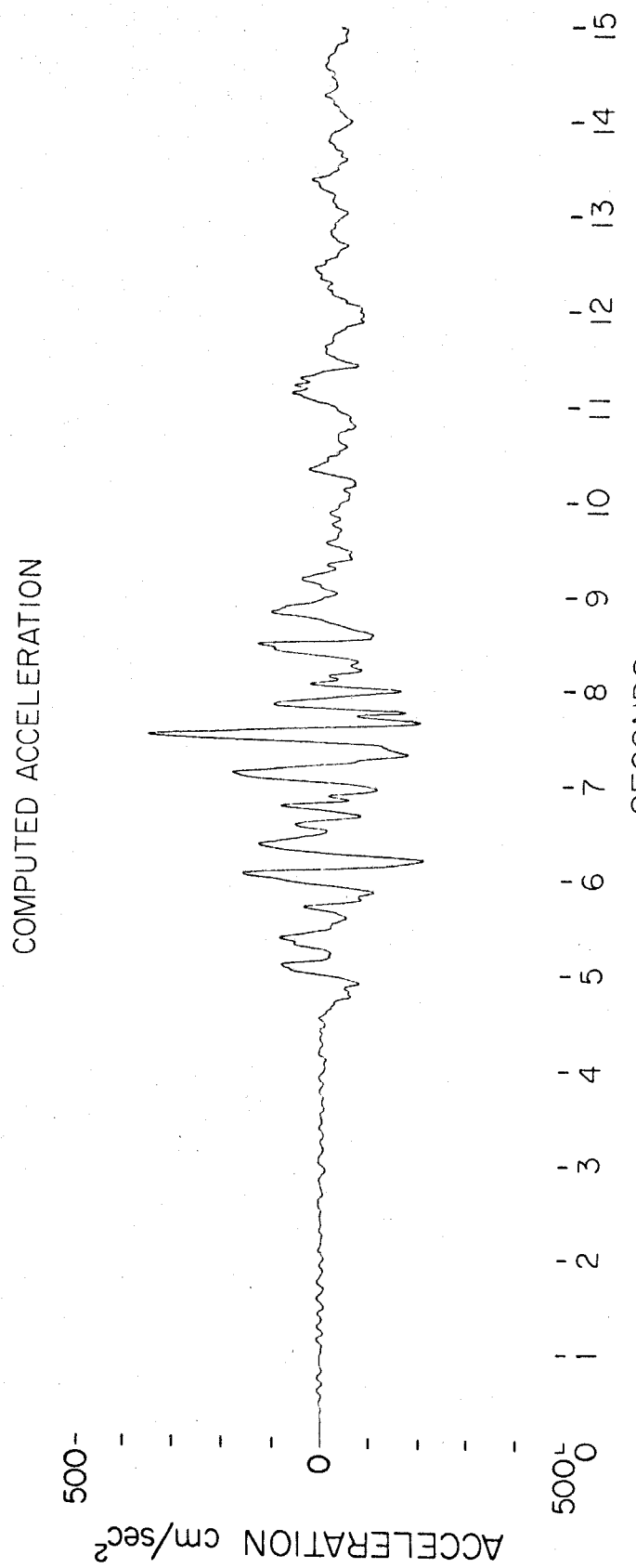

Figure G 11. Ground acceleration $\ddot{z}(t)$ reconstructed by using displacement response of a single degree of freedom oscillator given in Figure G 9.

accuracy. This fact opens new possibilities in seismic instrument design because it permits greater flexibility and releases many constraints which might otherwise limit other design features. Further, since it is not difficult to foresee that in the near future, most instrument recordings will tend to be on magnetic tapes rather than on the photographic paper or film, the method described above will become still simpler and easier to use. This is because analog to digital conversion facilities allow a high rate of accurate sampling, which is equally spaced in time and which is certainly much more accurate and reproducible than hand digitization.

Conclusions

Some of the main findings in this work can be summarized as follows:

1. Numerical differentiation can be performed successfully by employing a smoothing technique which is used to filter out high-frequency errors introduced by visual digitization of the record.

2. The ability to perform accurate differentiation provides a means for simple instrument correction leading to the reconstruction of the support acceleration. This is important because strong earthquake ground acceleration represents the basic information for studies of structural response during destructive earthquakes.

3. It is not necessary to design instruments so that their output is proportional to the quantity that is to be measure. The instruments

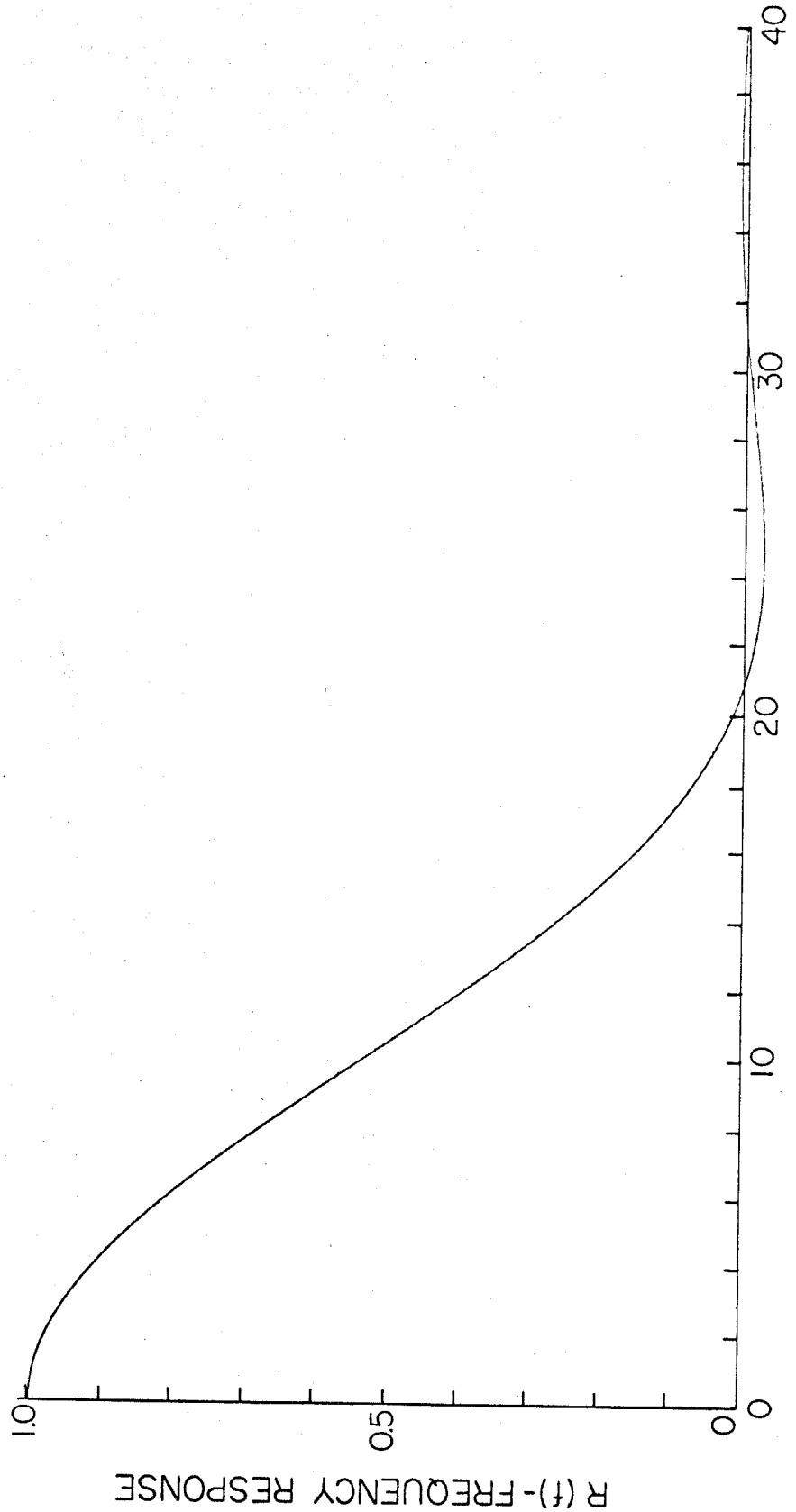

Figure G 12. Resulting frequency response of successive application of running mean filters with smoothing intervals T = 0.684, 0.032, and 0.016 seconds. This filtering was used in deriving $\ddot{z}(t)$ in Figure G 11.

may be designed in an optimum sense so that their characteristics coupled with suitable data processing gives the required information.

H. LABORATORY TESTS OF TRANSDUCER AND DATA PROCESSING TECHNIQUE ACCURACIES FOR TRANSIENT MOTION MEASUREMENTS

As a means of acquiring a feeling for the overall accuracies to be expected in the measurement of transient motions, the following simple experiment was performed. A laboratory shaking table was equipped with two instruments, a Statham ±2g accelerometer and a Schaevitz linear differential transformer in order to obtain simultaneous recordings of the table acceleration and displacement. The accuracy of these instruments has been ascertained by several years of calibration and repeated use for various measurements in the laboratory.

A nearly random signal from the Hewlett Packard Model 3722 random function generator was amplified and used along with the electro-magnetic shaker to produce typical table motions. Both the Statham accelerometer and the Schaevitz linear differential transformer were bolted to the table and recorded the motion in the same direction. The signals from the accelerometer and the displacement transformer were amplified by a carrier amplifier system and recorded on a two channel Brush Mark 280 recorder. In this way simultaneous records of table acceleration and table displacement were obtained.

In order to study the overall accuracy of the recording and data processing techniques, the acceleration and displacement records were digitized on the Benson-Lehner datareducer, digitizing about 160 points per second. The plots of these records are shown in Figure H. 1 (dashed

line) and Figure H. 2 (solid line). The overall accuracy of the differentiation and integration process, combined with the instrument accuracy, was studied.

First, the digitized version of the recorded acceleration record (Figure H. 1, dashed line) was baseline corrected using the parabolic baseline correction on the acceleration and minimizing the time integral of the square of the velocity. During integration it was assumed that the acceleration function is composed of straight lines between successive digitized points. This acceleration was integrated twice employing the simple trapezoidal rule (Brady, 1966). The initial velocity and displacement were set equal to zero. The integrated displacement curve is given in Figure H. 2 (dashed line). A comparison with the recorded displacement shows a slight long period drift. The agreement of the short period oscillations is excellent.

There are several possible reasons for the long period drifts. For example, the paper in the Brush recorder may experience minute transverse motions while the acceleration is being recorded, and this may cause long period drifts after double integration. The process of digitization also introduces similar effects. For the intermediate short periods, digitizing errors tend to average out because of their random character and zero mean, although they may cause long period fluctuations like those in Figure H. 2. For most applications, however, the agreement of the recorded and the computed displacement curves would be considered satisfactory.

For the second test, the recorded displacement curve of Figure H. 2 (solid line) was digitized and differentiated twice to obtain

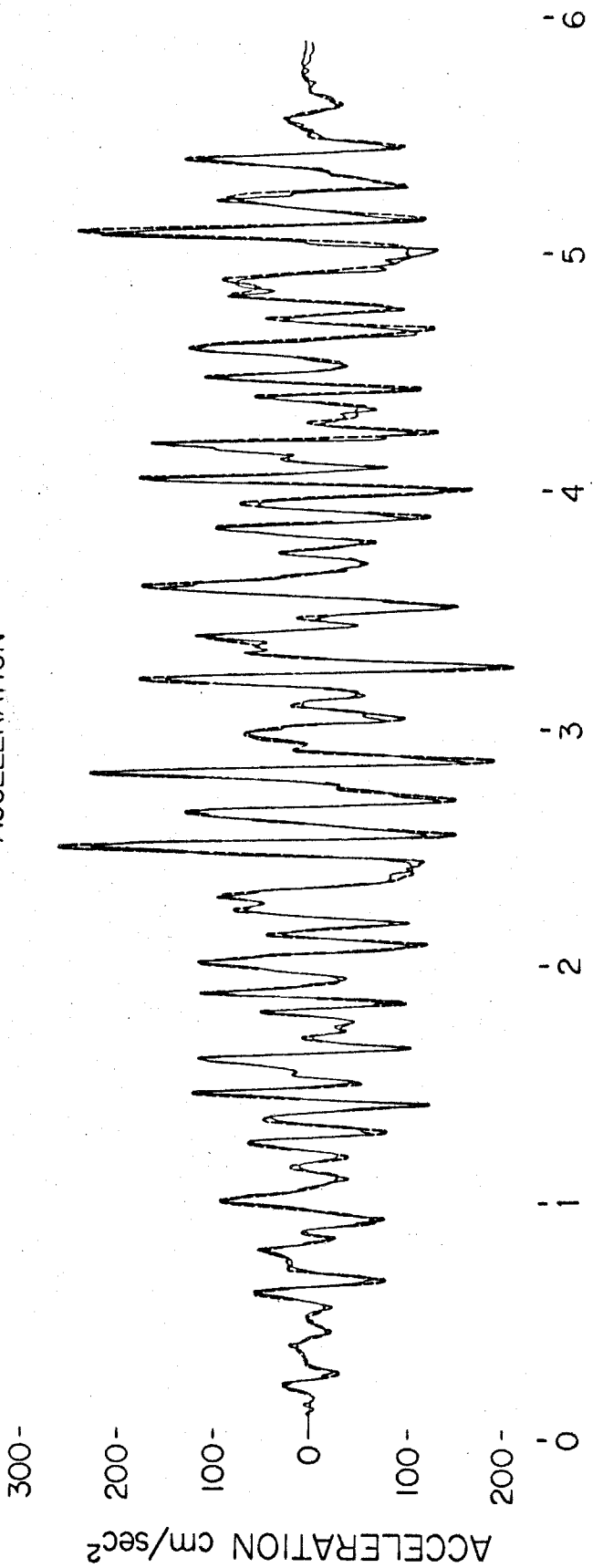

Figure H 1. A comparison of the recorded and computed acceleration curves.

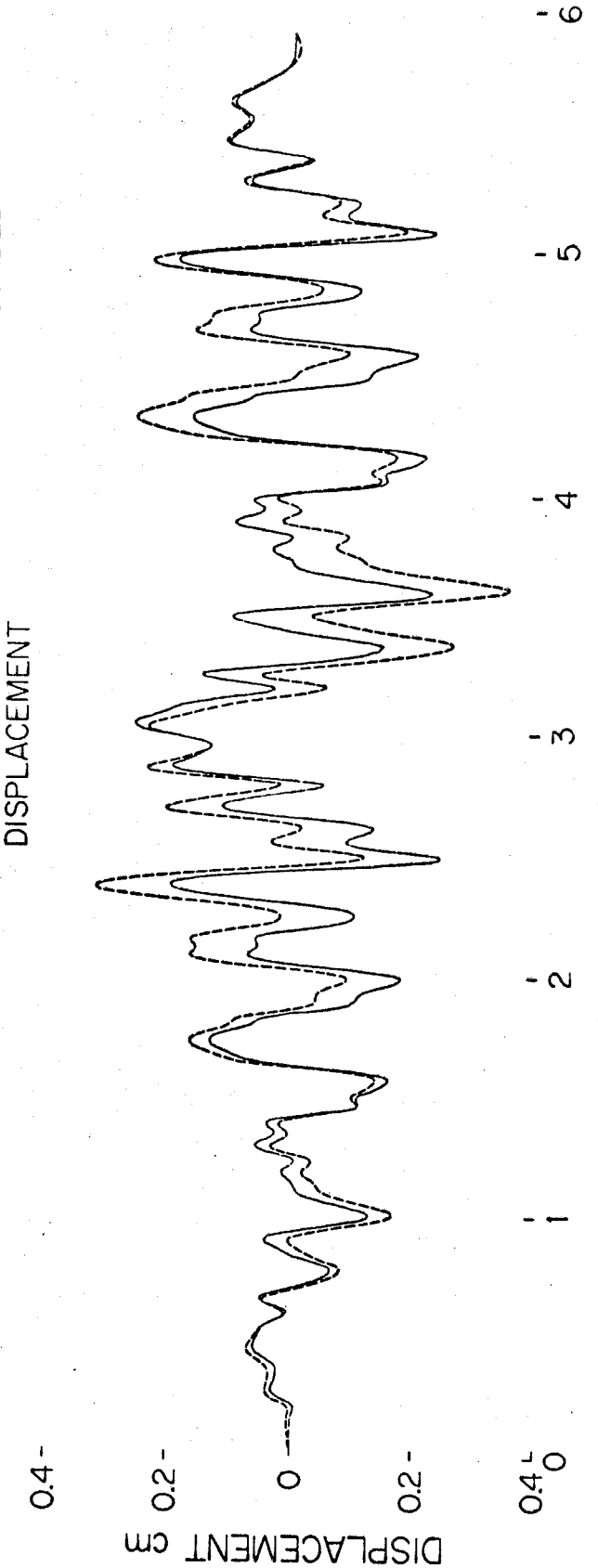

Figure H 2. A comparison of the recorded and computed displacement curves.

the acceleration curve. Before the differentiation, equally spaced data points were interpolated to the digitized displacement curve, generating 500 points per second. These equally spaced points were smoothed by successive equally weighted running means. The averaging intervals used in succession were $T_1 = 0.020$ seconds, $T_2 = 0.012$ seconds, and $T_3 = 0.008$ seconds. Double differentiation was then performed using a central difference scheme. The resulting acceleration is shown in Figure H.1 (solid line). The agreement with the recorded acceleration is excellent.

The above simple experiments were performed with the intention of giving to the reader quick and simple insight into the question of the expected overall accuracy of frequently used elementary measurement and data processing techniques. For a more detailed consideration of some aspects of this and other related topics see the paper by Hudson, et al, (1969).

ACKNOWLEDGMENTS

We are indebted to Professor W. O. Keightley of the University of Montana for conducting laboratory tests for evaluation of the RFT-250 accelerograph and for deriving relationships for angles of misalignment of the transducer sensitivity vectors. We are grateful to Mr. R. Dielman and Mr. J. Titlow for their help in some of the laboratory evaluation tests.

This research was supported in part by the grants from the National Science Foundation and the Earthquake Research Affiliates Program at the California Institute of Technology.

References

Brady, A. G. (1966). Studies of Response to Earthquake Ground Motion. Earthquake Engineering Research Laboratory, California Institute of Technology.

Holloway, J. L. (1958). Smoothing and Filtering of Time Series and Space Fields. Advances in Geophysics, 4, 351-389.

Hudson, D. E. (1962). Some Problems in the Application of Spectrum Techniques to Strong-Motion Earthquake Analysis. Bull. Seism. Soc. Amer., 52, 417-430.

Hudson, D. E., N. C. Nigam and M. D. Trifunac (1969). Analysis of Strong-Motion Accelerograph Records. Fourth World Conference on Earthquake Engineering, Santiago, Chile.

Jenschke, V. A. and T. Penzien (1964). Ground Motion Accelerogram Analysis Including Dynamical Instrument Correction. Bull. Seism. Soc. Amer., 54, 2087-2098.

Peters, B. R. (1968). Strong-Motion Accelerograph Evaluation. Earthquake Engineering Research Laboratory, California Institute of Technology.

Strong-Motion Earthquake Observation Council, Tokyo (1968). Some Recent Earthquake Engineering Research and Practice in Japan. The Japanese National Committee of the International Association for Earthquake Engineering, Tokyo, Japan, p. 1.

Trifunac, M. D. and D. E. Hudson (1970). Analysis of the Station No. 2 Seismoscope Record — 1966, Parkfield, California Earthquake. Bull. Seism. Soc. Amer., 60, 785-794.